การพัฒนาเมมเบรนไบโอเซนเซอร์และระบบของไหลจุลภาคแบบมัลติเพล็กซ์สำหรับการตรวจวัดสารบ่งชี้โรคเบาหวาน

นางสาวยุวดี บุญญสิทธิ์

วิทยานิพนธ์นี้เป็นส่วนหนึ่งของการศึกษาตามหลักสูตรปริญญาวิทยาศาสตรดุษฎีบัณฑิต
สาขาวิชาชีวเคมีคลินิกและอณูทางการแพทย์ ภาควิชาเคมีคลินิก
คณะสหเวชศาสตร์ จุฬาลงกรณ์มหาวิทยาลัย
ปีการศึกษา 2558

Development of Membrane-based and Multiplex Microfluidic Biosensors for Detection of Diabetic Markers

Miss Yuwadee Boonyasit

A Dissertation Submitted in Partial Fulfillment of the Requirements
for the Degree of Doctor of Philosophy Program in Clinical Biochemistry and Molecular Medicine
Department of Clinical Chemistry
Faculty of Allied Health Sciences
Chulalongkorn University
Academic Year 2015

Thesis Title	Development of Membrane-based and Multiplex Microfluidic Biosensors for Detection of Diabetic Markers
By	Miss Yuwadee Boonyasit
Field of Study	Clinical Biochemistry and Molecular Medicine
Thesis Advisor	Assistant Professor Dr. Wanida Laiwattanapaisal
Thesis Co-Advisor	Professor Dr. Orawon Chailapakul

Accepted by the Faculty of Allied Health Sciences, Chulalongkorn University in Partial Fulfillment of the Requirements for the Doctoral Degree

.....Dean of the Faculty of Allied Health Sciences
(Associate Professor Dr. Prawit Janwantanakul)

THESIS COMMITTEE

.....Chairman
(Associate Professor Dr. Rachana Santiyanont)

.....Thesis Advisor
(Assistant Professor Dr. Wanida Laiwattanapaisal)

.....Thesis Co-Advisor
(Professor Dr. Orawon Chailapakul)

.....Examiner
(Assistant Professor Dr. Tewin Tencomnao)

.....Examiner
(Professor Dr. Jenny Emnéus)

.....Examiner
(Associate Professor Dr. Arto Heiskanen)

.....External Examiner
(Associate Professor Dr. Weena Siangproh)

ยุวดี บุญญสิทธิ์ : การพัฒนาเมมเบรนไบโอเซนเซอร์และระบบของไหลจุลภาคแบบมัลติเพล็กซ์สำหรับการตรวจวัดสารบ่งชี้โรคเบาหวาน (Development of Membrane-based and Multiplex Microfluidic Biosensors for Detection of Diabetic Markers) อ.ที่ปรึกษาวิทยานิพนธ์หลัก: ผศ. ดร. วนิดา หลายวัฒนไพศาล, อ.ที่ปรึกษาวิทยานิพนธ์ร่วม: ศ. ดร. อรวรรณ ชัยลภากุล, หน้า.

โรคเบาหวานส่งผลกระทบร้ายแรงต่อคุณภาพชีวิตและค่าใช้จ่ายในการดูแลรักษาสุขภาพ ด้วยเหตุนี้การพัฒนาอุปกรณ์การวิเคราะห์เพื่อใช้ในการประเมินระดับน้ำตาลในเลือดจึงยังคงมีจำเป็นสำหรับผู้ป่วยที่เป็นโรคเบาหวานโดยเฉพาะอย่างยิ่งในพื้นที่ที่มีทรัพยากรอย่างจำกัด ในงานวิจัยนี้ ได้นำเสนออุปกรณ์การวิเคราะห์ที่หลากหลายในรูปแบบใหม่สำหรับวิเคราะห์สารบ่งชี้โรคเบาหวานเพื่อประเมินระดับน้ำตาลในเลือด ประการแรก ฟรุคโตซามีน (Fructosamine) และซีรัมอัลบูมิน (Serum albumin) ในตัวอย่างเลือดครบส่วนสามารถตรวจวิเคราะห์ได้พร้อมกันบนระบบของไหลจุลภาคฐานกระดาษ (Microfluidic paper-based analytical device) โดยอาศัยหลักการตรวจวัดจากการเกิดปฏิกิริยาของสี ซึ่งแสดงให้เห็นถึงศักยภาพในอนาคตที่จะพัฒนาต่อเป็นอุปกรณ์การตรวจวัดข้างเตียงผู้ป่วยสำหรับใช้ประเมินและติดตามระดับน้ำตาลในเลือดของผู้ป่วยโรคเบาหวาน ประการที่สอง ศึกษาและพัฒนาปรับปรุงผิวเยื่อเปลือกไข่ (Eggshell membrane) และชิปอิเล็กโทรดทอง (Interdigitated gold microelectrode array chip) ด้วย 3-aminophenylboronic acid (APBA) ให้มีความจำเพาะต่อการตรวจวิเคราะห์ฮีโมโกลบิน เอวันซี (HbA1c) ด้วยเทคนิคการตรวจวัดทางเคมีไฟฟ้าแบบไม่ติดฉลาก (Label-free electrochemical impedance spectroscopy) โดย APBA มีความจำเพาะกับฮีโมโกลบิน เอวันซี ผ่านอันตรกิริยาซิส-ไดออล (*Cis*-diol interactions) และประการสุดท้าย เพื่อเป็นการรวมการทดสอบสารบ่งชี้ทางชีวภาพหลายตัว (Multiplex biomarker assay) ด้วยระบบการวิเคราะห์จำเพาะที่มีต้นทุนต่ำ (Selective low-cost platform) จึงได้พัฒนาระบบการตรวจวัดทางเคมีไฟฟ้าแบบไม่ติดฉลากบนระบบของไหลจุลภาคฐานกระดาษแบบสามมิติ (Three-dimensional microfluidic paper-based electrochemical impedance devices) ร่วมกับระบบของไหลจุลภาคแบบมัลติเพล็กซ์ (Multiplexed microfluidic system) สำหรับการตรวจวัดสารบ่งชี้โรคเบาหวานได้พร้อมกันหลายตัวภายในระบบเดียวที่ค่าความถี่เดียวที่จำเพาะ

ภาควิชา	เคมีคลินิก	ลายมือชื่อนิสิต	.....
สาขาวิชา	ชีวเคมีคลินิกและอณูทางการแพทย์	ลายมือชื่อ อ.ที่ปรึกษาหลัก	.....
ปีการศึกษา	2558	ลายมือชื่อ อ.ที่ปรึกษาร่วม	.....

5476951137 : MAJOR CLINICAL BIOCHEMISTRY AND MOLECULAR MEDICINE
KEYWORDS: DIABETES MELLITUS, ALBUMIN-CORRECTED FRUCTOSAMINE VALUE, MICROFLUIDIC PAPER-BASED ANALYTICAL DEVICE, GLYCATED HAEMOGLOBIN, 3-AMINOPHENYLBORONIC ACID, EGGSHELL MEMBRANE, INTERDIGITATED MICROELECTRODE ARRAY, LABEL-FREE ELECTROCHEMICAL IMPEDANCE DETECTION, HAPTOGLOBIN, TOTAL HAEMOGLOBIN, THREE-DIMENSIONAL PAPER-BASED ELECTROCHEMICAL IMPEDANCE DEVICE, MULTIPLEX MICROFLUIDIC PLATFORM

YUWADEE BOONYASIT: Development of Membrane-based and Multiplex Microfluidic Biosensors for Detection of Diabetic Markers. ADVISOR: ASST. PROF. DR. WANIDA LAIWATTANAPAISAL, CO-ADVISOR: PROF. DR. ORAWON CHAILAPAKUL, pp.

Diabetes has the devastating impacts on the quality of life and healthcare expenditures. Thus, the further improvements on glycaemic assessment test devices have been still required for patients with diabetes, particularly in resource-limited settings. Herein, various novel analytical devices for measuring diabetic markers were proposed as trustworthy assays for glycaemic monitoring. Firstly, the colourimetric determination of fructosamine and serum albumin in whole blood samples could be performed simultaneously on the microfluidic paper-based analytical devices (μPADs), demonstrating considerable future potential for independent bedside glycaemic monitoring in diabetic individuals. Secondly, selective 3-aminophenylboronic acid (APBA)-modified eggshell membrane (ESM) and APBA-modified interdigitated gold microelectrode array (IDA) chip were constructed as specific binding components of a device for label-free electrochemical impedance spectroscopy (EIS) measurement of glycated haemoglobin (HbA1c). The APBA plays a prominent role in the selective binding of HbA1c via cis-diol interactions with a boronate-recognition group. Lastly, to combine a multiplex biomarker assay with a selective low-cost platform, the three-dimensional paper-based electrochemical impedance device (3D-PEID) and the multiplexed microfluidic system were fabricated for measuring multiple diabetic markers using a single platform in combination with a specific single-frequency impedance measurement.

Department: Clinical Chemistry
Field of Study: Clinical Biochemistry and Molecular Medicine
Academic Year: 2015

Student's Signature .....
Advisor's Signature .....
Co-Advisor's Signature .....

ACKNOWLEDGEMENTS

I owe a huge debt of gratitude to my principal advisor, Asst. Prof. Dr. Wanida Laiwattanapaisal, who has always encouraged and supported me during my study on undergraduate and graduate degrees. As a matter of fact, she is not only like a mother to me, but also a highly revered mentor. She also opens a window of opportunity for me to take further steps forward towards my academic career aspiration. I particularly wish to thank Prof. Dr. Orawon Chailapakul, my co-advisor, for providing excellent support and professional advice. With her considerable encouragement, it makes me work under her a pleasurable experience. She has always been a source of inspiration for me.

I am deeply grateful to my supervisor, Prof. Dr. Jenny Emnéus, the leader of Bioanalyitcs group at the Department of Micro- and Nanotechnology, Technical University of Denmark, who gave me a once-in-a-lifetime opportunity to spend a one-year research stay at DTU Nanotech and to attend the PolyNano PhD Summer School course. Not only did I gain the new skills and scientific knowledge during my stay at DTU, but I also augmented the network of relationships. I have found some sparkling inspiration and derived much intense pleasure over a one-year period. The project on the development of a multiplexed microfluidic platform was also conducted under the constant supervision of Assoc. Prof. Dr. Arto Heiskanen. I am very appreciative of his expert guidance and the experiences shared, which are potentially valuable. Aside from the technical expertise I acquired from him, I also gain a new perspective on the light of microfluidics.

I would like to extend my thanks to all the staff at DTU Danchip for providing the technical know-how to deal with all aspects of the state-of-the-art cleanroom facilities and microfabrication process. All my colleagues at the Department of Clinical Chemistry, Department of Chemistry, Chulalongkorn University and the Department of Micro- and Nanotechnology, Technical University of Denmark are recognised for providing the social companionship. I have found the contentment for working with these individuals. For being a part of my committees and their valuable time, I feel a deep sense of gratitude to Assoc. Prof. Dr. Rachana Santiyanont, Asst. Prof. Dr. Tewin Tencomnao, and Assoc. Prof. Dr. Weena Siangproh.

I am deeply indebted to the Thailand Research Fund through the Royal Golden Jubilee Ph.D. Program (under grant No. PHD/0164/2553), and the Graduate School, Chulalongkorn University for the Tuition Fee Scholarship.

Lastly, and with no less gratitude, I would like to express my appreciation to my parents, Pol. Lt. Col. Somkiat Boonyasit and Jamsai Boonyasit, for being supportive and encouraging. Any merit of this thesis, I wish to dedicate this work as a token of my indebtedness to my parents and all my revered mentors.

CONTENTS

Page

Page

Page

Page

LIST OF FIGURES

LIST OF TABLES

PREFACE

This dissertation is organised in a manuscript format. It consists of seven chapters: Chapter I provides an introduction and research objectives; Chapter II is published on *Bioanalysis*; Chapter III is accepted for publication in *Anal Bioanal Chem*; Chapter IV is accepted for publication in *Anal Chim Acta*; Chapter V is prepared for manuscript submission; Chapter VI introduces a multiplexed microfluidic platform for measuring multiple diabetes markers; Chapter VII presents the conclusions of this study. All the published articles are submitted in partial fulfillment of the requirements for the degree of doctor of philosophy program in clinical biochemistry and molecular medicine.

CHAPTER I

INTRODUCTION

1.1 Background and Rationale

Diabetes, one of the most challenging health problems worldwide, has become the potentially devastating impacts on the quality of life and healthcare expenditures [1]. Accordingly, the intensive monitoring of glycaemic status is really needed to avoid the worsening diabetic complications. Traditionally, the glycated serum proteins, i.e., fructosamine, glycated albumin, and glycated haemoglobin (HbA1c) have become the predominant biomarkers for the assessment of glycaemic control. HbA1c, which corresponds to the 100 to 120-day lifespan of erythrocytes, is the standard for monitoring long-term glycaemic control in clinical practice, whereas fructosamine, which has a shorter half-life than HbA1c (1-3 weeks), along with glycated albumin, has been proposed as an alternative glycaemic index for the management of diabetes in kidney dialysis patients [2-4]. The American Diabetes Association (ADA) strongly recommends maintaining tight control over the level of HbA1c, with recommended values lower than 7%, and using HbA1c as a diagnostic criterion for diabetes [5]. However, HbA1c may be affected by shortened lifespan of red blood cells, iron deficiency anaemia, and the uraemic state. Although fructosamine is not altered by haemoglobin metabolism disorders, the protein turnover disorders directly affect the fructosamine levels. Regarding diabetes-associated nephropathy cases, most patients have lower serum albumin concentrations

and higher urine albumin excretion. Therefore, routine measurement of both fructosamine and albumin to correct for variations in serum albumin concentration is recommended [6].

Currently, clinical diagnosis and follow-up are performed in the hands of professionals. In such cases, if point-of-care (POC) instruments were available, patient inconvenience and an extra visit to the clinic could be possibly avoided. Numerous approaches have been employed to quantify fructosamine, including furosine/high pressure liquid chromatography (HPLC) [7, 8], affinity chromatography [9], electrochemical techniques [10], and colourimetric methods based on thiobarbituric acid (TBA) [11] and nitroblue tetrazolium chloride (NBT) dye [12-14]. However, most of these techniques require sophisticated instruments, extensive cost, and multiple operational steps, resulting in portability difficulties for meeting clinical demands. Consequently, developing a more selective, high sensitivity, trustworthy, and portable biosensor for the measurement of diabetic markers is highly desirable. For the application of simple telemedicine in remote areas, the use of the microfluidic paper-based analytical devices (μPADs) has emerged for clinical off-site diagnoses. During recent years, μPADs coupled with optical imaging for colourimetric detection provide an affordable point-of-care platform for analysis of biomarkers such as multiplexed transaminase assay for liver function testing [15, 16], metabolic biomarkers for glycaemic control [17, 18], urinalysis assays [19, 20], and simultaneous detection of glucose, uric acid and lactate [21]. Alternatively, other detection methods for assaying multiple biomarkers on a single μPAD have been demonstrated, including electrochemical [22-27], chemiluminescence [28], and electrochemiluminescence [29] techniques, most of which relied on ultrasensitive

immunodevices for multiplexed quantification of cancer biomarkers. Such a multi-parameter point-of-care platform provides great opportunities for ubiquitous healthcare monitoring in remote areas [30, 31]. Hazardous waste that results from the use of μPAD-based bioanalytical devices can be easily disposed by incineration [32]. Therefore, if an albumin-corrected fructosamine assay based on μPADs were available, diabetic patients in low-resource settings could continuously monitor their glycaemic levels.

Considering HbA1c detection, although available methods for HbA1c analysis have been developed using a wide range of techniques including mass spectrometry [33-35], ion-exchange chromatography [36], boronate affinity chromatography [37], isoelectric focusing [38], piezoelectric sensors [39-41], chemiluminescent probes [42], immunoanalytical approaches [43-47], amperometric detection [48-50], voltammetric measurement [51-53], potentiometric method [54], EIS sensing [55-57], surface plasmon resonance [58], and surface-enhanced resonance Raman spectroscopy [59], further improvements on diagnostic POCT system are still required for clinical assessment of glycaemic status in patients with diabetes. So far no previous report in the literature exists regarding the simultaneous detection of both total haemoglobin and HbA1c based on a single affinity sensing device. A technique for selective HbA1c biosensing by means of electrochemical impedance spectroscopy (EIS) has been reported to enable the determination of HbA1c concentrations with high sensitivity [56, 60, 61], where the principle of this technique depended primarily on a self-assembled monolayer (SAM) of thiophene-3-boronic acid (T3BA) on gold electrodes. However, the dynamic detection range has yet to match the physiological range of HbA1c in real blood samples. Thus, improvements of the sensing interface

are still needed to provide an acceptable linear range for the clinical assessment of HbA1c.

Currently, EIS-based point-of-care diagnostic platforms for determining a panel of biomarkers have attracted great interest in clinical assessment of early disease detection. The biological reaction between each target and its molecular recognition element results in a unique binding frequency that is specific to each reaction. Thus, the differences in frequency signals from each reaction can be detected on a single platform due to its effective way of distinguishing binding frequencies from the others. According to this underlying principle, by immobilising recognition elements for different biomarkers on a sensor interface, each target molecule can be measured simultaneously by monitoring their optimal binding frequency, thereby making this platform suitable for assaying multiple markers in a single device. Electrochemical affinity sensors have considerable potential for developing portable analytical devices due to its sensitivity, low cost (e.g. no or minimal reagent needs), simplicity, and possibility to miniaturise [62]. For sensor applications, boronate-based ligands are now frequently used for the development of affinity sensing interfaces to capture glycosylated biomolecules, since the boronate groups are able to form reversible bonds with the *cis*-diol groups from glycated proteins under alkaline conditions [63]. This concept can be extended to the development of high-throughput and selective biosensor for distinguishing HbA1c from non-glycated haemoglobin (HbAo). Therefore, if electrochemical boronate-based approaches were on offer, it would be best suited for independent bedside HbA1c monitoring devices.

Interdigitated electrode arrays (IDAs) have emerged as an interesting aspect of improving sensitivity due to its unique electrochemical properties. Individually

addressable microelectrode arrays offer great potential for multiple analyte sensing using different microelectrodes in the array, enabling the possibility of developing into a single multiplexed biomarker sensor. Due to these distinctive characteristics, the use of IDAs as an electrochemical platform is eminently suitable for biosensor applications. Considering a low-cost platform for immobilisation, the eggshell membranes (ESMs) consisting of highly cross-linked protein fibres and cavities have attracted much attention. ESM, a naturally occurring biological polymer, has the distinct property of an interconnected porous structure, making ESM a useful biomaterial to use as a template for surface modification. The amines and amides on its surface present positively charged functional groups, which in turn can be functionalised or modified [64]. Moreover, ESM is generally available, affordable, abundant, biocompatible, and environmentally benign. Regarding the sustainable utilisation of ESM, there have been no relevant data as yet on label-free biosensing with boronate-affinity applications.

Herein, various novel analytical devices for measuring diabetic markers are proposed as trustworthy assays for glycaemic monitoring for clinical usage. Firstly, the colourimetric determination of fructosamine and serum albumin in whole blood samples could be performed simultaneously on μPADs, demonstrating considerable future potential for independent bedside glycaemic monitoring in diabetic individuals, particularly in resource-limited settings. Secondly, selective 3-aminophenylboronic acid (APBA)-modified ESM and APBA-modified IDAs were constructed as specific binding components of a device for label-free electrochemical impedance spectroscopy measurement of HbA1c. The APBA plays a prominent role in the selective binding of HbA1c via cis-diol interactions with a boronate-recognition

group. Lastly, to combine a multiplex biomarker assay with a selective low-cost platform, the three-dimensional paper-based electrochemical impedance device (3D-PEID) and the multiplexed microfluidic system were fabricated for measuring multiple diabetic markers using a single platform in combination with a specific single-frequency impedance measurement.

1.2 Research Objectives

1. To develop μPADs for simultaneous detection of serum albumin and fructosamine from whole blood samples
2. To construct a selective APBA-modified ESM for label-free electrochemical impedance measurement of HbA1c
3. To develop a single multiplexed 3D-PEID for measuring multiple diabetic markers at a specific single-frequency value
4. To demonstrate the applicability of APBA-modified IDAs chip for assaying HbA1c in patient-derived real blood samples
5. To construct a multiplexed microfluidic platform for impedimetric assaying of both the total and glycated haemoglobin levels from two independent samples measured simultaneously using a unique single-frequency value

1.3 Scope of the Study

All the manuscripts presented in this dissertation report studies concerning the development of innovative and novel analytical devices for practical applications in medicinal diagnostics. As an alternative to the existing methods for glycaemic

monitoring, the proposed affinity-based analytical devices provide a more economical, accurate, reproducible, and reliable assay for assessing the glycaemic levels in diabetic patients. Analytical performance characteristics of the proposed methods were also investigated, including linearity, detection limits, reproducibility, interferences, stability, selectivity, real sample analysis, and assay comparison. The proposed systems passed validation with patient-derived blood samples in comparison with a standard method accepted in clinical practice. Unless otherwise stated, the presented development and validation of the proposed affinity membrane-based and multiplexed microfluidic sensors for detection of diabetic markers can serve as a basis for further development of reliable point-of-care systems for glycemic control of diabetes patients.

1.4 Significance/ Implications

Up to date, the ongoing problem with the developed sensors for detection of diabetic markers is that the analytical performance of the devices has failed in terms of one or more key analytical parameters – limit of detection, range of linearity, assay reproducibility, interferences, storage stability, and validation using patient-derived real samples. In this study, the results show that the proposed affinity-based analytical devices meet the aforementioned analytical criteria. On virtue of the optimized construction of the affinity-based devices, the proposed sensor systems

- have sufficient sensitivity to determine the concentration of serum albumin, fructosamine, HbA1c, and total haemoglobin levels in real blood samples.

- have a linear range covering clinically relevant serum albumin, frutosamine, HbA1c, and total haemoglobin concentrations covering both healthy and diabetic individuals.
- provide good reproducibility for the assessment of serum albumin, fructosamine, HbA1c, and total haemoglobin levels.
- are insensitive to the presence of interferences.
- offer a long-term stability.
- are validated to suit the clinical requirements for assessing the glycaemic levels in diabetic patients.

The presented manuscripts dealing with innovative instrumental are of great interest to the fundamental knowledge in analytical science and demonstrate considerable advantages over existing methods. Indeed, the proposed analytical devices are particularly helpful for long-term glycaemic monitoring in diabetic individuals.

CHAPTER II

PUBLISHED ARTICLE

A Microfluidic Paper-based Analytical Device for the Assay of Albumin-corrected Fructosamine Values from Whole Blood Samples

Yuwadee Boonyasit[1], Wanida Laiwattanapaisal[2,*]

[1]Graduate Program in Clinical Biochemistry and Molecular Medicine, Faculty of Allied Health Sciences, Chulalongkorn University, Bangkok, 10330, Thailand

[2]Department of Clinical Chemistry, Faculty of Allied Health Sciences, Chulalongkorn University, Bangkok, 10330, Thailand

Accepted for publication in *Bioanalysis*, Vol. 7(1), pp. 79-90, 2015

2.1 Abstract

Background: A method for acquiring albumin-corrected fructosamine values from whole blood using a microfluidic paper-based analytical system that offers substantial improvement over previous methods is proposed. **Results:** The time required to quantify both serum albumin and fructosamine is shortened to 10 minutes with detection limits of 0.50 g dL^{-1} and 0.58 mM, respectively (S/N=3). The proposed system also exhibited good within-run and run-to-run reproducibility. The results of the interference study revealed that the acceptable recoveries ranged from 95.1%-106.2%. The system was compared with currently used large-scale methods (n =15), and the results demonstrated good agreement among the techniques. **Conclusion:** The microfluidic paper-based system has the potential to continuously monitor glycaemic levels in low resource settings.

Key Terms

Diabetes mellitus: A group of disorders resulting from insulin deficiency and/or insulin resistance.

Glycated serum proteins: Ketoamine formed during the non-enzymatic oxidation of serum proteins by excess circulating glucose.

Fructosamine: A glycaemic index for monitoring glycaemic status over the preceding 1-3 weeks.

Albumin-corrected fructosamine value: The fructosamine level that is corrected for variation in the serum albumin concentration.

Microfluidic paper-based analytical device: A paper-based platform that contains barriers to the transport of small volumes of fluid to multiple sites of detection via capillary action.

2.2 Introduction

Diabetes mellitus, an underlying cause of mortality and morbidity worldwide, is an increasing international health burden with pernicious effects on health-care costs and quality of life [65]. Additionally, the chronic glycosylation of serum proteins contributes substantially to secondary complications in diabetes, including arteriopathy, retinopathy, nephropathy, and neuropathy. In chronic kidney disease (CKD), approximately 44% of new end-stage renal disease (ESRD) cases have a primary diagnosis of diabetes [66]. In such cases, most patients have undergone renal replacement therapy by haemodialysis, peritoneal dialysis, or kidney transplant, all of which lead to increased health care expenditures [67]. To avoid unnecessary expense and suffering, the long-term blood glucose level of a diabetic patient should be monitored closely and should be regulated to levels found in healthy individuals. Intensive glycaemic control can reduce the risk of chronic complications, delay the progression of diabetic nephropathy, and decrease cardiovascular mortality [68, 69].

Glycated haemoglobin (HbA1c) and glycated serum proteins, such as fructosamine and glycated albumin, have become noteworthy markers for the assessment of glycaemic control, the effectiveness of therapy, and patient compliance. Traditionally, HbA1c is the standard for monitoring long-term glycaemic control in clinical practice. However, HbA1c may be an unreliable measure in kidney dialysis patients. This is because HbA1C may be affected by the shortened lifespan of red blood cells, iron deficiency anaemia, the uraemic state, an increased turnover of immature red cells due to frequent blood transfusions or the use of erythropoietin therapy. Additionally, HbA1C can be overestimated when the carbamylated haemoglobin in a patient with CKD interferes with the chromatography method,

which is based on charge-dependent assays [70]. Fructosamine, which has a shorter half-life than HbA1c (1-3 weeks), along with glycated albumin, has been proposed as an alternative glycaemic index for the management of diabetes in kidney dialysis patients [2-4]. Fructosamine originates from the spontaneous non-enzymatic glycation of serum proteins, particularly albumin, which is the most abundant protein in serum. Therefore, fructosamine is not altered by haemoglobin metabolism disorders. However, protein turnover disorders directly affect fructosamine levels. Therefore, the routine measurement of both fructosamine and albumin to correct for variations in the serum albumin concentration is recommended [6]. More recently, Mittan et al. reported that albumin-corrected fructosamine (AlbF) levels were more closely associated with morbidity than HbA1c in diabetic haemodialysis patients [8]. In general, the content of circulating serum albumin is relatively constant. However, in the diabetes-associated nephropathy cases, most patients have lower serum albumin concentrations and higher urine albumin excretion. Thus, the albumin-corrected fructosamine value can be a reliable marker for the monitoring of glycaemic levels. Fructosamine values corrected for serum albumin were also suggested to be justifiable in patients with stages 3 and 4 CKD, these patients have lower serum albumin concentrations and higher urine albumin excretion [71].

Numerous approaches have been employed to quantify fructosamine, including furosine/high pressure liquid chromatography (HPLC) [7, 8], affinity chromatography [9], electrochemical techniques [10], and colourimetric methods based on thiobarbituric acid (TBA) [11] and nitroblue tetrazolium chloride (NBT) dye [12-14]. The furosine/HPLC and affinity chromatography procedures require expensive and sophisticated instruments; therefore, they are not available for routine

use in a clinical laboratory. Under alkaline conditions, fructosamine is converted to its eneaminol tautomer, which is a chemically active reducing substance that lends itself to the electrochemical determination of fructosamine in blood samples. Other reducing agents found in serum samples, such as uric acid and ascorbic acid, can be oxidised at a similar pH and voltage as fructosamine and interfere with assay performance. Similar to other colourimetric methods of detection, the TBA assay suffers from the major drawbacks of a long analysis time and the involvement of many steps. These steps include dialysis to remove interfering endogenous glucose, thus making the TBA assay a labour- and time-intensive procedure that is not suitable for clinical practice. NBT indicator dye has gained popularity in clinical laboratories due to its fast reaction time, reproducibility, low cost, and the ease of automation. Although it is quite reasonable to perform the NBT assay and obtain an accurate interpretation at clinical levels, the liquid waste produced is strongly alkaline and pollutes the environment.

One approach to minimising the chemical waste produced by wet-chemistry methods is to implement dry-chemistry methods that utilise microfluidic paper-based analytical devices (μPADs) [72]. For the application of simple telemedicine in remote areas, the use of μPADs has emerged for clinical off-site diagnoses and for the performance of multiplexed measurements for various biochemical markers such as urinalysis assays [19, 73], liver function tests [15], tumour markers [22, 29], salivary nitrite [73, 74] uric acid [75], and the combination of glucose, lactate, and uric acid [21]. Such a multipliable point-of-care platform provides great opportunities for ubiquitous healthcare monitoring in remote areas [30, 31]. Additionally, the hazardous waste that results from the use of μPAD-based bioanalytical devices can be

easily disposed by incineration [32]. Therefore, if an albumin-corrected fructosamine assay based on μPADs were available, diabetic patients in low-resource settings could continuously monitor their glycaemic levels. As this can result in increased effectiveness in therapeutic regimens, the healthcare costs resulting from serious complications associated with hyperglycaemia can be reduced. A point-of-care testing (POCT) system, which is an enzymatic method used to determine glycated albumin levels, has been proposed. However, the POCT system requires a tremendous amount of enzyme (protease, ketoamine oxidase, and peroxidase) for a single reaction as well as a pre-analytical measurement step (blood separation) prior to the analysis [18].

In our study, colourimetric assays for the determination of both fructosamine and serum albumin in whole blood samples could be performed simultaneously in a single step on the proposed μPADs. To the best of our knowledge, the use of μPADs for the acquisition of albumin-corrected fructosamine values is reported for the first time. This process can be performed in a single step. For medical diagnosis, our system is something of a novelty. This is due to the precise and quantitative measurement of albumin-corrected fructosamine values within a clinically relevant range. Additionally, we also demonstrated a feasible solution to the problem of background colour due to real blood plasma, which can affect the measured colour intensities in paper-based analytical assays. The turnaround time required for assaying albumin-corrected fructosamine levels using the proposed μPADs was shortened to 10 minutes, making them useful for obtaining glycaemic levels near a patient's bedside. This is particularly helpful when treating patients suffering from diabetic nephropathy. In other words, the availability of a trustworthy albumin-corrected fructosamine diagnostic assay on a μPAD provides a more economical, accurate,

reproducible, reliable, and rapid platform to monitor and assess diabetic treatments of glycaemic levels for clinical use.

2.3 Experimental

2.3.1 Chemicals and reagents

The chemicals and materials used to prepare the paper-based microfluidic devices, including beeswax pellets, magnets, glass slides, and a custom-ordered iron mould, were readily available from local service providers. Blood separation paper (LF1) and Whatman No.1 filter paper were acquired from Whatman International Ltd. (Maidstone, England). A hot plate equipped with an electronic contact thermometer was manufactured by IKA® (Wilmington, NC, USA). A compact digital camera, the Casio EX-S600 (10.1 megapixels, Tokyo, Japan), was used to record the results from the paper-based microfluidic devices.

Analytical grade chemicals were used throughout this study. For the serum albumin and fructosamine assays, *p*-nitroblue tetrazolium chloride (NBT), 1-deoxy-1-morpholino-*D*-fructose (DMF), uricase from *Candida sp*., haemoglobin, human serum albumin, γ-globulins, *D*-glucose, uric acid, *L*-ascorbic acid, poly(vinylpyrrolidone) (PVP), Triton™ X-100, sodium azide, sodium chloride, potassium chloride, potassium carbonate, and potassium bicarbonate were acquired from Sigma (St. Louis, MO, USA). Brij® 35 (polyoxyethylene (23) lauryl ether detergent), succinic acid, and sodium hydroxide were obtained from Merck (Darmstadt, Germany). Bromcresol green sodium salt (BCG) was supplied by BDH chemicals (Poole, England) and bilirubin was purchased from Fluka (Buchs, Switzerland).

For method validation, commercial Cobas® kits from Roche Diagnostics (Mannheim, Germany) were assayed using Roche automated clinical chemistry analysers to determine the serum albumin and fructosamine levels in the whole blood samples based on the standard methods for BCG and NBT, respectively. To measure fructosamine, an in-house wet chemistry method based on the method described by Kruse-Jarres et al. [76] was performedusing the NBT reagent and the uricase enzyme. In this way, a direct correlation between the DMF standard and the calibrator used in the commercial kit (glycated poly-L-lysine) was established.

2.3.2 Fabrication of µPADs

The custom-ordered iron mould and a detailed description of its dimensions are illustrated in Figure 1(A). It is comprised of a blood separation zone and four circular detection areas, which are used to obtain duplicates of each assay. The designed pattern of the proposed µPAD was fabricated in a relatively simple and low-cost method using a wax-dipping process; this process can be performed in low-resource settings in developing countries, as described in our previous works [77, 78]. In this study, the following two membranes were selected to prepare the µPAD: LF-1 and Whatman No.1. Briefly, each membrane was cut to an equal size and overlapped on a glass slide with the permanent magnet underneath. The whole assembly was then overlaid with the custom-designed iron mould before being dipped into the melted wax. After being allowed to cool to room temperature, the membrane was peeled off the iron mould. A hydrophobic region was defined at the edge of membranes, which were then adhered to the backing card before use in the clinical analysis of serum albumin and fructosamine from whole blood samples. A drop (0.5 µL) of the working

BCG dye solution (2.5X, pH 4.2), modified using the method described by Doumas et al. [79], and a drop of the NBT reagent (2.5 mM NBT, 0.5 U mL^{-1} of uricase, 100 mM KCl, 2% Triton X-100, and 0.5% poly(vinylpyrrolidone), prepared in 0.1 M carbonate buffer at pH 10.3), were applied at each of two circular detection areas to quantify the amounts of serum albumin and fructosamine, respectively. As depicted in Figure 1(B), the reagent spots were subsequently allowed to dry at room temperature before the whole blood samples were dropped into the separation zone.

(A)

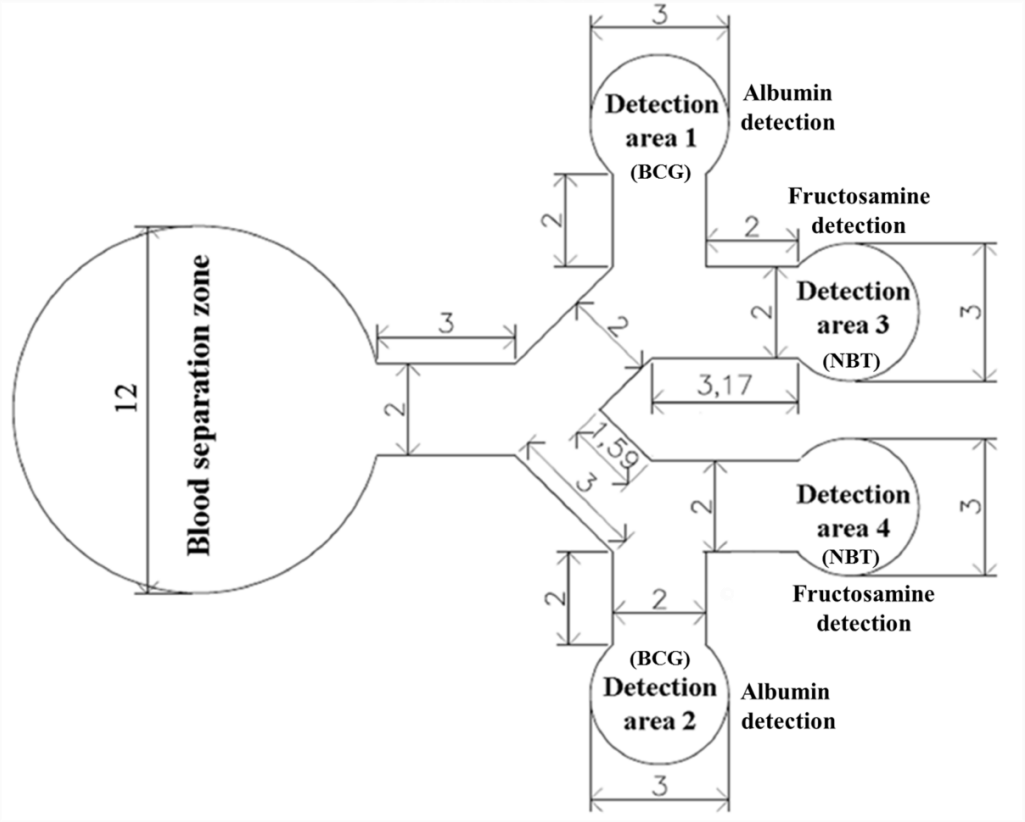

(B)

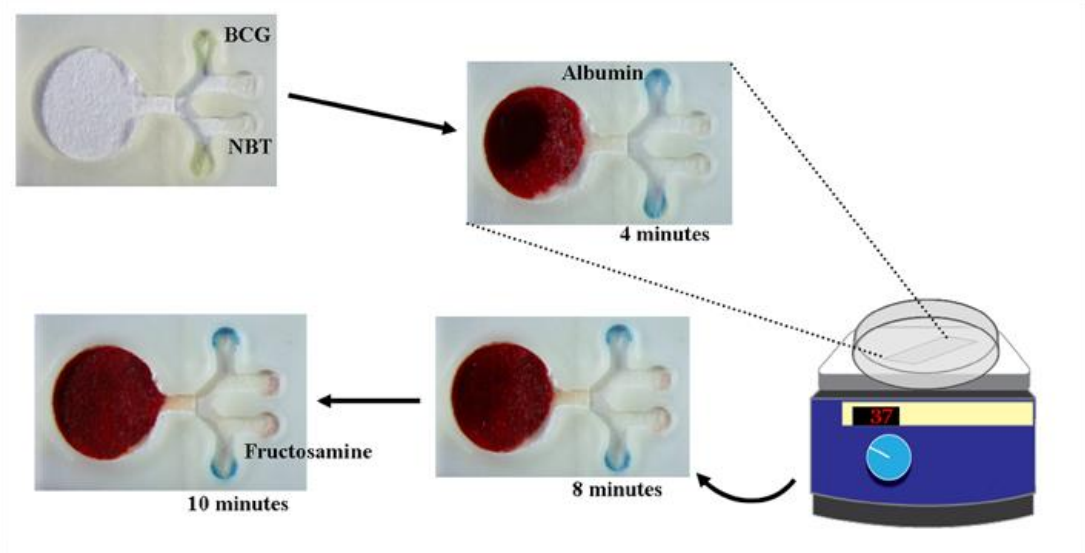

Figure 1. Schematic diagram of the proposed designed pattern illustrating (A) a detailed picture of its dimensions (mm) and (B) images of the device before and after the whole blood sample is dropped into the separation zone and upon the completion of the chemical reactions.

2.3.3 Sample preparation

Healthy volunteers and diabetes mellitus (DM) patients, as defined by the American Diabetes Association criteria [80], were enrolled in our study of their own volition. The individual participants provided written and informed consent before being enrolled in this study. Whole blood samples were drawn into vacuum blood collection tubes using K_3EDTA as an anticoagulant. To prepare the samples, a standard addition technique was used to quantify the intensity measurement of the colourimetric reaction due to the natural colour and viscosity of the plasma. Various concentrations of serum albumin and DMF dissolved in physiological saline were spiked into the whole blood samples before the clinical analysis was performed. DMF

was selected as a calibrator because it has a reducing activity similar to physiological fructosamine. The NBT principle relies on the ability of ketoamines (fructosamines) to act as reducing agents in the alkaline solution.

2.3.4 Determining albumin-corrected fructosamine levels with the proposed μPADs

When the whole blood samples contacted the proposed device, white and red blood cells were trapped at the separation membrane. Plasma was able to flow through and reach the four testing detection zones, which contained the reagents (the BCG solution and the NBT indicator dye) used to assay the levels of serum albumin and fructosamine in duplicate. The measurement of albumin is based on its binding to the indicator dye BCG at pH 4.2 to form a blue coloured complex. The intensity of the blue colour is directly proportional to the concentration of albumin in the blood sample. The complete reaction of the serum albumin occurred immediately when the plasma and the BCG dye made contact. The paper-based microfluidic device was then transferred to a 37 °C hot plate, to continuously monitor the fructosamine reaction in a series of 1-minute intervals. Fructosamines in alkaline solution form eneaminols that act as reducing agents on NBT, further reducing the dye to formazan. The rate of formazan formation is directly proportional to the fructosamine concentration. This rate is expressed as the DMF content; DMF is the synthetic ketoamine used as the primary standard. The colourimetric reaction in the detection zones was captured using a digital camera, and the grey intensity of each image was analysed using Adobe Photoshop software. The fructosamine values were corrected for the serum

albumin concentrations based on the following formula described by Lamb et al. [6]: Albumin-corrected fructosamine (AlbF) = (fructosamine (μM) x 100/albumin (gL^{-1}))

2.4 Results and Discussion

2.4.1 Optimal performance of the albumin and fructosamine assay

2.4.1.1 Reaction time optimisation

Approximately 45 μL of the spiked whole blood samples was deposited on the LF1 membrane (1.13 cm^2) and the plasma flowed through the Whatman No.1 membrane to reach the four circular detection zones within 3 to 4 minutes. In this experiment, the serum albumin-BCG and fructosamine-NBT dye complexes were continuously observed until the colour formation reached a constant signal. A digital camera was used to capture images at 1-minute intervals. The grey intensity of each digital image was measured using Adobe Photoshop software.

The preliminary results revealed that the serum albumin-BCG reaction was immediately apparent within 3 to 4 minutes, at the time when the plasma gradually came into contact with the immobilised BCG dye at both of the circular detection zones. The piece of μPAD was then transferred to the hot plate to obtain careful observations of the chemical reaction of the fructosamine-NBT dye complex at 37°C. When assays were performed with two levels of serum albumin concentrations prepared using the standard addition technique (0.25 and 0.75 g dL^{-1}), constant signals were observed 4 to 10 minutes after the spiked whole blood samples were dropped; these results are shown in Figure 2(A). Thus, the appropriate time for the albumin measurement was determined to be 4 minutes.

For the fructosamine reaction on the proposed µPAD, the magenta colour of the fructosamine-NBT complex continued to develop after the device was transferred to the 37 °C hot plate. Major changes in colour intensities occurred between 5 and 30 minutes after the whole blood samples were dropped; these results are shown in Figure 2(B). When samples with the two spiked DMF concentrations (0.25 and 0.75 mM) were assayed, the linear relationship between intensity and time was observed between 5 and 10 minutes. The sensitivity of the assay did not improve over longer periods of time. The change in intensity between 8 and 10 minutes was calculated and selected for use in further experiments. After an adequate elapsed time, an accurate fructosamine determination was accomplished by allowing the fructosamine contents in whole blood samples to interact with the NBT dye reagent.

In brief, the use of the proposed µPAD requires a shorter turnaround time. Both the fructosamine and the serum albumin levels could be determined within 10 minutes after the whole blood sample was dropped onto the proposed device.

(A)

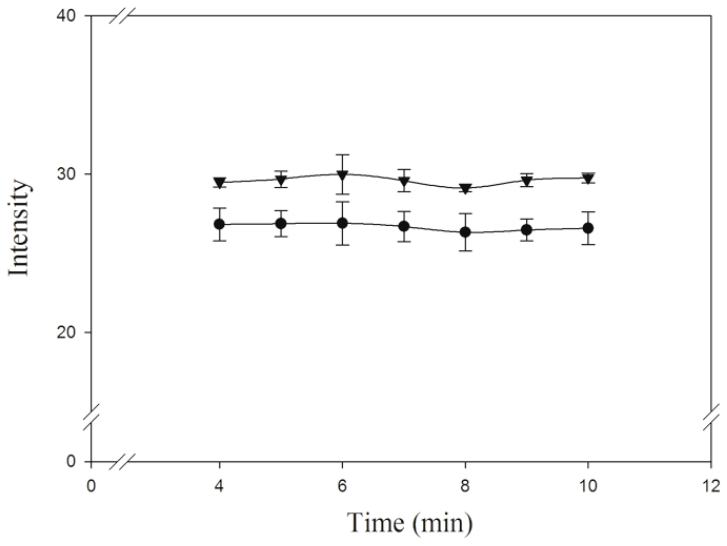

(B)

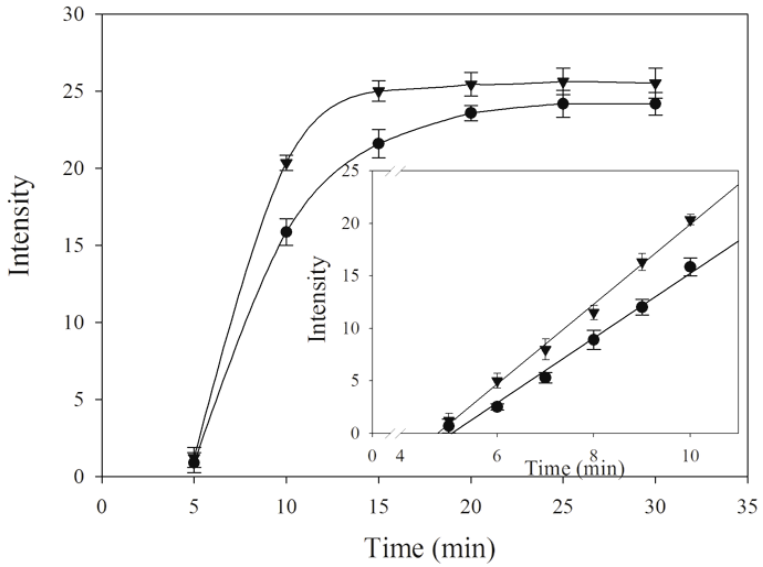

Figure 2. Experimental results from reaction time optimisation for the albumin and fructosamine assay. The plot shows colour intensity versus time points from (A) the formation of the serum albumin-BCG complex when assaying the albumin concentrations; samples spiked with (●) 0.25 g dL^{-1} and (▼) 0.75 g dL^{-1}; (B) the formation of the fructosamine-NBT complex when assaying DMF concentrations; samplesspiked with (●) 0.25 mM and (▼) 0.75 mM.

2.4.1.2 The effects of BCG and NBT concentrations

To determine the distinctive characteristics of the proposed device, the indicator dye concentration was optimised to improve clinical performance. In general, the amount of indicator reagent should be sufficient to provide a detectable and differentiable colour transition by visualisation or instrument detection. The amount of indicator dye directly affected the colour intensity and the ability of the dye to interact with the analyte of interest. Accordingly, the effect of the chromogenic

indicator dye concentration (BCG and NBT) on assay sensitivity was investigated using various spiked concentrations of the serum albumin standards (0-1 g dL^{-1}) and the DMF standards (0-1 mM). Each whole blood sample was prepared by spiking with stock solutions of serum albumin and DMF dissolved in physiological saline to desired final concentrations before the clinical analysis was performed on the proposed device in duplicate.

The signal intensity in response to the BCG concentration could not be plotted linearly against the total serum albumin concentration (a combination of the unknown concentration of serum albumin in the sample and the standard serum albumin) at concentrations of 1X, 5X, and 10X of the working BCG solution due to indistinguishable colour intensities at each level of spiked serum albumin concentration. As demonstrated in Figure 3(A), the 1X working BCG solution barely provided sufficient sensitivity to differentiate between spiked serum albumin concentrations ranging from 0 to 1 g dL^{-1}. When assaying spiked serum albumin concentrations greater than 0.5 g dL^{-1}, changes in the intensity of the instantaneous colour development significantly decreased at 5X and 10X BCG concentrations due to the plateau effect. This plateau response implied that the saturation of the BCG indicator dye with serum albumin occurred at this concentration. A 2.5X BCG solution was preferable as the standard addition plot could be linear in the concentration range of 0-1 g dL^{-1} (data not shown). The intensity values increased in direct proportion to the increasing spiked serum albumin concentrations, up to 1 g dL^{-1}.

For fructosamine measurements, the intensity responses for each spiked DMF sample were clearly distinguishable and varied linearly. Accordingly, a standard

addition graph could be plotted to compare various concentrations of the NBT indicator dye. The preliminary results demonstrated that the sensitivity of the fructosamine assay increased with increasing NBT concentration, as depicted in Figure 3(B). When assays were performed with 5 mM NBT, spiked DMF concentrations of 0.75 and 1 mM reached saturation and the assay signal did not improve. These results suggest that the use of NBT at this concentration allows for a narrow analysis range. As a consequence, an NBT concentration of 2.5 mM was selected for all subsequent experiments. This concentration allowed for the strongest sensitivity and provided an acceptable linear range. Compared with previous reports [81, 82], our proposed device was impregnated with a lower NBT concentration. Therefore, we are more closely aligned withthe concept of green chemistry as reagent consumption is markedly decreased.

(A)

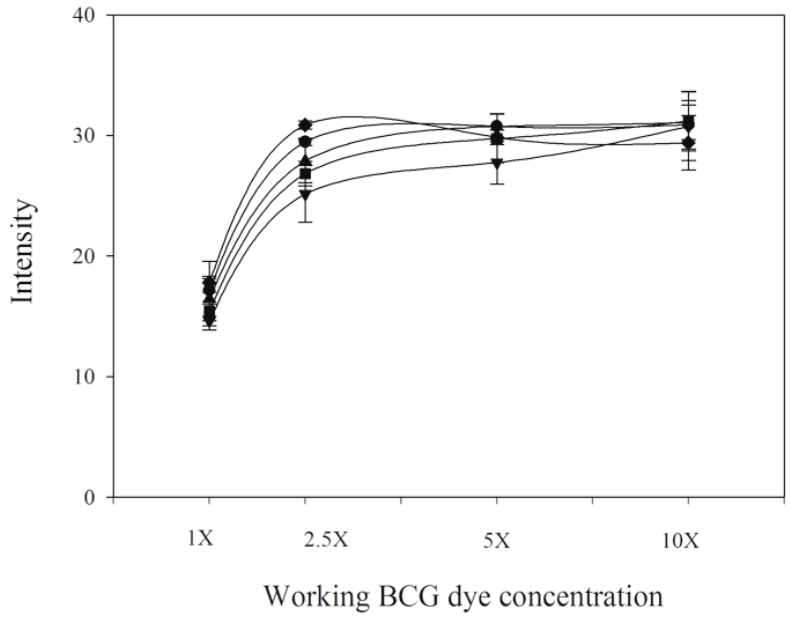

(B)

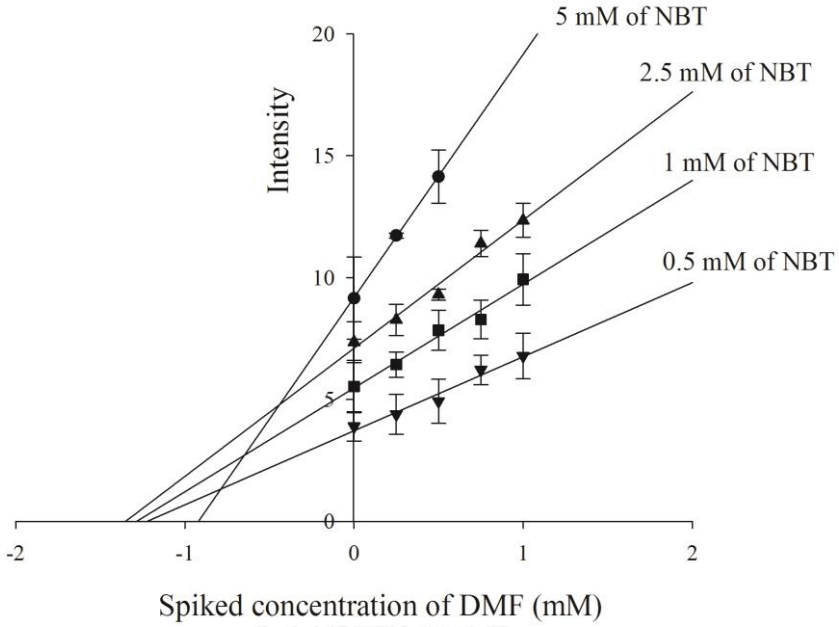

Figure 3. The effect of (A) working BCG concentrations on response signals when assaying samples spiked with the following serum albumin concentrations: (▼) 0 g dL^{-1}, (■) 0.25 g dL^{-1}, (▲) 0.5 g dL^{-1}, (●) 0.75 g dL^{-1}, and (◆) 1 g dL^{-1} albumin; and the influence of (B) the following NBT concentrations on assay sensitivity: (▼) 0.5 mM, (■) 1 mM, (▲) 2.5 mM, and (●) 5 mM NBT. Each spiked concentration of serum albumin and DMF was assayed in duplicate, and the standard deviation of the assays is depicted as an error bar.

2.4.2 Analytical characteristics

2.4.2.1 Standard addition technique

The natural straw or pale yellow colour of blood plasma can interfere with the measured colour intensities in colourimetric assays. Thus, the standard addition technique was selected for our experiments. Vella et al. also discussed the problem of

background colour with red blood cells and blood plasma, suggesting that it would be better to generate calibration curves using known amounts of analytes in whole blood samples [15]. In general, the viscosity of plasma is almost twice that of water; plasma viscosity is also frequently elevated in diabetes patients [83]. Plasma viscosity is therefore likely to influence wicking time when samples are penetrating into the porosity of each membrane compared to standard solutions or artificial blood plasma. Additionally, our preliminary results revealed that serum albumin and DMF standard solutions arrive at the four detection zones within 1 to 2 minutes of the application of each solution to the separation membrane. These findings explain why discrepancies emerged between the results obtained from standard solutions and those from the spiked whole blood samples when μPADs were used for the assays. In regards to the complex matrix of biological fluids (i.e. whole blood samples), the standard addition method should be utilized by the addition of a small volume of standard solutions to the unknown samples. In this study, small volumes of serum albumin and DMF stock solutions dissolved in physiological saline were used to spiked whole blood samples to obtain several samples at each concentration. The volumes added were small enough that the matrix compositions of the whole blood samples, including the viscosity of plasma, were not disturbed.

Under proper conditions, each reagent solution used in the albumin and fructosamine assay, i.e., a 2.5X working BCG dye solution (pH 4.2) and a NBT reagent solution with 2.5 mM NBT, 0.5 U mL^{-1} uricase, 100 mM KCl, 2% Triton X-100, and 0.5% poly(vinylpyrolidone) in 0.1 M carbonate buffer (pH 10.3), was dropped onto the circular detection areas of the proposed device and allowed to air dry before the spiked whole blood samples were applied. The poly(vinylpyrrolidone)

polymer was an optional ingredient that was incorporated into the indicator dye solution to improve colour uniformity, intensity and stability on the proposed µPADs. The instantaneous colour formation resulting from the serum albumin-BCG complex was completed after 4 minutes. The difference between the intensity of the blank BCG solution and that of the whole blood sample spiked with the serum albumin was calculated and plotted against the final concentration of the spiked serum albumin, as shown in Figure 4(A). The results revealed that the intensity response was linear up a spiked albumin concentration of 1 g dL^{-1}, with a regression equation of $y = 5.64x + 25.22$ ($r^2 = 0.996$), that projects linearity up to 6 g dL^{-1} of albumin. The negative intercept on the x-axis corresponds to the amount of serum albumin in the whole blood sample multiplied by its dilution factor, thus resulting in an albumin concentration of 4.97 g dL^{-1}.

In fructosamine-NBT reaction, the difference in the intensities of the NBT blank solution and the whole blood sample spiked with the DMF was determined over successive two-minute intervals (with a total duration of 8 to 10 minutes); the results are presented in Figure 4(B). A linear relationships was observed when the spiked DMF concentrations was between 0 to 1 mM, with correlation coefficients of 0.978; the regression equation was $y = 5.258x + 7.105$, which extended the linearity to a fructosamine concentration of 4 mM (data not shown). The intercept on the x-axis corresponds with the fructosamine level, which appeared to be 1.50 mM. When calculating the intensities of the blank solutions in each assay, the detection limits for albumin and fructosamine were found to be 0.50 g dL^{-1} and 0.58 mM, respectively. These findings suggest that the proposed devices provided sufficient sensitivity to measure albumin and fructosamine concentrations in whole blood samples and

covered the clinically relevant range of serum albumin (3.5 - 5.5 g dL^{-1}) and fructosamine (1.61 - 2.68 mM) [84]. However, each individual laboratory should determine the reference values in its own population. In comparison with the POCT system described by Yamaguchi et al., the proposed μPADs were slightly more sensitive; the μPADs also provided acceptable linear ranges for the assessment of serum albumin and fructosamine [18].

Although the standard addition technique is a relatively sophisticated method of calibration, it can reduce errors in the measured colour intensities that results from the background colour of the plasma. The standard addition technique also provides a more accurate assessment of the total reaction time, which can be affected by plasma viscosity. To further improve upon background correction, a different μPAD design should be created that introduces an additional zone for the subtraction of plasma colour and for use as a negative control (serum blank); however, such a design relies heavily on the test principle of the analyte of interest. In our point of view, the full preparation of a 5-point standard addition assay as a reagent test kit would outweigh the potential benefits of portability and ease-of-use at the point of care that such a test could provide. The albumin-corrected fructosamine measurement takes only 15 minutes if five μPADs are run in parallel with each other. For the sake of simplicity in field analysis, we investigated whether the two-point standard addition could be used in lieu of five-point assay. As shown in Table 1, results obtained from five-point and two-point standard addition spiked with 0.75 mM DMF or 1 g dL^{-1} albumin showed no statistical differences, at the 95% confidence interval with p-value = 0.089 and 0.424, respectively. Moreover, sample preparation and processing can be performed

in a single device. Such capabilities are worthwhile when used in telemedicine for quantitative off-site diagnosis.

(A)

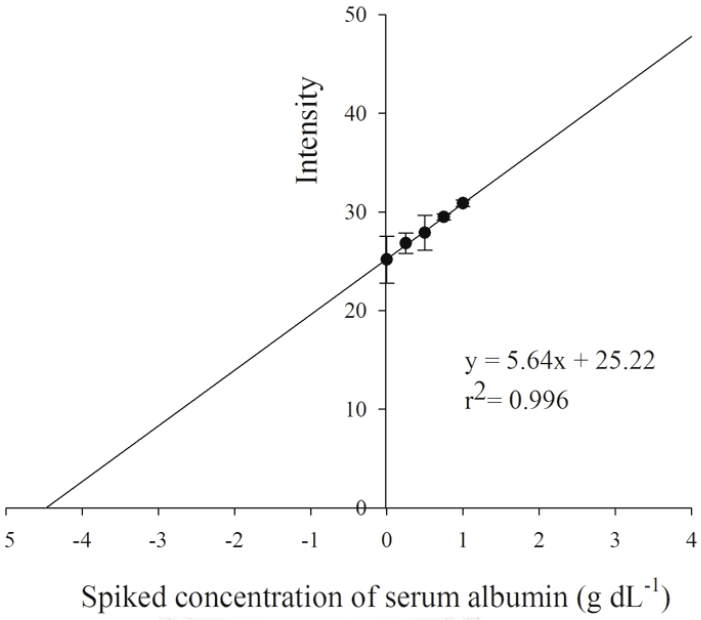

(B)

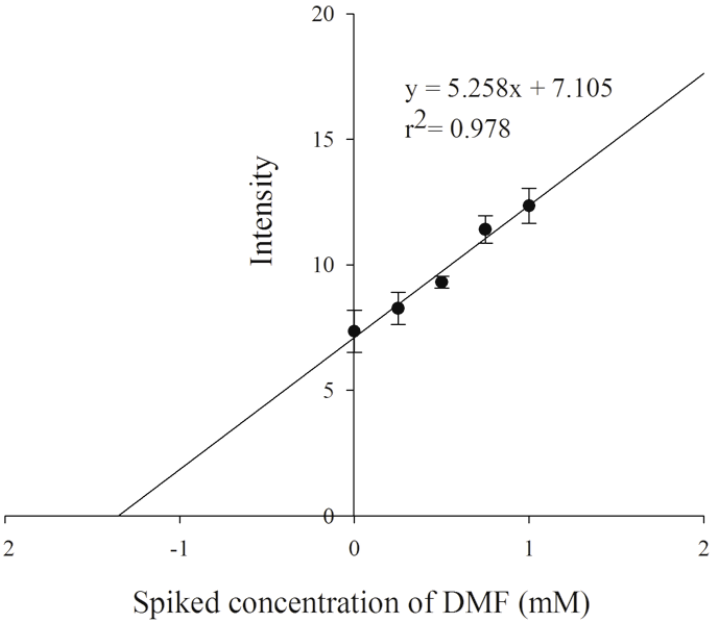

Figure 4. The standard addition technique was used to determine the quantity of (A) serum albumin and (B) fructosamine contents using the proposed microfluidic paper-based analytical devices.

Table 1. Concentrations of fructosamine and serum albumin calculated from 5-point standard addition and 2-point standard addition.

Sample No.	Fructosamine (mM)					Albumin (g dL^{-1})				
	5-point standard addition	2-point standard addition (spiked concentration, mM)				5- point standard addition	2-point standard addition (spiked concentration, g dL^{-1})			
		0.25	0. 5	0.75*	1.0		0. 25	0. 5	0.75	1.0*
1	1.50	2.24	2.09	1.51	1.63	4.38	7.38	4.63	4.50	4.62
2	1.39	1.52	1.54	1.32	1.45	4.82	3.73	4.77	4.61	4.69
3	2.11	2.19	2.22	1.93	2.19	4.66	3.31	4.40	4.37	4.49
4	1.75	6.31	3.09	1.92	2.01	4.08	6.84	4.21	4.00	4.38
5	1.94	1.68	1.85	1.75	1.96	4.66	3.52	4.59	4.24	4.60
6	1.90	1.55	1.76	1.69	1.89	4.71	3.44	4.51	4.44	4.55
7	2.70	1.65	2.03	2.30	2.55	4.82	3.73	4.77	4.61	4.69
8	2.12	2.26	2.26	1.96	2.21	4.43	3.00	4.10	3.93	4.31
9	1.69	4.16	2.27	1.79	1.89	4.72	3.46	4.53	4.45	4.56
10	2.18	2.58	2.43	2.05	2.31	4.78	3.61	4.67	4.55	4.64
11	3.02	2.42	2.47	2.87	2.93	4.27	3.06	3.91	3.81	4.20
12	1.64	3.36	2.11	1.71	1.82	4.57	3.31	4.40	4.13	4.49

13	1.46	1.98	1.95	1.45	1.58	4.26	3.04	3.89	3.80	4.18
14	1.47	2.00	1.96	1.45	1.58	4.15	7.83	4.40	4.12	4.49
15	1.79	3.76	2.64	1.89	1.98	4.39	2.90	4.01	3.87	4.25

* Indicates concentrations that showed no significance differences from 5-point standard addition based on paired t-test with 95% confidence interval (p = 0.05)

2.4.2.2 Reproducibility

To study the reproducibility of the proposed devices, whole blood samples were spiked with one of two concentrations of serum albumin standard solutions, 0.25 and 1 g dL^{-1}, and assayed for albumin content. The results revealed that the within-run reproducibility at 0.25 and 1 g dL^{-1} (n = 10) resulted in CVs of 2.43% and 2.19%, respectively. Furthermore, the run-to-run reproducibility at 0.25 and 1 g dL^{-1} was CVs of 4.26% and 3.98%, respectively; this was assessed on three consecutive days (n =30). The reproducibility of the fructosamine assay was investigated in parallel with the albumin assay. Within-run reproducibility was 2.23% and 2.08% CV, when assaying samples spiked with DMF concentrations of 0.25 mM and 1 mM, respectively. The run-to-run reproducibility was CVs of 3.84% and 3.6% when assaying samples spiked with DMF concentrations of 0.25 mM and 1 mM, respectively. These results clearly indicated that our proposed device provided good reproducibility for the assessment of serum albumin and fructosamine levels.

2.4.2.3 Interference study

An interference study was conducted to assess the effectiveness of the proposed device in the determination of serum albumin and fructosamine contents in whole blood samples. Endogenous substances present in body fluids may interfere with the colourimetric measurement of serum albumin and fructosamine; these include haemoglobin and bilirubin, which frequently interfere with chromophoric assays. Therefore, a known quantity of each interfering substance was spiked into the whole blood samples. The recovery percentage was assessed to determine how much the spiked signal increased or decreased from the initial response signals. The possible interference of ɣ-globulin in the albumin assay was also studied to evaluate the specificity of the proposed system. The tetrazolium salt dye suffers from a major drawback; other physiologically relevant active reducing agents are found in blood serum, including glucose, ascorbic acid, and uric acid, and these blood components cause nonspecific reductions in the colour indicator. Although we used uricase, an enzyme with oxidising activity in the reagent to decompose the uric acid and shorten the assay time, its interference effect was still carefully examined in parallel.

As shown in Table 2, 200 mg dL^{-1} haemoglobin impacted both assays. The resulting sample recoveries were 142.8% and 136.2% for the serum albumin and fructosamine measurements, respectively. However, the measured recoveries dropped to the satisfactory levels of 106.2% and 103.8% when the amount of haemoglobin was decreased to 100 mg dL^{-1}. Similarly, a bilirubin concentration of 1.5 mg dL^{-1} generated reasonable recovery signals of 101.7% and 99.5% for both assays. The effect of another serum protein, ɣ-globulin, at a concentration of 2000 mg dL^{-1} on the performance of the proposed device was also evaluated; the recovery value of this

protein was 105.1%. Other reducing components such as glucose and ascorbic acid, which were capable of reducing the indicator dye, had acceptable recoveries between 101.1% and 102.3%. With the expectation of eliminating the non-specifically reducing component uric acid, 0.5 U mL^{-1} of uricase enzyme was employed as an oxidising agent to remove interference. Uricase had a reasonable recovery level of 95.1% when spiked at concentrations up to 10 mg dL^{-1}. This result implied that the uricase enzyme was used at a concentration sufficient to prevent the non-specific reduction.

Table 2. The influence of various tested substances on the determination of serum albumin and fructosamine contents by the proposed system.

Added interferences	Added concentration (mg dL^{-1})	Albumin assay (%Recovery)	Fructosamine assay (%Recovery)
None	-	100	100
Haemoglobin	200	142.8	136.2
	100	106.2	103.8
Bilirubin	1.5	101.7	99.5
ɣ-Globulin	2000	105.1	-
Glucose	1000	-	101.1
Ascorbic acid	5	-	102.3
Uric acid	10	-	95.1

2.4.2.4 Assay comparison

The serum albumin and fructosamine levels of 15 samples obtained from non-diabetic and diabetic volunteers were analysed using our proposed system in parallel with the current large-scale method. To obtain albumin-corrected fructosamine values, the fructosamine levels were corrected and calculated using the formula previously described by Lamb et al. [6]. To calculate the close correlation between the DMF standard solution and the calibrator used in commercial kit, we also used an in-house NBT reagent composition based on the same principle as the large-scale Roche automatic machine. The agreement and relation between the two approaches in the measurement of albumin-corrected fructosamine values were assessed using the Bland-Altman bias plot and the Passing-Bablok regression analysis, respectively. The results revealed a reliable relationship between the proposed microfluidic paper-based analytical system and the conventional method within two standard deviation limits (± 1.96 SD). These results suggest that the two methods could be used interchangeably, as depicted in Figure 5(A). As shown in Figure 5(B), the results derived from our system and those obtained from the commercial kit were highly correlated, with a Passing-Bablok regression equation of $y = 0.9680x - 31.4271$, when the albumin-corrected fructosamine value was assayed. Based on a 95% confidence interval, the values of the y-intercept (-31.4281) and the slope (0.9680) were trustworthy and covered a range of -69.6364 to 20.0344 and 0.8638 to 1.0361, respectively. In other words, these data demonstrate good agreement between these two methods and provide an alternative approach to monitoring albumin-corrected fructosamine level in whole blood samples such that the glycaemic status in each individual can be determined.

Nevertheless, Figure 5(A) and 5(B) suggest about 10% low bias of results obtained by our new assay. This low bias could cause by the differences in platform used in our new paper-based system. Unlike conventional batch methods, it is probable that small amount of proteins could be trapped in the channels of the paper used to fabricate our device resulting in a lower amount of target analytes reaching the detection zone. In comparison with the conventional methods for determination of serum albumin and fructosamine, the bias of our assay slightly exceeds the minimum allowable total error as recommended by Westguard [85]. This finding suggests that new reference intervals of both serum albumin and fructosamine should be further reviewed and investigated to obtain a desirable specification within acceptable bias value for albumin-corrected fructosamine levels. However, this level of bias should be acceptable for a point-of-care screening assay for serum glycaemic levels.

(A)

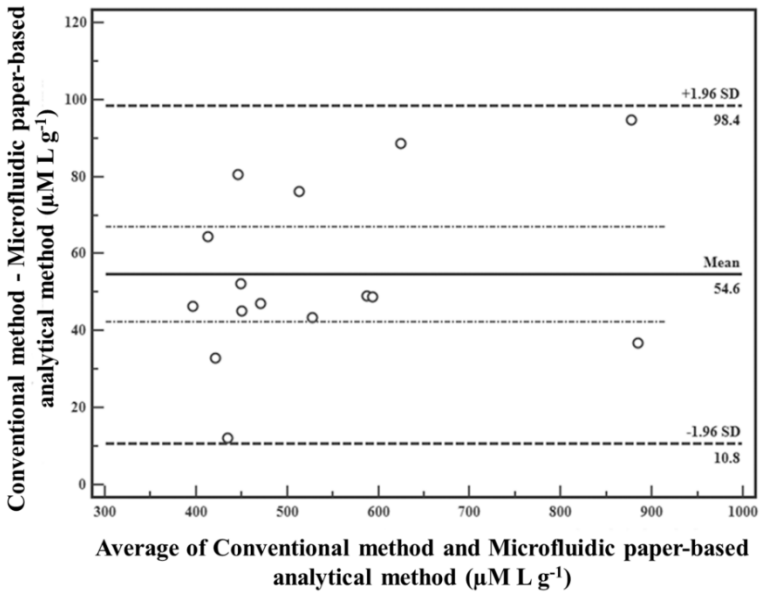

(B)

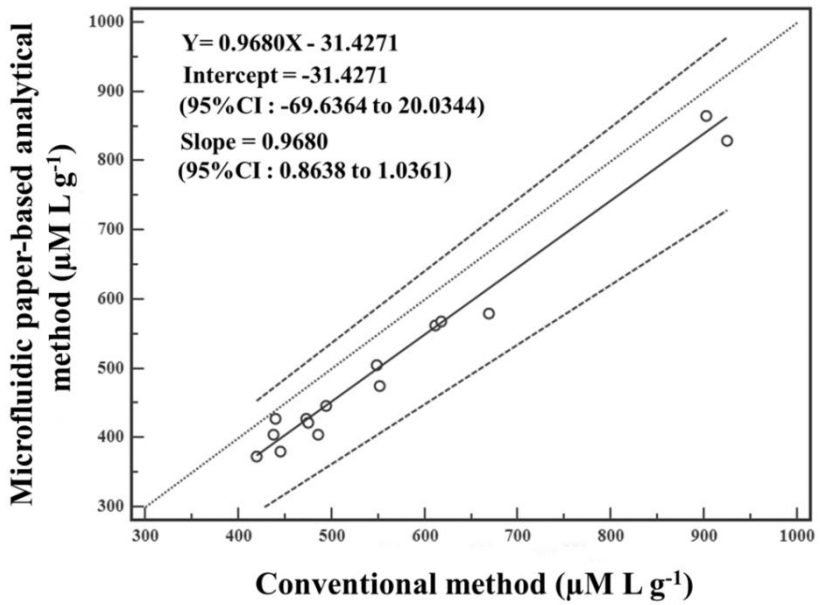

Figure 5. Comparison of the proposed microfluidic paper-based analytical device and the conventional method for albumin-corrected fructosamine measurement using (A) a Bland-Altman bias plot and (B) Passing-Bablok regression analysis.

2.5 Conclusions

As demonstrated here, the proposed μPADs provide considerable improvement in both simplicity and speed and exhibit sufficient sensitivity. The burden of the large, cumbersome machinery currently used in laboratories can also be avoided. In addition to being easy to perform, these μPADs devices provide accurate determinations at clinically significant levels. To confirm its non-specificity, the uricase enzyme was employed as part of the NBT reagent to suppress uric acid and to shorten times. Two-point measurements of changes in intensity over successive two-minute intervals (with a total duration between 8 and 10 minutes) were used to

minimise fast-reacting interferences, resulting in a more accurate and reliable assay. To enhance the uniformity, intensity and stability of the colourimetric reaction on the μPADs, poly(vinylpyrrolidone) was the hydrophilic polymer of choice. Regarding the intensity measurement, we also demonstrated that the standard addition technique could be used to subtract background colour contributed by real blood plasma; this allows for ease-of-use at the point of care. When the proposed device was used, the corrected fructosamine values for serum albumin were acquired simultaneously. These results indicate that we have made great strides in providing a reliable marker for glycaemic control in diabetes associated with chronic kidney disease, particularly for dialysis patients.

2.6 Financial and Competing Interests Disclosure

This research was financially supported by the Ratchadaphiseksomphot Endowment Fund of Chulalongkorn University (RES 560530212-HR). Y.B. acknowledges the Thailand Research Fund through the Royal Golden Jubilee Ph.D. Program (under grant No. PHD/0164/2553) and the Graduate School, Chulalongkorn University for the Tuition Fee Scholarship. The authors have no relevant affiliations or financial involvement with any organization or entity with a financial interest in or financial conflict with the subject matter or materials discussed in the manuscript apart from those disclosed. No writing assistance was utilized in the production of this manuscript.

2.7 Ethical Conduct of Research

This project was approved by the Ethics Review Committee for Research Involving Human Research Subjects, Health Sciences Group, Chulalongkorn University (ECCU) under the approval number COA No. 132/2556.

CHAPTER III

PUBLISHED ARTICLE

Selective Label-Free Electrochemical Impedance Measurement of Glycated Haemoglobin on 3-Aminophenylboronic Acid-Modified Eggshell Membranes

Yuwadee Boonyasit[1], Arto Heiskanen[2], Orawan Chailapakul[3,4], and Wanida Laiwattanapaisal[5,*]

[1] Graduate Program in Clinical Biochemistry and Molecular Medicine, Faculty of Allied Health Sciences, Chulalongkorn University, Bangkok, 10330, Thailand.

[2] Department of Micro- and Nanotechnology, Technical University of Denmark, Kgs. Lyngby, 2800, Denmark.

[3] Electrochemistry and Optical Spectroscopy Research Unit (EOSRU), Department of Chemistry, Faculty of Science, Chulalongkorn University, Bangkok, 10330, Thailand.

[4] Center of Excellence on Petrochemical and Materials Technology (PETROMAT), Chulalongkorn University, Bangkok, 10330, Thailand.

[5] Department of Clinical Chemistry, Faculty of Allied Health Sciences, Chulalongkorn University, Bangkok, 10330, Thailand.

Accepted for publication in *Anal Bioanal Chem,* Vol. 407, pp. 5287-5297, 2015

3.1 Abstract

We propose an alternative approach to long-term glycaemic monitoring that uses eggshell membranes (ESMs) as a new immobilising platform for the first time in the selective label-free electrochemical sensing of glycated haemoglobin (HbA1c), which is a vital clinical index of the glycaemic status in diabetic individuals. Due to the unique features of a novel 3-aminophenylboronic acid-modified ESM, selective binding was obtained via cis-diol interactions. Such a device provides clinical applicability as an affinity membrane-based biosensor for the identification of HbA1c over a clinically relevant range (2.3%-14%) with a detection limit of 0.19%. The proposed membrane-based biosensor also exhibited good reproducibility. When assaying normal and abnormal HbA1c levels, the within-run coefficients of variation were 1.68% and 1.83%, respectively, and the run-to-run coefficients of variation were 1.97% and 2.02%, respectively, demonstrating that this method achieved the precise and selective measurement of HbA1c. Compared with a currently used commercial method (n =15), the results demonstrated excellent agreement between the techniques, demonstrating the clinical applicability of this sensor for monitoring glycaemic control. Additionally, the low cost of this sensing platform makes using the proposed membrane-based biosensor ideal for point-of-care diagnostics.

Keywords: Glycated haemoglobin (HbA1c), diabetes mellitus, 3-aminophenyl boronic acid, eggshell membrane, membrane-based biosensor, selective label-free electrochemical detection.

3.2 Introduction

The alarming increases in mortality and health care expenditures resulting from diabetes have brought about considerable efforts to make disease-related measurements outside clinical settings, especially at a patient's bedside. High blood glucose contributes significantly towards many chronic complications, e.g., atherosclerosis, kidney failure, retinopathy, and cognitive degeneration [86, 87]. The frequent monitoring of glycaemic levels is of great importance for preventing the serious complications associated with diabetes and also for delaying the clinical progression of the disease. Traditionally, glycated haemoglobin (HbA1c) has been the predominant biomarker for the long-term assessment of glycaemic control in clinical practice. HbA1c is irreversibly formed by a slow, non-enzymatic glycation process at one or both of the N-terminal valine residues of the β-chains of haemoglobin over a long period of time, which corresponds to the average lifespan of erythrocytes in the preceding 2-3 months. The American Diabetes Association (ADA) strongly recommends maintaining tight control over the level of HbA1c, with recommended values lower than 7%, and using HbA1c as a diagnostic criterion for diabetes [5]. A quantitative measurement of HbA1c should be performed at least twice a year in patients with good glycaemic control and at least once every three months in individuals with poor glycaemic control [5].

Currently, the quantitative analysis of HbA1c is performed with a variety of analytical techniques, including electrophoresis [88], ion-exchange chromatography [36], boronate affinity chromatography [89], mass spectrometry [33-35], immunoassays[43, 44, 90, 91], electrochemical detection [48, 50, 51, 92-94], piezoelectric sensors [39-41], chemiluminescence [42], surface plasmon resonance

[58], and surface-enhanced resonance Raman spectroscopy [95]. Among these available techniques, the major drawbacks are that such methods are inevitably rather complicated and, as such, require a long time for analysis [43], the use of labelled antibodies [92], expensive equipment [39, 41], and/or sample preparation [96]; the effects of haemoglobin variants and chemically modified derivatives may also complicate these methods [88]. Although boronate affinity chromatography and mass spectrometry appear to be unaffected by interference from haemoglobin derivatives, the prohibitive cost and sophisticated instruments required make these methods unsuitable for routine clinical diagnosis [34].

Due to the unique features of boronic acid binding, this compound is of interest in developing an alternative detection method to distinguish between non-glycated haemoglobin (HbAo) and HbA1c. Boronate groups are able to form stable complexes with the diol groups from glycated proteins under alkaline conditions [63]. Consequently, a boronate derivative is a critical component of an affinity biosensor for the analysis of glycosylated biomolecules. More recently, to amplify the electrochemical signal, Song et al. proposed the competition assay between HbA1c and glucose oxidase on the boronate-modified electrode surface for HbA1c determination in whole blood samples [93]. The proposed biosensor provided a linear response covering the clinical reference range of diabetes (4.5-15%). However, in contrast to the voltammetric and amperometric methods, impedimetric measurements gain the full benefits of understanding the chemical reaction mechanisms, including electron transfer, absorption, conductance and mass transport of the redox probe [97]. Therefore, for this purpose, the use of electrochemical impedance spectroscopy for investigating chemical characteristics is highly desirable. A technique for selective

HbA1c biosensing by means of impedance spectroscopy has been previously reported to enable the determination of HbA1c concentrations with high sensitivity [56, 60, 61], where the principle of this technique depended primarily on a self-assembled monolayer (SAM) of thiophene-3-boronic acid (T3BA) on gold electrodes. However, the dynamic detection range has yet to match the physiological range of HbA1c in real blood samples (3-13 mg mL^{-1}) [40]. Thus, improvements of the sensing interface are still needed to provide an acceptable linear range for the clinical assessment of HbA1c.

Porous fibres consisting of proteins, e.g., eggshell membranes (ESMs), have attracted much attention because of the wide potential applications of these fibres as low-cost platforms for immobilisation. In previous studies on other selective microporous membranes [98, 99], the potential problems of delicate operation and high cost arose as crucial hurdles for the development of membrane-based biosensors. ESM, a naturally occurring biological polymer, has the distinct property of an interconnected porous structure, making ESM a useful biomaterial to use as a template for surface modification. ESM is generally available, affordable, abundant, biocompatible, and environmentally benign. Moreover, the amines and amides on its surface present positively charged functional groups, which in turn can be functionalised or modified [64]. Due to these properties, ESM has been employed in biomedical applications as a membrane for guided bone regeneration [100], a biological dressing to promote the infection-free healing of wounds [101], and a platform for protein immobilisation [102, 103].

Regarding the sustainable utilisation of ESM, there have been no relevant data as yet on label-free biosensing with boronate-affinity applications. Therefore, the

primary aim of this work was to investigate the possibility of using ESM as a new immobilising platform for surface modification with boronate derivatives. Such a platform can be applied to the creation an affinity-based biosensor to identify HbA1c. In this study, a novel ESM-based analytical device for the quantitative measurement of HbA1c in authentic blood samples was proposed as a great advancement in HbA1c analysis. The selective 3-aminophenylboronic acid (APBA)-modified ESM was constructed as a specific binding component of a device for the label-free electrochemical impedance spectroscopy measurement. The APBA plays a prominent role in the selective binding of HbA1c via cis-diol interactions with a boronate-recognition group. To our knowledge, no previous attempts have been made to develop ESM-based biosensors for determining HbA1c in blood samples. In other words, with the intriguing use of ESM as a new immobilising platform, this work demonstrates the development of a reliable and inexpensive device for assaying HbA1c.

3.3 Materials and Methods

3.3.1 Reagents and chemicals

For assaying HbA1c levels, a Lyphochek® HbA1c Linearity Set and Lyphochek® Diabetes Controls were purchased from BioRad Laboratories (Hercules, CA, USA). Analytical grade chemicals were used throughout this study. APBA, 4-ethylmorpholine, sodium chloride, potassium chloride, potassium hexacyanoferrate II, potassium hexacyanoferrate III, a glutaraldehyde solution (25% w/w), ethanolamine, sodium acetate trihydrate, potassium cyanide, sodium phosphate monobasic, sodium phosphate dibasic, potassium ferricyanide, sodium bicarbonate, and haemoglobin-Ao

were obtained from Sigma (St. Louis, MO, USA). Hydrochloric acid, Brij® 35 [polyoxyethylene (23) lauryl ether detergent], and acetic acid were acquired from Merck (Darmstadt, Germany). The materials used to determine the haematocrit (Hct) values, including micro-haematocrit tubes, a micro-capillary reader, and a micro-haematocrit centrifuge, were manufactured by Vitrex Medical A/S (Herlev, Denmark), International Equipment Company (Needham Heights, MA, USA), and Hawksley and Sons Ltd. (Sussex, England), respectively. A cyanmethaemoglobin standard solution was available from a local service provider. A commercial platinum screen-printed electrode was supplied by DropSens (Asturias, Spain). To determine the HbA1c levels in the whole blood samples, commercial in2it^{TM} (II) A1c test kits from Bio-Rad Laboratories (Hercules, CA, USA) were employed to validate the method based on well-established boronate affinity chromatography.

3.3.2 ESM preparation

Chicken eggs were purchased from the local supermarket and stored at 4 °C before use. The ESM is a double-layered membrane inside the eggshell composed of highly cross-linked proteins. According to the method described by F. Yeni et al. [104], to obtain the whole ESMs, eggs were soaked in absolute acetic acid at 4 °C for 18 hours, and the membrane was subsequently peeled off of the broken eggshell. Afterwards, the membranes were cleansed with a copious amount of deionised water before cutting into circles with a diameter of approximately 13 mm. The circular ESMs were stored in a 10 mM 4-ethylmorpholine buffer containing 0.25 M KCl and 0.1 M NaCl until further use.

To characterise the microstructure of the ESM with and without the immobilised HbA1c, a scanning electron microscope (JSM-5410LV, JEOL, Tokyo, Japan) and transmission electron microscope (TEM-2100, JEOL, Tokyo, Japan) were used to study the surface and internal structure of the ESMs. For scanning electron microscopy (SEM), the dried circular membranes were placed on a specimen stub and coated with a thin layer of gold before analysis. To prepare the ESMs for transmission electron microscopy (TEM), the membranes were initially fixed with a 2.5% (w/w) glutaraldehyde solution and 1% (w/v) osmium tetroxide before being dehydrated with a series of washes with ethanol at concentrations ranging from 35% to 95%. The membranes were further immersed in propylene oxide, embedded in an epoxy resin solution, dried, and then cut to 90-nm thickness using an ultramicrotome before being placed on a copper grid. Finally, to increase the contrast level of the image, the membranes were stained with uranyl acetate and lead citrate before the TEM investigation.

3.3.3 Label-free electrochemical impedance spectroscopy system set-up

The label-free electrochemical impedance spectroscopy measurement was carried out with a potentiostat/galvanostat instrument (Autolab PGSTAT30, Eco Chemie, The Netherlands) equipped with the Frequency Response Analyser system software. In this study, the impedance detection system was connected to a commercial platinum screen-printed electrode (DropSens, Asturias, Spain) for the selective electrochemical sensing of HbA1c. This new configuration is illustrated in Figure 5(A). A circle-sized APBA-modified ESM (13 mm) was positioned on the platinum screen-printed electrode surface covering all of three electrodes, consisting

of counter (CE), working (WE), and reference electrodes (RE). The membrane was carefully placed over the electrode to prevent the formation of air bubbles between both layers. The whole assembly, i.e., an integrated electrode with a thin layer of ESM, an O-ring, and a custom-ordered holder, was clamped together through magnetic force. The electronic connections were accomplished by a customised designed electronic connector. The impedance measurement was conducted over a frequency range of 100 kHz to 10 mHz with an alternating-current amplitude of 10 mV. The redox ions, i.e., a 5 mM $Fe(CN)_6^{3-/4-}$ solution containing 0.25 M KCl and 0.1 M NaCl dissolved in 10 mM 4-ethylmorpholine buffer, were prepared and used as an electroactive probe throughout the experiment. The impedance data were fitted to an equivalent-circuit model using the NOVA 1.9 software.

3.3.4 Surface modification with APBA

Unless otherwise stated, for fabrication of the APBA-modified ESM, a drop of glutaraldehyde solution was placed on the surface of the membrane, which was then thoroughly washed with 10 mM 4-ethylmorpholine buffer before the addition of 2.5 mg mL^{-1} of APBA. The excess aldehyde groups were subsequently removed by rinsing with 10 mM ethanolamine followed by an additional wash. Finally, various concentrations of HbA1c were used to investigate whether HbA1c could bind to the selective sensing surface via cis-diol interactions. Each consecutive step was carried out on the same piece of platinum screen-printed electrode with the use of the electroactive redox probe. The electrochemical impedance spectroscopy measurement was conducted in a step-wise manner. The APBA-modified ESMs could be used repeatedly after washing with a regeneration buffer, 10 mM sodium acetate at pH 5,

which reversed the HbA1c binding reaction. A sodium acetate buffer could be used to remove HbA1c from the APBA-modified membranes because the binding of boronate groups with diol groups has been shown to be quite unstable under acidic conditions [105].

Glutaraldehyde was used as a coupling agent and served as a homo-bifunctional crosslinker between the amine moiety of APBA and the amine groups on the surface of the ESM, as depicted in Figure 5(B). The aldehyde group is expected to attach to the amine group of APBA. Afterwards, any remaining aldehyde groups were then blocked with the ethanolamine buffer. In such a case, the specific binding between the boronic acid groups and HbA1c occurs via cis-diol interactions.

(A)

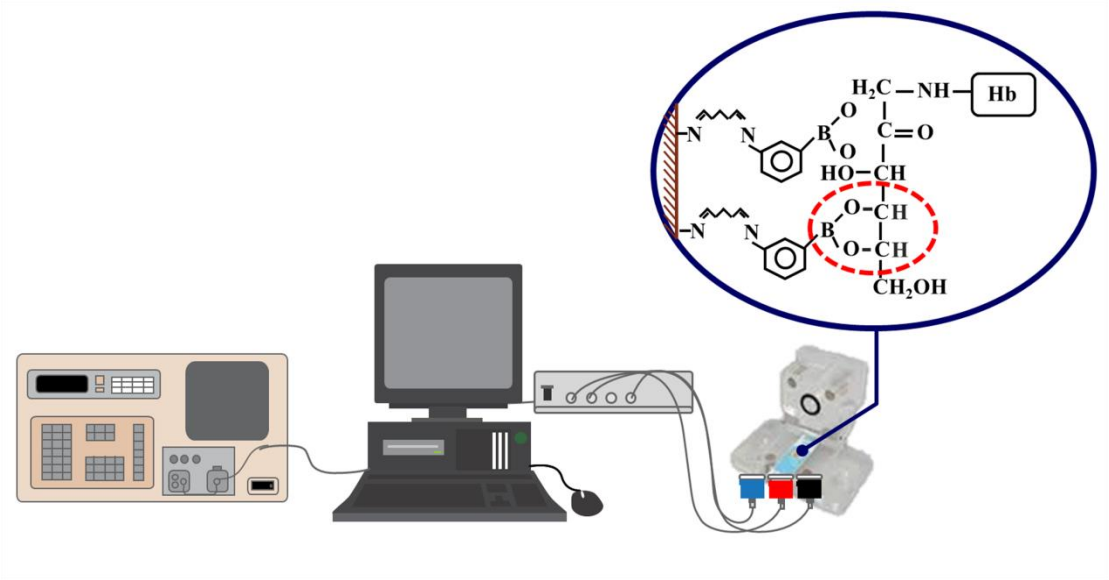

(B)

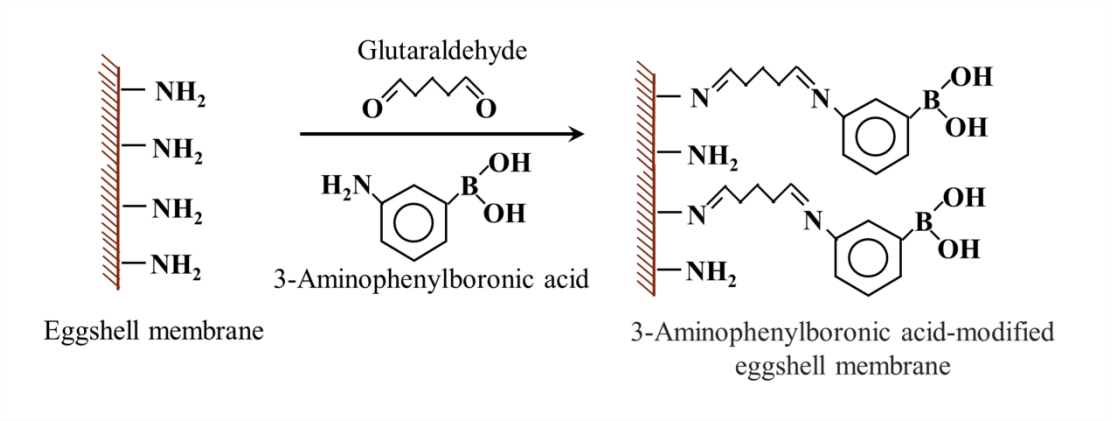

Figure 6. Schematic diagram of the proposed ESM-based biosensor illustrating (A) a configuration of the label-free electrochemical impedance system set-up and (B) a reaction scheme for immobilising APBA on the surface of ESMs.

3.3.5 Sample preparation

Healthy participants and diabetic patients, as defined by the American Diabetes Association criteria [80], volunteered to take part in our study. Written informed consent was obtained from all the individuals before the study began. The project regarding the development of membrane-based biosensors was approved by the Ethics Review Committee for Research Involving Human Research Subjects, Health Sciences Group, Chulalongkorn University (ECCU) under approval number COA No. 057/2557. Whole blood samples were collected in vacuum blood collection tubes using tripotassium ethylenediaminetetraacetic acid (K_3EDTA) as an anticoagulant. The Hct and total haemoglobin (Hb) were quantified using the micro-capillary and cyanmethaemoglobin methods (Drabkin's reagent), respectively. After measuring the Hct and total Hb, centrifugation was used to separate the plasma from cells, and then the plasma was discarded to eliminate glucose and other glycated

proteins existing in the plasma. The red blood cells remaining were carefully washed three times with physiological saline (a 0.9% sodium chloride solution) to remove the plasma completely. To prepare the red blood cell lysates, a haemolysing buffer solution (26 mM NaH_2PO_4, 7.4 mM Na_2HPO_4, and 13.5 mM KCN), as prepared according to a previous study [48], was used to lyse the red blood cells prior to the electrochemical impedance measurement.

3.4 Results and Discussion

3.4.1 Surface characterisation of the ESM

The ESM, a thin film adhering inside the eggshell, is composed of three thin membranes, namely, the outer ESM, inner ESM, and limiting membrane, from outside to inside [106]. In our study, the entire ESM was used as a sheet membrane, and the membrane surface that contacts the shell was called the outer surface, whereas the opposite surface was called the inner surface. Figure 7 displays scanning electron micrographs (Panels A-D) and transmission electron micrographs (Panels E-F) of ESMs with and without the immobilised red blood cell lysates. The surface structure was found to be different side of an ESM, as shown in Figure 7(A). The total thickness of the ESM was approximately 60-70 μm, which is in agreement with the work of Takiguchi et al. [107]. A network-like structure was observed on the ESM surface [Figure 7(B)], indicating that the ESM consisted of highly cross-linked protein fibres and cavities. The fibres of the inner layer were smaller and smoother than those of the outer layer [Figure 7(C)]. After the immobilisation of APBA, the red blood cell lysates were able to adhere to the surface of the ESM, as depicted in Figure 7(D). Our analysis indicated that the red blood cell lysates were successfully immobilised on the

surface of the ESM. Figure 7(E) presents the TEM micrograph showing that the membrane fibres are 1-4 μm in diameter and separated by extra-fibre spaces. Each fibre consists of a collagen-rich core that is surrounded by a glycoprotein-rich mantle [108]. The internal cavity of the ESM was occupied by HbA1c after exposure to the red blood cell lysates [Figure 7(F)]. These results implied that some components of the red blood cell lysates attached to the surface of the ESM, while other components entered into the interlacing network of ESM fibres.

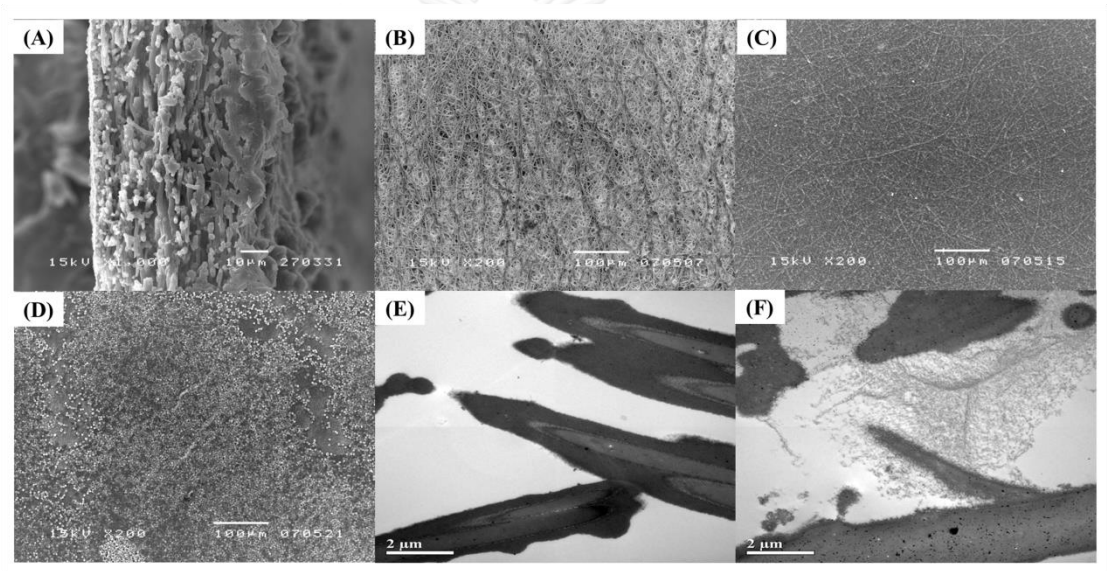

Figure 7. SEM images of the ESM: (A) cross-section, (B) outer surface, (C) inner surface, (D) after exposure to HbA1c; and TEM images of ESM: (E) membrane fibres consisting of a collagen-rich core surrounded by a mantle layer and extra-fibre spaces, (F) after exposure to HbA1c.

3.4.2 Optimisation of the HbA1c assay

3.4.2.1 Effect of pH

The effect of pH has been widely perceived to be the most crucial factor for affinity binding between HbA1c and the boronate groups. In general, under alkaline conditions, boronic acid is transformed to its tetrahedral anionic form, which subsequently reacts with the diol group of a glycated protein to form a cyclic ester. A pH above the pK_a value of APBA is typically considered optimal for this reaction; however, it has been suggested that determining the optimum pH for binding is not this simple [109]. Therefore, in this study, the effect of pH on binding was investigated with a 10 mM 4-ethylmorpholine buffer solution containing 0.25 M KCl and 0.1 M NaCl to maintain the pH at 8, 8.5, 9, or 9.5. As shown in Figure 8, the normalized ratio of stimulated resistance plotted against the HbA1c concentration was greatly impacted by pH. The results revealed that the sensitivity of the HbA1c assay increased with increasing pH. Although the binding of HbA1c to the boronate complexes at pH 9.5 provided the highest sensitivity, this pH was disregarded due to the narrow linearity also obtained at this pH. Furthermore, under extremely alkaline conditions, the tertiary and quaternary structures of glycated proteins would be subject to denaturation. Thus, a pH of 8.5 was instead selected for all subsequent experiments because this pH provided a wider linear range that extended to 14% HbA1c. At pH values close to the pK_a of APBA, the boronate group is expected to exist in an anionic form, which is able to bind specifically with a diol to form the boronate ester. Similarly, Přibyl et al. also suggested that a pH above 8 can generally be accepted as an optimum condition [41].

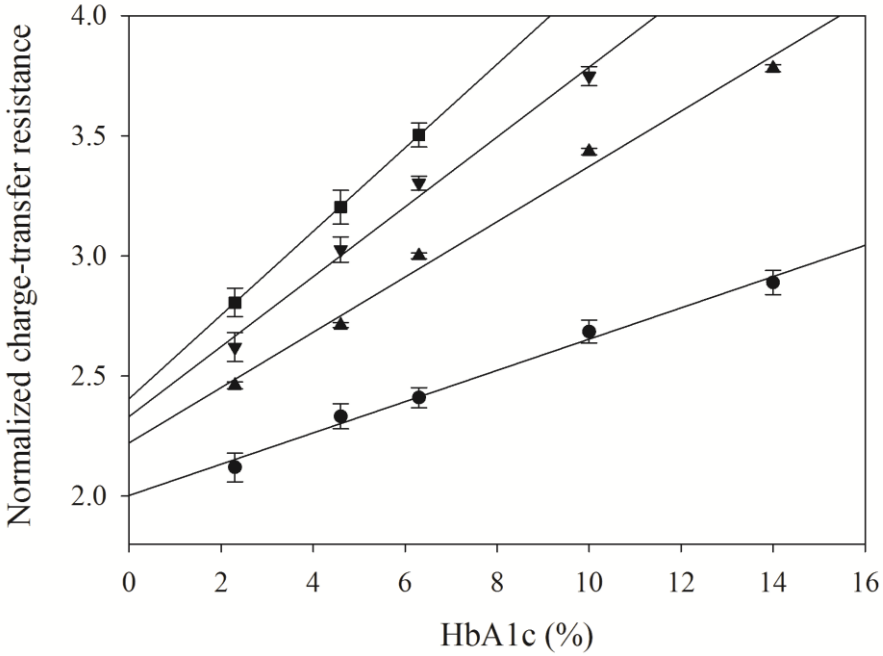

Figure 8. The effect of pH on HbA1c binding; (●) pH 8, (▲) pH 8.5, (▼) pH 9, and (■) pH 9.5.

3.4.2.2 Effects of glutaraldehyde and APBA concentrations

In our system, the glutaraldehyde solution was used as a cross-linking agent to achieve covalent bonding between the amino groups of the ESMs and amine functional groups of APBA. Two levels of an HbA1c standard solution were employed to investigate the effect of glutaraldehyde concentration on the impedance signal response of the APBA-modified ESMs at a concentration of 0.25 mg mL^{-1} APBA. After 5 minutes of glutaraldehyde immobilisation, when normal and high levels of HbA1c were assayed, the impedance response of the membrane-based biosensor increased with increasing concentrations of glutaraldehyde, as depicted in Figure 9(A). Hence, a 25% (w/w) glutaraldehyde solution was the optimum condition

and was selected for all subsequent experiments. In comparison, when using ESM as an enzyme immobilisation platform, higher glutaraldehyde concentrations lead to a decrease in the sensitivity of the biosensor due to the denaturation of the enzyme. In general, a 2.5% (w/w) glutaraldehyde solution has been chosen as the optimal cross-linking agent for enzyme immobilisation; however, the immobilisation normally occurs over a prolonged period ranging from 30 minutes to 8 hours, permitting long-term contact of the enzymes with glutaraldehyde [110-112]. In contrast, the method of choice in this study involved an immobilisation strategy that utilised a higher concentration of glutaraldehyde and a short contact time. This approach is not without precedent because several instances of using high concentrations of glutaraldehyde have been reported in the literature [113-115].

The concentration of APBA was also a relevant factor that directly affected the binding of HbA1c to the ESM-based biosensor. The signal response increased with an increasing concentration of APBA, as depicted in Figure 9(B). However, when the concentration of APBA was higher than 0.25 mg mL^{-1}, the response reached a maximum value, indicating that the amount of APBA had achieved equilibrium. Thus, 0.25 mg mL^{-1} of APBA was used for all subsequent experiments.

(A)

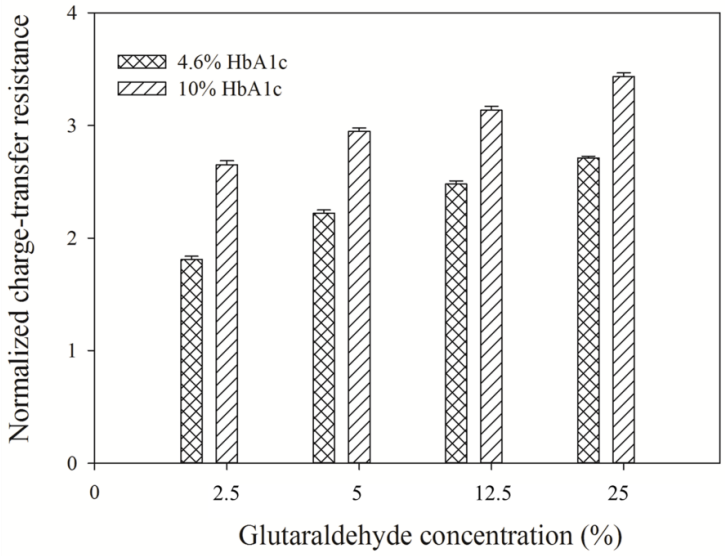

(B)

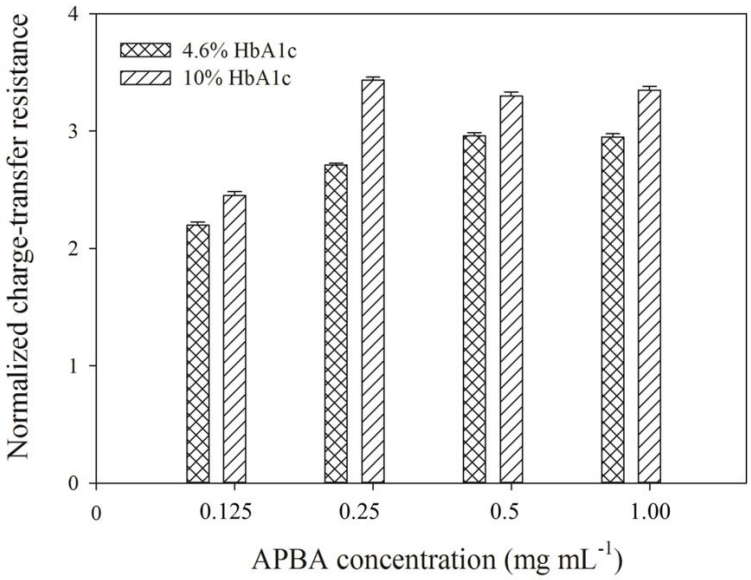

Figure 9. Optimisation parameters regarding (A) glutaraldehyde concentration and (B) APBA concentration.

3.4.2.3 Effect of incubation time

Alteration of the times for the APBA and HbA1c immobilisations on the ESMs could affect the amount of immobilised boronic acid functional groups and HbA1c molecules, respectively, on the surface of the ESMs, which are in direct proportion to the sensitivity of the membrane-based sensors. Thus, the effect on HbA1c detection on APBA immobilisation times from 10 to 40 minutes was also investigated (Figure 10(A)). When assaying 2 levels of HbA1c with 0.25 mg mL^{-1} of APBA, the impedance signal increased gradually as the immobilisation time increased from 10 to 20 minutes, and the signal reached a steady state after 20 minutes of incubation. Therefore, the optimum immobilisation time for APBA was determined to be 20 minutes. Figure 10(B) illustrates the effect of HbA1c immobilisation time on the impedance signal obtained from the APBA-modified ESM. In this case, when assaying 2 levels of HbA1c, the signal response increased with an increasing incubation time and approached the maximum value after 15 minutes. Thus, considering a compromise between the signal response and analysis time, a 15-minute incubation time was used throughout our studies.

(A)

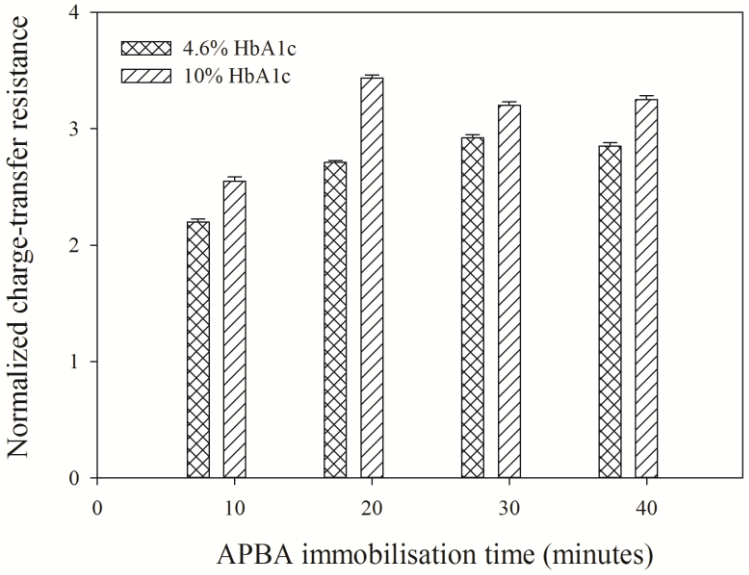

(B)

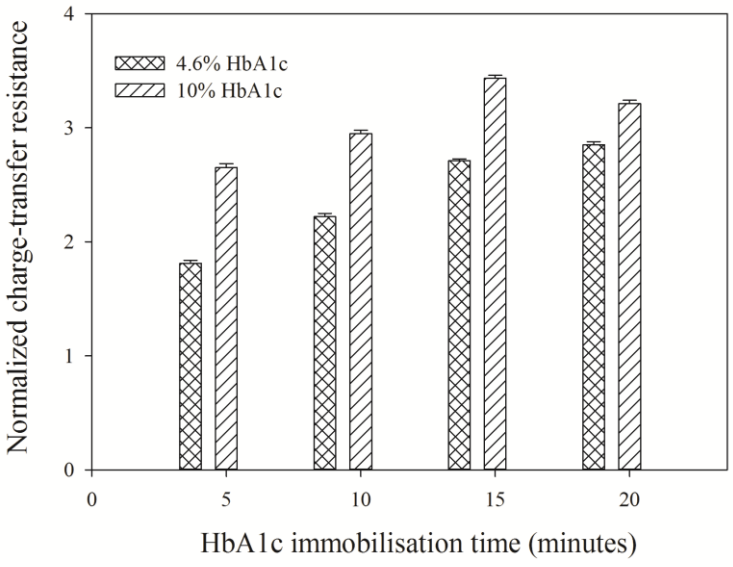

Figure 10. Optimisation parameters regarding (A) immobilisation time with 0.25 mg mL^{-1} of APBA and (B) HbA1c immobilisation time assayed on the proposed membrane-based biosensor.

3.4.3 Analytical characteristics

3.4.3.1 EIS characterisation of the sensing interface

One of the distinctive features of ESM is that its structure is composed of an intricate lattice meshwork of large and small fibres interlocking with each other, and the ESM surface is expected to contain reactive functional groups, i.e., amines and amides, that are expected to react with APBA via the glutaraldehyde coupling agent. In our study, the inner surface of the ESM was subjected to step-wise boronate modifications with a platinum screen-printed electrode underneath. Label-free electrochemical impedance measurements were subsequently performed following each step of the surface modification. Figure 11 shows Nyquist plots for the kinetic redox process, using $[Fe(CN)_6]^{3-/4-}$ as an electroactive probe, on a bare platinum screen-printed electrode, and on the ESM, glutaraldehyde-activated ESM, and APBA-modified ESM. Compared to the impedance data obtained from a bare electrode, a 2-fold increase in the charge-transfer resistance (Rct) was observed when the membrane was placed on the electrode. This evidence implies that the fibrous ESM immobilised on the surface of the platinum electrode was blocking redox species movement. When the glutaraldehyde solution was applied, the curve broadened significantly, indicating a dramatic increase in resistance. Surprisingly, when the glutaraldehyde-activated ESM was further modified with APBA, the Rct significantly decreased, indicating neutralisation of the negative charges of the redox probes. The observed decrease in the Rct may result from the almost neutral net charge of APBA in a buffer with a pH close to the pK_a of APBA. In addition, APBA may directly bind to the surface of the ESM because the network of protein fibres in this type of membrane is composed of a collagen-rich core and a glycoprotein-rich mantle [116]. To investigate whether the

impedance changes were due to the resistance of the membrane, a control experiment was also performed using the screen-printed electrode without ESM prepared in the same manner as the electrode in the proposed system. Nyquist plots for the stepwise modification of screen-printed electrodes are shown in Figure 12. The impedance response obtained from the glutaraldehyde-treated electrode was significantly decreased compared to that obtained from the bare electrode. Additionally, the glutaraldehyde-treated electrode was not responsive to the 0.25 mg mL^{-1} APBA. The impedance signals of the APBA-modified electrode were not in direct proportion to the various concentrations of HbA1c, implying that the changes in impedance of the proposed membrane-based system were due to the resistance of the membrane.

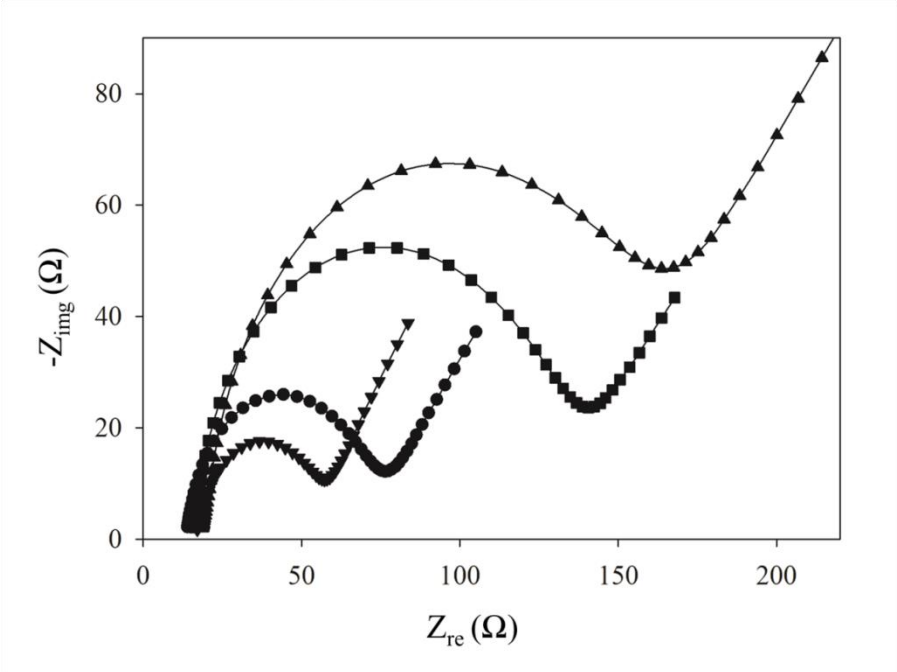

Figure 11. Nyquist plots for the stepwise analysis of the (●) bare electrode, (■) ESM, (▲) glutaraldehyde treated-ESM, and (▼) APBA-modified ESM surface in the presence of a 5 mM $Fe(CN)_6^{3-/4-}$ redox probe in 10 mM 4-ethylmorpholine buffer (pH 8.5).

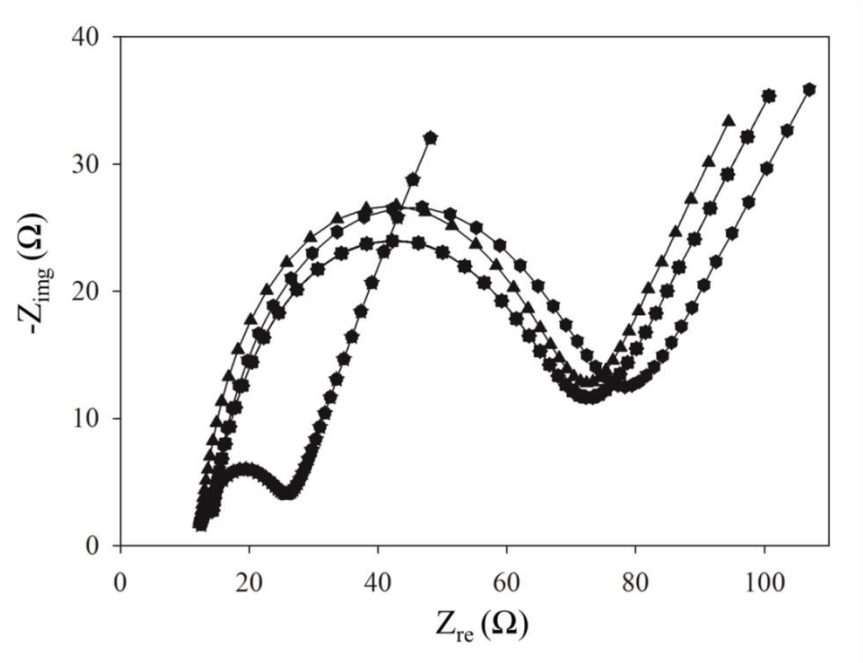

Figure 12. Nyquist plots for the step-wise modification of the screen-printed electrodes without ESM for HbA1c biosensing: (✕) bare elctrode, (●) glutaraldehyde-treated electrode, (★) 0.25 mg mL^{-1} APBA, (■) 2.3% HbA1c, (▲) 4.6% HbA1c, (▼) 6.3% HbA1c, (◆) 10% HbA1c, and (⬢) 14% HbA1c.

3.4.3.2 Calibration curve for the detection of HbA1c

The differential change in impedance with increasing HbA1c concentrations is clearly indicated in the Nyquist plot, as depicted in Figure 13(A). After exposure to the HbA1c, the Rct was significantly increased due to the ability of HbA1c to interact with APBA on the modified ESM and thus hinder the movement of redox species to the platinum electrode surface below the ESM. A control experiment was also carried out using an ESM without immobilised APBA, which was prepared in a manner similar to the proposed system. The impedance signal response towards HbA1c over the concentration range of 2.3% to 14% remained unchanged compared to the

baseline signal of the ESM (Figure 14). This result confirmed that the impedance signal arose from the specific binding between the APBA-modified ESM and HbA1c via cis-diol interactions. Additionally, as shown in Figure 13(B), a significant phase shift was observed after attachment of the HbA1c, and a less obvious change occurred with increasing concentrations of HbA1c. Dramatic changes in impedance were noticed at the lower frequency ranges [Figure 13(C)], thereby demonstrating the sensitive response of the APBA-modified ESM towards HbA1c.

The impedance data are satisfactorily described by the behaviour of a system with the equivalent circuit shown in Figure 13(D) (inset), which comprises a series of two constant-phase elements (CPEs) in parallel with two resistances (Rp) and the Warburg impedance element (W), along with the solution resistance (Rs). The good fitting results are shown in Figure 15. In this model, Rs corresponds primarily to the resistance of the electrolyte solution, whereas Rp1 and Rp2 are the Rct values that correspond to the membrane resistance and charge-transfer kinetics at the platinum screen-printed electrode, respectively. A CPE is used to describe the non-Faradic process at the membrane-solution and electrode-solution layers. The CPE is defined as $Z_{CPE}= (A\omega)^{-\alpha}$, where A is a proportionality factor, ω is the angular factor, and α is an exponential term with a value between 0 and 1. When the value of α is equal to 1, the CPE acts as a pure capacitor [97]. Based on the results of fitting the electrochemical impedance data to this equivalent circuit, an increase in the membrane resistance Rp1 response is observed in the presence of increasing HbA1c concentrations. These results implied that the immobilised HbA1c could fully occupy the porous network of the ESM; therefore, the electroactive probe was not accessible to the surface of the platinum electrode, resulting in an increase in the Rct. The rate

constant for the Faradic reaction of $[Fe(CN)_6]^{3-/4-}$, an electroactive probe, has been described using the electrochemical basis of the Rct, as indicated in the following equation [117]: $Rct = RT/(n^2F^2Ak^0_{app}C)$ where R is the gas constant, T is the temperature, n is the number of electrons transferred, F is the Faraday constant, A is the electrode area, k^0_{app} is the rate constant of the redox process, and C is the concentration of the redox species. In our proposed system, the electrode surface area (A) and the rate of the redox process (k^0_{app}) can be altered by the stepwise modification process.

The normalised ratio of the resistances derived from the fitted resistance values was plotted versus the various concentrations of HbA1c, as illustrated in Figure 13(D). The results revealed that the normalised response was linear up to 14% of HbA1c, with a regression equation of $y = 0.1151x + 2.2216$ ($r^2 = 0.990$). The detection limit, defined by a signal-to-noise ratio of 3, was found to be 0.19%, a slightly higher sensitivity than that described by Kim et al. [48]. These findings suggest that the proposed system provides sufficient sensitivity to measure the concentration of HbA1c within the required clinically relevant range of HbA1c, where 4–6% is considered normal and covers the clinical reference range of diabetes (6.5-15%) [5]. Compared with other electrochemical impedance measurements of HbA1c, the proposed membrane-based biosensor provides a wider linear range for assaying HbA1c [56, 60, 61]. ESM has a distinctive property. The higher the porous fibres, the higher the immobilisation surface areas, is available for boronate-binding sites. Hence, the high surface density of the available boronate groups increases the sensitivity and linearity of the proposed biosensor. With the proposed ESM biosensor, samples can be directly tested without requiring additional sample dilution steps and

avoiding pipetting errors. In addition, this label-free affinity platform provides us with a better understanding of interfacial sensing mechanisms and a great tool for glycaemic monitoring in diabetic patients, especially those in developing countries. A favourable comparison of the analytical characteristics for HbA1c determination using boronate-based electrochemical methods is provided in greater detail in Table 5. Importantly, according to the standard interpretation norms of HbA1c in clinical practice, the HbA1c concentration should be expressed as the percentage of total haemoglobin (i.e., mmol mol^{-1} or %). Thus, in our studies, the HbA1c haemolysate standards (% HbA1c), which are currently used for commercial instruments, were selected as being representative of real clinical samples. As demonstrated here, the proposed membrane-based system leads to a substantial improvement in the dynamic detection range of HbA1c (up to 14%) and also exhibits excellent sensitivity. Such capabilities make this method useful for real sample analysis and for assessing the glycaemic levels for clinical diagnosis.

(A)

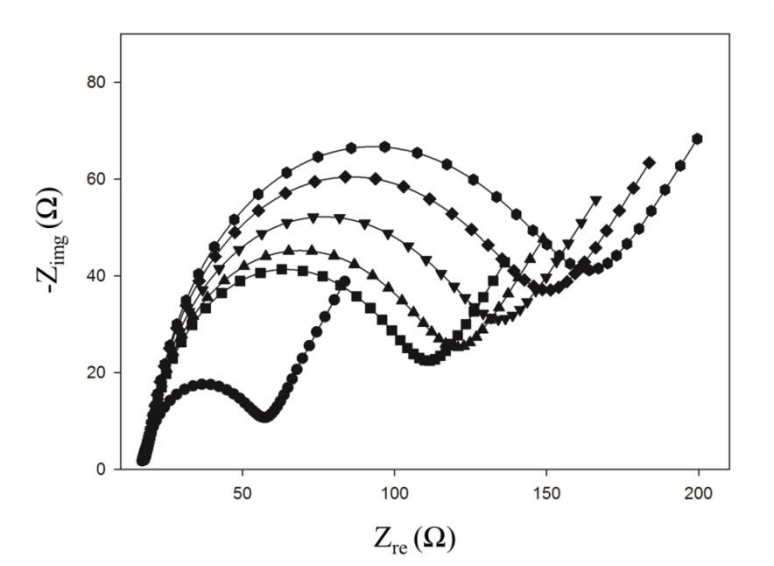

(B)

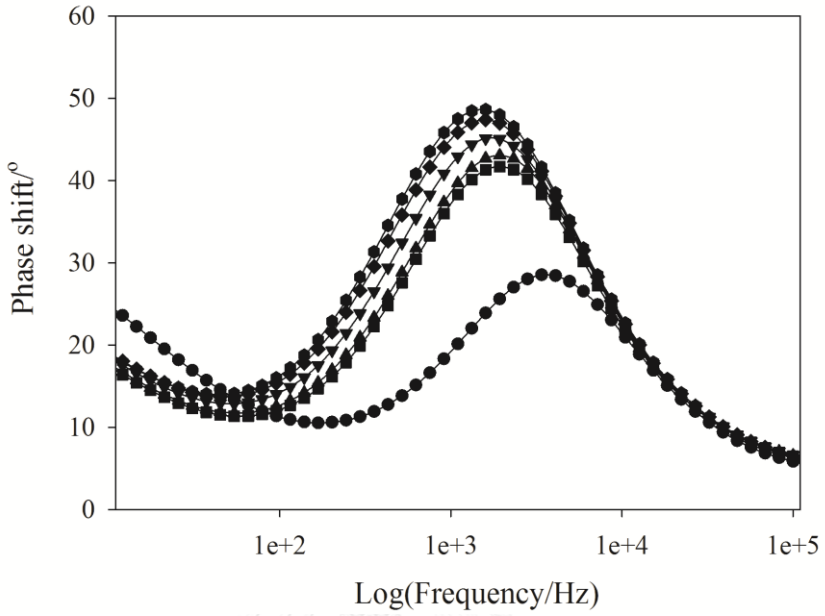
60
50
40
30
20
10
0
Phase shift/°
1e+2
1e+3
1e+4
1e+5
Log(Frequency/Hz)

(C)

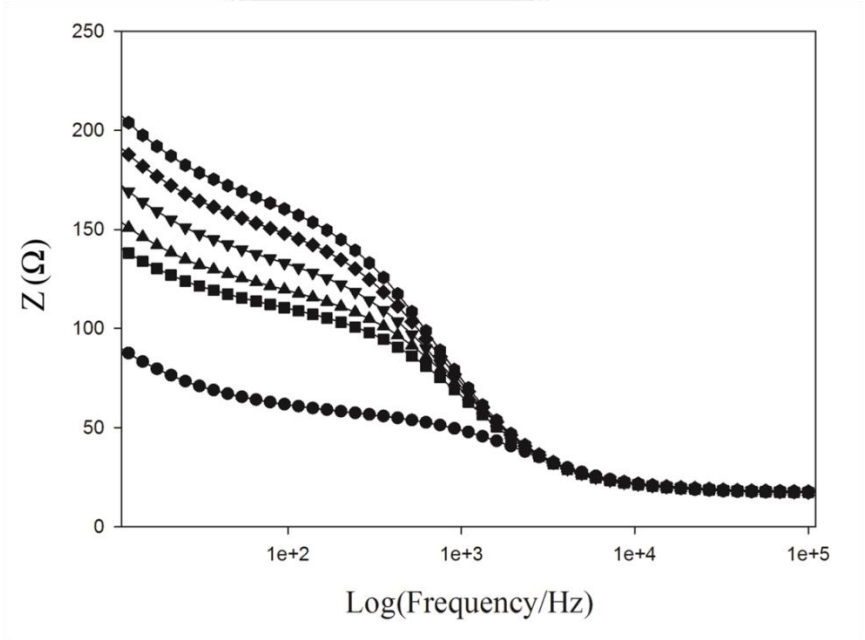
250
200
150
100
50
0
Z (Ω)
1e+2
1e+3
1e+4
1e+5
Log(Frequency/Hz)

(D)

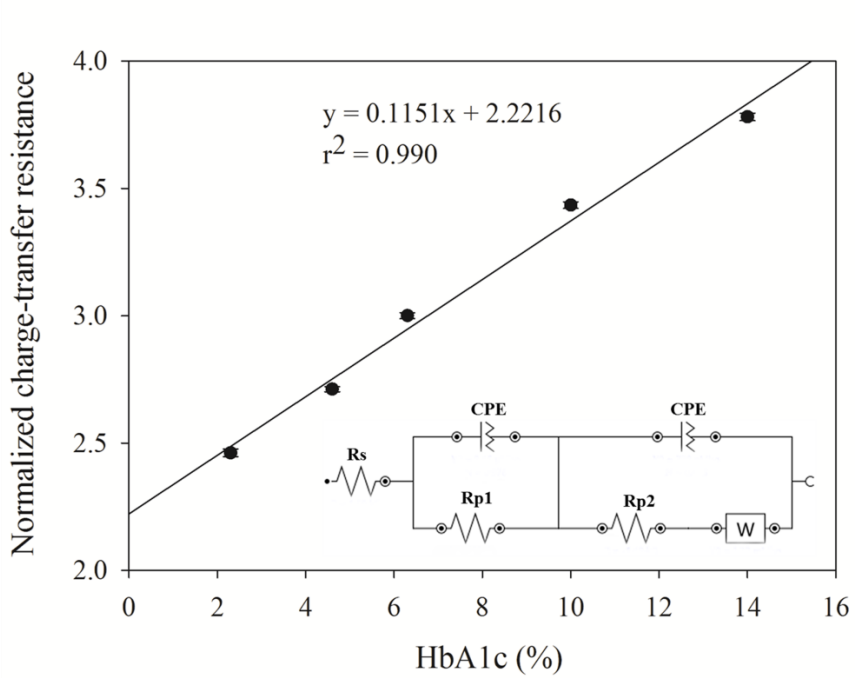

Figure 13. Impedance data obtained from (A) Nyquist plot, (B) Bode-phase plot of the APBA-modified ESM before and after it was exposed to various concentrations of HbA1c: (●) APBA-modified ESM, (■) 2.3%, (▲) 4.6%, (▼) 6.3%, (◆)10%, and (⬢) 14% HbA1c; (C) Bode-modulus plot and (D) variation of the normalised Rct with respect to the concentration of HbA1c (%). Inset right: an equivalent circuit for analysing the impedance data; Rs, Rp, CPE, and W represent the solution resistance, charge-transfer resistance (Rct), constant-phase element, and Warburg impedance, respectively.

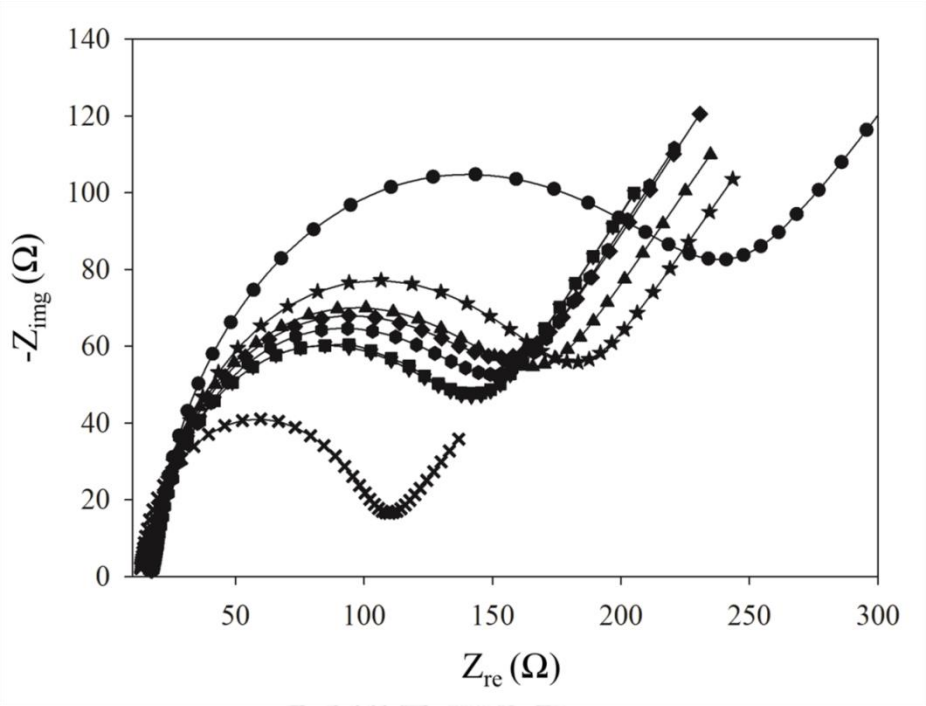

Figure 14. Impedance data obtained from the control experiment using an ESM without immobilised APBA for HbA1c detection: (✕) bare electrode, (★) ESM, (●) glutaraldehyde-treated ESM, (■) 2.3% HbA1c, (▲) 4.6% HbA1c, (▼) 6.3% HbA1c, (◆) 10% HbA1c, and (⬢) 14% HbA1c.

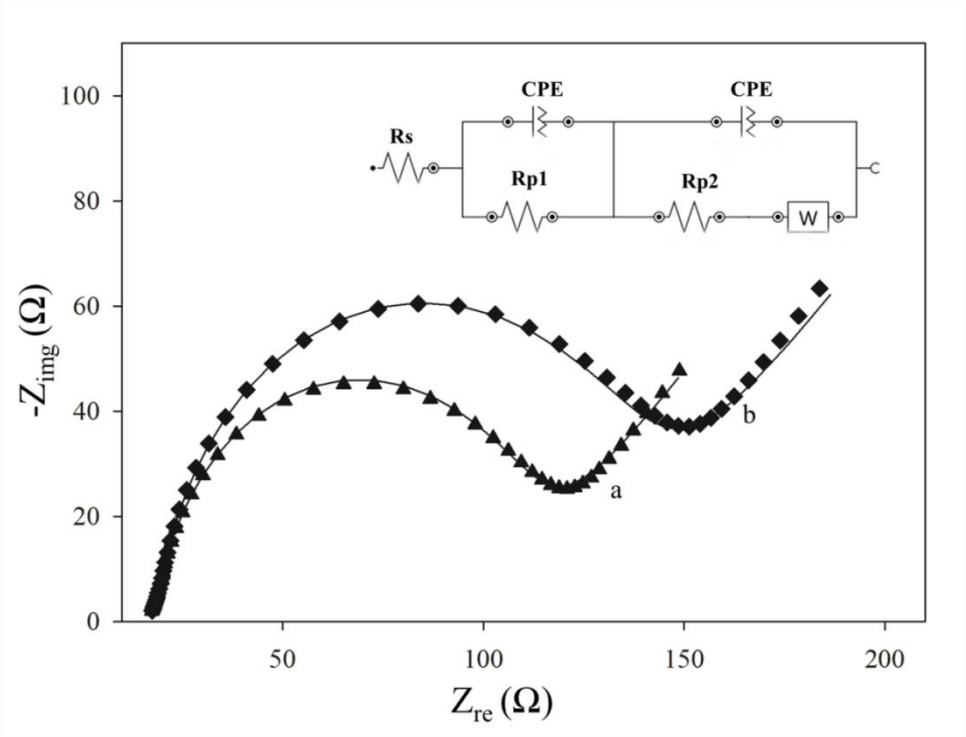

Figure 15. The experimental electrochemical impedance spectra (scattered points) and the fitted results (solid line): (a) incubation of a normal HbA1c concentration (4.6% HbA1c) and (b) diabetic HbA1c concentration (10% HbA1c) in the presence of a 5 mM $Fe(CN)_6^{3-/4-}$ redox probe in 10 mM 4-ethylmorpholine buffer (pH 8.5) containing 0.25 M KCl and 0.1 M NaCl. Nyquist plots of an APBA-modified ESM after exposure to the various concentrations of HbA1c. Inset: the equivalent circuit for the impedance spectroscopy measurement.

Table 3. Comparison of analytical characteristics for HbA1c determination using boronate-based electrochemical methods.

Approach	Dynamic detection range ($\mu g\ mL^{-1}$)	Limit of detection ($\mu g\ mL^{-1}$)	Real sample analysis	Ref.
Thiophene-3-boronic acid monolayer-covered gold electrodes	0.1 - 1	ND	ND	Park et al., 2008
Thiophene-3-boronic acid-modified ring-shaped interdigitated electrodes	10 - 100	1	ND	Hsieh et al., 2013
Thiophene-3-boronic acid-modified gold electrodes integrated into a microfluidic device	10-100	ND	ND	Chuang et al., 2012
Amperometric sensor (poly(terthiophene benzoic acid)/gold nanoparticle-modified electrodes)	0.1 – 1.5 %	0.052 ± 0.02 % (0.27 %; impedance analysis)	Haemo-lysates	Kim and Shim, 2013
Flow immunoassay system	0 - 500	ND	Haemo-	Tanaka

(boronate-affinity on-chip column)			lysates	et al., 2007
Voltammetric measurement (boronic acid-modified pyrroloquinoline quinine/reduced graphene oxide composites)	9.4 – 65.8	1.25	Haemo-lysates	Zhou et al., 2015
Voltammetric measurement (poly(amidoamine) G4 dendrimer/formylphenylboronic acid-modified electrodes)	2.5 – 15 %	ND	ND	Song and Yoon, 2009
Voltammetric measurement (cystamine/formylphenylboronic acid-modified electrodes)	4.5 – 15 %	ND	Whole blood	Song et al., 2012
Potentiometric method	ND	ND	Haemo-lysates	Liu and Crooks, 2013
Ferroceneboronic acid-based amperometric biosensor (Zirconium dioxide nanoparticle-modified electrodes)	6.8 – 14 %	ND	Whole blood	Liu et al., 2006

ND: not determined.

3.4.3.3 Reproducibility

The reliability of the proposed membrane-based biosensor was determined with a precision assay that included two levels of HbA1c, i.e., normal (4.6%) and diabetic (10%) HbA1c concentrations, performed on the same day and on three consecutive days. The results revealed that the within-run reproducibility (each concentration; n = 10) was indicated by CVs of 1.68% and 1.83% when assaying normal and abnormal levels of HbA1c, respectively. Furthermore, the run-to-run reproducibility studies at normal and abnormal levels resulted in CVs of 1.97% and 2.02%, respectively, assessed on three consecutive days (each concentration; n =30). The regeneration experiment is also demonstrated in Figure 16. Due to the reversible binding between HbA1c and boronate-recognition groups, the proposed membrane-based biosensor could be used as a reusable sensing platform. After repeated usage of the proposed membrane-based biosensor, similar signal responses were observed up to 10 cycles without losing APBA activity. Recently, Sacks et al. recommended that an intra-laboratory CV should be less than 2% (NGSP units; National Glycohemoglobin Standardization Program) because a difference of 0.5% HbA1c between successive patient samples represented a significant change in glycaemic control [118]. Therefore, these findings clearly demonstrate that our proposed system provides an accurate assessment of HbA1c with great precision and also meets the performance goal for HbA1c measurement. Additionally, the storage stability of the screen-printed electrode covered with the boronate-modified ESM was also investigated by soaking the system in ultrapure water. Unfortunately, our results showed that the activity of APBA sensing interface was greatly diminished after storing the electrode for a few days. The decrease in signal response could be due to

the detachment of the boronate group from the ESM. Thus, the future studies on the storage stability of the boronate-modified ESM will be needed to be investigated.

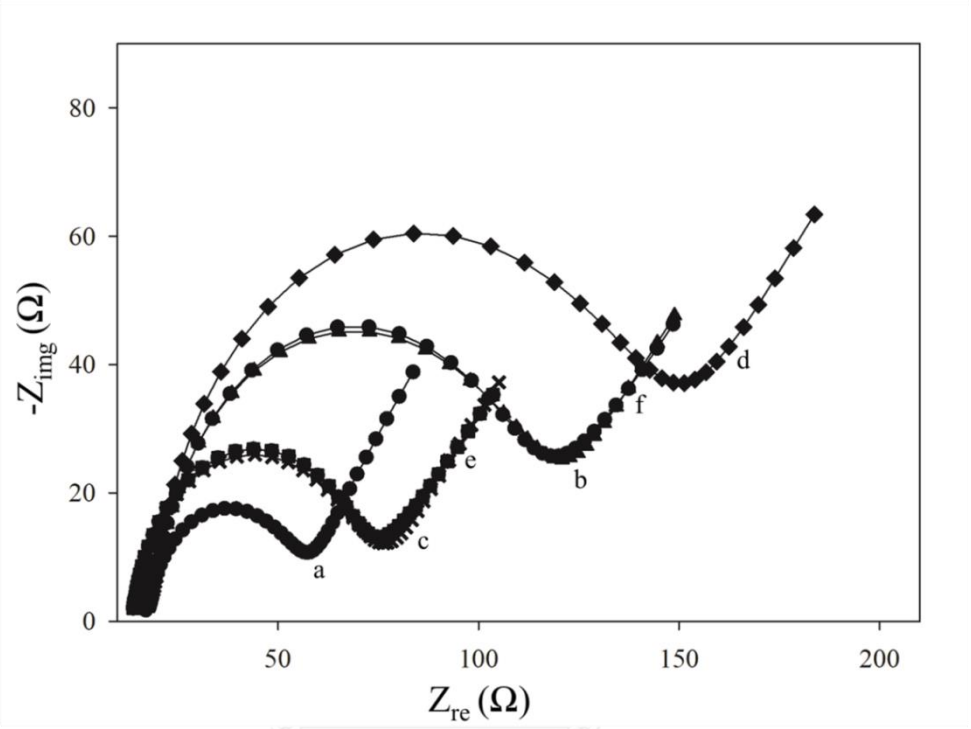

Figure 16. Nyquist plots for step-wise modification of (a) an APBA-modified ESM, (b) incubated with 4.6% HbA1c, (c) regenerated with sodium acetate buffer at a pH of 5, (d) incubated with 10% HbA1c, (e) washed with regeneration buffer, (f) re-incubated with 4.6% HbA1c.

3.4.3.4 Selectivity study

For clinical purposes, a whole-blood specimen is the most complex matrix because there are many interfering molecules present, including endogenous (unconjugated bilirubin, glucose, glycated proteins, or high hypertriglyceridaemia) and exogenous substances (commonly prescribed drugs and supplements).

Considering the underlying principles of the boronate affinity measurement method, this analytical concept is based on a unique structural characteristic of HbA1c. The boronate recognition group is able to covalently bind to the diol group of any glycated protein or sugar. Accordingly, the method described here may not be specific only to HbA1c but may also bind to glucose, glycated albumin, and other glycated proteins interfering in whole-blood samples. However, in our study, these endogenous interfering substances present in plasma were negligible because these substances were completely removed from the red blood cells by centrifugation and washing with physiological saline. As stated earlier, the red blood cell lysates were prepared before being subjected to the impedance analysis. Therefore, to evaluate the selectivity of the proposed membrane-based biosensor for the determination of HbA1c in authentic blood samples, the use of HbAo was one possible way to investigate whether the non-glycated protein could interfere with the specificity of the proposed assay. The experiment was carried out utilising the boronate-modified ESM prepared in a manner similar to that for HbA1c determination, as described in the method section, but HbAo was used instead. Compared with the signal response of boronate-modified membranes, the impedance data in the response towards HbAo remained unchanged over the concentration range of 10 to 20 g dL^{-1} (data not shown). These results imply that our proposed membrane-based system is able to very precisely determine the HbA1c content in authentic blood samples, indicating the clinical applicability of the present method to monitor glycaemic levels in diabetic individuals.

Most importantly, for the correct interpretation of HbA1c measurements in clinical practice, the analytical interference of genetic variants, i.e., HbS, HbC, HbD, HbF, and HbE, and chemical derivatives of haemoglobin, i.e., carbamyl-Hb, and pre-

HbA1c, is of particular note when guaranteeing the reliability of the results. However, to our knowledge, compared with the other available methods for HbA1c determination, the boronate affinity binding method is generally considered to be less affected by the presence of haemoglobin variants and modified derivatives [119, 120]. Recent data obtained from a comparison between the International Federation of Clinical Chemistry and Laboratory Medicine (IFCC) reference method and boronate affinity method showed that boronate affinity method was not affected by the presence of most common haemoglobin variants [56]. However, the characteristics of patient population should be carefully considered during the selection of HbA1c assay method, including the prevalence of haemoglobin variants. Additional physiological factors, such as severe iron-deficiency anaemia, haemolytic anaemia or any conditions that directly affect the erythrocyte lifespan, should be considered as potential restrictions for interpreting HbA1c assay results.

3.4.3.5 Assay comparison

Fifteen red blood cell lysate samples obtained from non-diabetic and diabetic volunteers were analysed for HbA1c levels using the proposed membrane-based system in parallel with the current commercially available method. All of the samples were analysed for haemoglobin and haematocrit values, which were determined to be within the ranges of 11-18 g dL^{-1} and 30-47%, respectively. The agreement and correlation between the two approaches were assessed using the Bland-Altman bias plot and a Passing-Bablok regression analysis, respectively. The results revealed a reliable relationship between the proposed membrane-based system and the commercially available method within an agreement interval of ± 1.96 SD. As

demonstrated in Figure 17(A), these results suggest that the two methods could be used interchangeably. The results derived from our system were highly correlated with those obtained using the commercially available kit, with a Passing-Bablok regression equation of y = 1.0000x + 0.0100, as shown in Figure 17(B). Based on a 95% confidence interval, the values of the y-intercept (0.0100) and the slope (1.0000) were trustworthy and covered a range of -0.4600 to 0.3017 and 0.9478 to 1.1000, respectively. In other words, these data demonstrate a good agreement between these two methods, and the proposed ESM-based method provides an alternative approach to monitoring HbA1c levels in authentic blood samples. In this case, the glycaemic status of each individual can be determined.

(A)

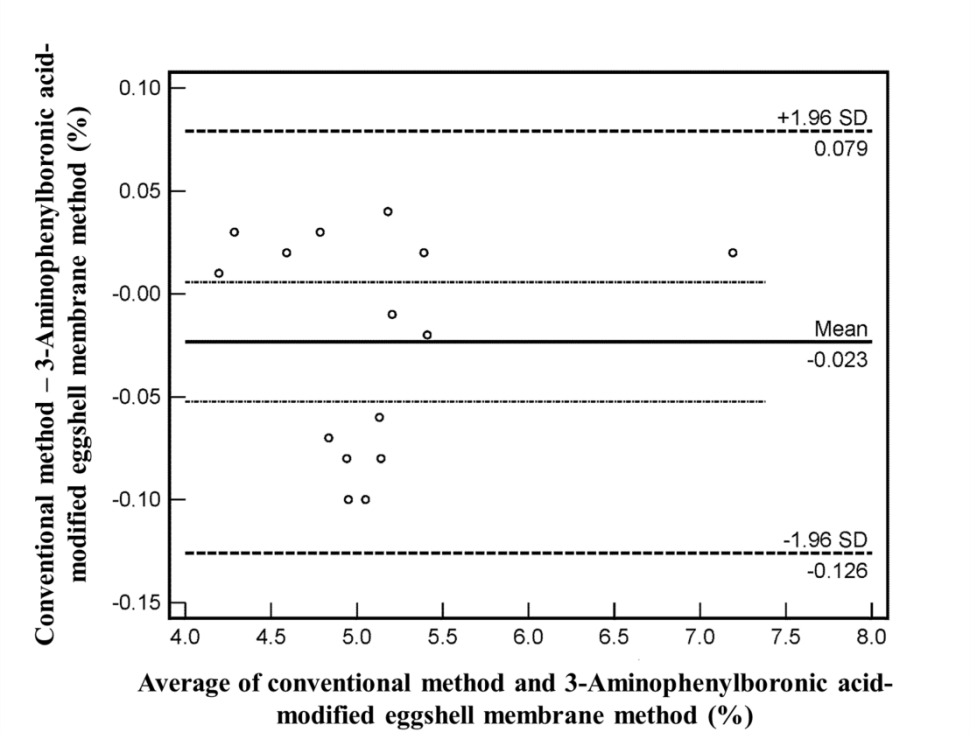

(B)

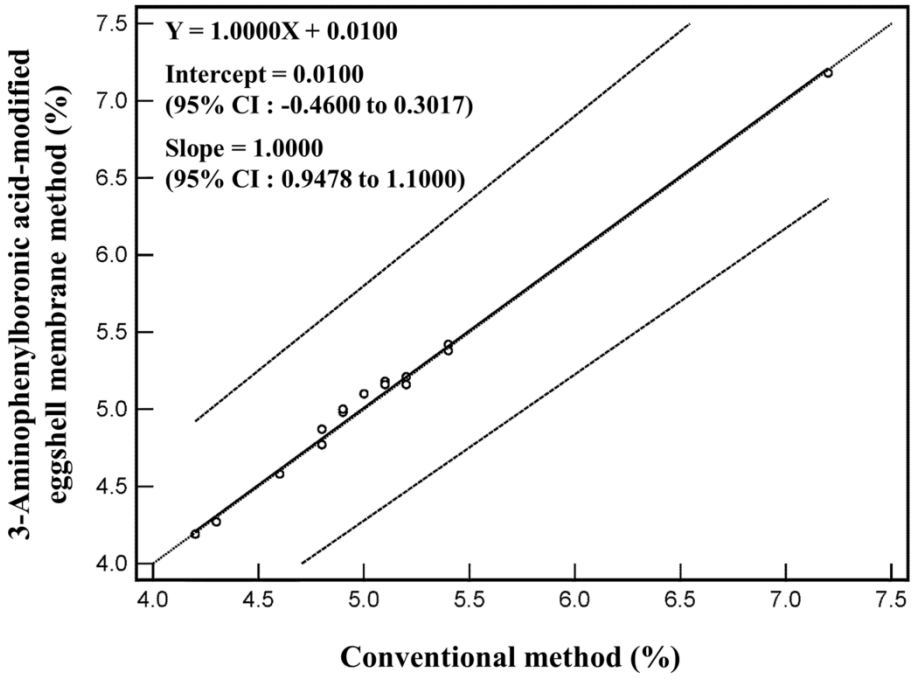

Figure 17. Comparison of the proposed ESM-based analytical system and the current commercially available method for HbA1c measurement using (A) a Bland-Altman bias plot and (B) Passing-Bablok regression analysis.

3.5 Conclusions

The proposed ESM-based biosensor was remarkably selective in determining HbA1c levels because this method was successfully applied to the analysis of authentic samples via a label-free electrochemical impedance measurement, in which the results demonstrated good agreement with the commercially available affinity method. The results showed in a step-wise process that the boronate-modified ESM was highly responsive to a wide range of HbA1c levels, indicating that this method is suitable for the clinical monitoring of glycaemic control. A novel APBA-modified

ESM also provides a cost-effective biosensor for the diagnosis of diabetes, which is highly desirous in under-developed countries. Without the use of other detection labels, such as antibodies, dyes, or fluorescent materials, the proposed system has the merit of great simplicity. With the utilisation of an affinity membrane-based biosensor, this method has the potential for continuously monitoring glycaemic levels in diabetic patients and can be applicable to determining the presence other glycated proteins, e.g., glycated albumin, found in plasma.

3.6 Acknowledgements

This research was financially supported by the Ratchadaphiseksomphot Endowment Fund of Chulalongkorn University (RES 560530212-HR) and the Thailand Research Fund (RTA5780005). Y.B. acknowledges the Thailand Research Fund through the Royal Golden Jubilee Ph.D. Program (under grant No. PHD/0164/2553) and the Graduate School, Chulalongkorn University for the Tuition Fee Scholarship.

CHAPTER IV

PUBLISHED ARTICLE

A Multiplexed Three-Dimensional Paper-Based Electrochemical Impedance Device for Simultaneous Label-Free Affinity Sensing of Total and Glycated Haemoglobin: the Potential of using a Specific Single-Frequency Value for Analysis

Yuwadee Boonyasit[1], Orawon Chailapakul[2], and Wanida Laiwattanapaisal[3,*]

[1] Graduate Program in Clinical Biochemistry and Molecular Medicine, Faculty of Allied Health Sciences, Chulalongkorn University, Bangkok, 10330, Thailand.

[2] Electrochemistry and Optical Spectroscopy Research Unit (EOSRU), Department of Chemistry, Faculty of Science, Chulalongkorn University, Bangkok, 10330, Thailand.

[3] Department of Clinical Chemistry, Faculty of Allied Health Sciences, Chulalongkorn University, Bangkok, 10330, Thailand.

Accepted for publication in *Anal Chim Acta*, Article in Press, 2016

4.1 Abstract

A novel three-dimensional paper-based electrochemical impedance device (3D-PEID) is first introduced for measuring multiple diabetes markers. Herein, a simple 3D-PEID composed of a dual screen-printed electrode on wax-patterned paper coupled with a multilayer of magnetic paper was fabricated for label-free electrochemical detection. The results clearly demonstrated in a step-wise manner that the haptoglobin (Hp)-modified and 3-aminophenylboronic acid (APBA)-modified eggshell membranes (ESMs) were highly responsive to a clinically relevant range of total (0.5–20 g dL^{-1}; r^2 = 0.989) and glycated haemoglobin (HbA1c) (2.3%–14%; r^2 = 0.997) levels with detection limits (S/N = 3) of 0.08 g dL^{-1} and 0.21%, respectively. The optimal binding frequencies of total haemoglobin and HbA1c to their specific recognition elements were 5.18 Hz and 9.99 Hz, respectively. The within-run coefficients of variation (CV) were 1.84%, 2.18%, 1.72%, and 2.01%, whereas the run-to-run CVs were 2.11%, 2.41%, 2.08%, and 2.21%, when assaying two levels of haemoglobin and HbA1c, respectively. The CVs for the haemoglobin and HbA1c levels measured on ten independently fabricated paper-based sheets were 1.96% and 2.10%, respectively. These results demonstrated that our proposed system achieved excellent precision for the simultaneous detection of total haemoglobin and HbA1c, with an acceptable reproducibility of fabrication. The long-term stability of the Hp-modified eggshell membrane (ESM) was 98.84% over a shelf-life of 4 weeks, enabling the possibility of storage or long-distance transport to remote regions, particularly in resource-limited settings; however, for the APBA-modified ESM, the stability was 92.35% over a one-week period. Compared with the commercial automated method, the results demonstrated excellent agreement between the

techniques (p-value < 0.05), thus permitting the potential application of 3D-PEID for the monitoring of the glycaemic status in diabetic patients.

Keywords: Glycated haemoglobin; three-dimensional paper-based electrochemical impedance device; 3-aminophenylboronic acid; haptoglobin; eggshell membrane; label-free electrochemical detection.

4.2 Introduction

The implementation of microfluidic paper-based analytical devices (μPADs) in clinical off-site diagnoses has recently emerged as a distinctive field of simple telemedicine in remote areas [19]. The multiplexed measurement of a panel of biomarkers has recently attracted considerable interest due to its great potential for monitoring patient compliance, evaluating the effectiveness of therapy, and early screening for diseases. During recent years, μPADs coupled with optical imaging for colourimetric detection have provided an affordable point-of-care platform for the multiplexed analysis of biomarkers, such as the transaminase assays for liver function assessment [15, 16], detection of metabolic biomarkers for glycaemic control [17, 18], urinalysis assays [19, 20], and simultaneous detection of glucose, uric acid and lactate [21]. Alternatively, other detection methods for assaying multiple biomarkers on a single 3D-μPAD have been demonstrated, including electrochemical [22-27], chemiluminescence [28], and electrochemiluminescence [29] techniques, most of which relied heavily on ultrasensitive immunodevices for multiplexed quantification of cancer biomarkers. To date, considering the existing paper-based electrochemical devices for measuring metabolic biomarkers, considerable efforts have been focused

only on establishing a proof-of-concept work on the determination of glucose, uric acid, and lactate [121, 122]. However, there has been minimal validation of µPADs using actual clinical specimens. Thus far the label-free impedimetric sensing of diabetes markers for the long-term assessment of glycaemic control on a single 3D-µPAD has yet to be investigated. As an alternative to the single-analyte assays, the multiplexed 3D-µPAD allows simultaneous measurement of multiple analytes on a single device, which provides an accurate basis for clinical diagnoses and decreases the assay time. To our knowledge, there have been no attempts to use a single three-dimensional paper-based electrochemical impedance device (3D-PEID) for measuring multiple diabetes markers.

Currently, electrochemical impedance spectroscopy (EIS)-based point-of-care diagnostic platforms for determining a panel of biomarkers have attracted great interest in the clinical assessment of early disease detection. Known as an informative and nondestructive technique for biosensing applications, EIS has an enormous potential for the label-free and ultrasensitive biomarker detection with the capability to measure multiple markers simultaneously as it can be used to study the interfacial events or diffusion effects occurring at the surface of the electrodes. Because acquisition of impedance spectra is relatively time consuming, many attempts have been made to use a single frequency value for analysis [123-127]. More recently, multiplexed sensor array designs, most of which depend on antibody-based molecular recognition, have been implemented for the determination of various inflammatory markers using a unique frequency upon binding of the target molecule to the sensor [128, 129]. The biological reaction between each target and its molecular recognition element results in a unique binding frequency that is specific to each reaction. Thus,

the differences in frequency signals from each reaction can be detected on a single platform due to the effective discrimination of the target binding frequencies from the others. Using this underlying principle, by immobilising recognition elements for different biomarkers on the sensor interface, each target molecule can be measured simultaneously by monitoring their optimal binding frequency, thereby making this platform suitable for multiplexed assays of makers in a single device. The specific optimal binding frequency depends on several factors such as the sensor material, molecular recognition element, and the linkers used for immobilisation [130]. For instance, EIS in combination with technology for the management of patients with diabetes mellitus (DM) was implemented using a specific frequency for glucose-glucose oxidase binding interaction [131]. A few years later, the feasibility of EIS in detecting 1,5-anhydroglucitol levels at its optimal binding frequency was also demonstrated using the enzyme pyranose oxidase [132]. However, there are no relevant data as of yet on the label-free affinity biosensing for measuring multiple diabetes markers on a single device. Hence, a multiplexed single-sensor diabetes marker assay needs to be further developed to meet the clinical requirements for a point-of-care testing (POCT) system.

Typically, in clinical practice, the quantitative measurement of glycated haemoglobin (HbA1c) is an indispensable index for the long-term monitoring of glycaemic control in both the diagnosis and routine management of diabetes. The intensive monitoring of glycaemic status is needed to avoid diabetic complications. In general, the HbA1c level is measured as the percentage of glycated haemoglobin in the total haemoglobin (i.e., mmol mol^{-1} or %). According to the consensus statement of the International Federation of Clinical Chemistry and Laboratory Medicine

(IFCC) and the National Glycohemoglobin Standardization Program (NGSP) on the standard interpretation norms of HbA1c values, HbA1c results are reported worldwide together with the haemoglobin value as mmol of HbA1c or a percentage of HbA1c in the total haemoglobin, respectively [133]. HbA1c analysis has been accomplished using a wide range of techniques, including mass spectrometry [33-35], electrophoresis [38], chromatography [36, 37], immunoassays [43-47], electrochemistry [48-54, 56, 60, 61], enzyme assays [96, 134-136], piezoelectric sensing [39-41], and optical spectroscopy [42, 58, 59]. However, most of the aforementioned approaches require the use of highly sophisticated instruments at high operating costs by experienced personnel. Moreover, they fail to satisfy the analytical requirements of sensitivity, specificity, reproducibility, storage stability, simplicity, and portability. For these reasons, further improvements of cost-effective diagnostic POCT devices are still required for the clinical assessment of glycaemic status in diabetes patients. Thus far, there have been no reports in the literature regarding simultaneous detection of both total haemoglobin and HbA1c based on a single affinity-based sensing device. In our preceding work, the label-free boronate-modified eggshell membrane (ESM)-based affinity sensor for long-term glycaemic monitoring was first demonstrated via the cis-diol interaction between HbA1c and the boronate recognition element [137]. Using the boronate-modified sensing surface, our device could distinguish between HbA1c and non-glycated haemoglobin (HbAo). However, acquisition of impedance spectra typically required a scanning time of 15 for the entire frequency range. Therefore, in the present work, we have further developed the affinity membrane-based analytical device for detecting HbA1c in parallel with total

haemoglobin contents using a specific single-frequency value for analysis to circumvent the time-intensive procedure of acquiring entire impedance spectra.

Herein, to combine a multiplexed biomarker assay with a selective low-cost platform, we demonstrated a simple 3D-PEID for simultaneous quantitative detection of total haemoglobin and HbA1c using an ESM-based affinity sensor. The impedance response as a function of analyte concentration was also investigated in a single- or limited-frequency range by attaching the molecular recognition elements, i.e., haptoglobin (Hp) or 3-aminophenylboronic acid (APBA), to the sensor surface. Due to the distinctive features of Hp and APBA, which are promising recognition elements for total haemoglobin and HbA1c, selective binding was obtained via non-covalent protein-protein interactions and cis-diol interactions, respectively. Therefore, each target analyte could be detected by monitoring the optimal binding frequency specific to that reaction using a single 3D-PEID platform. This affinity device was also validated to suit the clinical requirements and applied to the determination of the total haemoglobin and HbA1c levels in real clinical blood samples. To our knowledge, no previous attempts have been made to assess the clinical applicability of a label-free 3D-PEID for assaying both total haemoglobin and HbA1c in actual patient-derived specimens. This reliable and inexpensive device for assaying total haemoglobin in parallel with HbA1c is an ideal sensing platform for point-of-care diagnostics. Our proposed system demonstrates the considerable future potential for long-term independent bedside monitoring of the glycaemic status of diabetes patients, particularly in resource-limited settings.

4.3 Materials and Methods

4.3.1 Reagents and chemicals

All reagents and chemicals were of analytical grade or the highest purity available and used as received without further purification. APBA, human haptoglobin phenotype 1-1 (Hp), human haemoglobin, 4-ethylmorpholine, sodium chloride (NaCl), potassium chloride (KCl), potassium hexacyanoferrate II, potassium hexacyanoferrate III, a glutaraldehyde solution (25% w/w), ethanolamine, sodium acetate trihydrate, potassium cyanide, sodium phosphate monobasic, sodium phosphate dibasic, potassium phosphate monobasic, potassium phosphate dibasic, sodium hydroxide, urea, and haemoglobin-Ao were acquired from Sigma (St. Louis, MO, USA). Hydrochloric acid, ethanol, and absolute acetic acid were purchased from Merck (Darmstadt, Germany). A Lyphochek® HbA1c linearity set and Lyphochek® diabetes controls were obtained from BioRad Laboratories (Hercules, CA, USA). Ultrapure water obtained from a Millipore water purification system (18 MΩ cm, Milli-Q, Millipore) was used throughout the study. The instruments used for measuring the haematocrit (Hct) values, including micro-haematocrit tubes, a micro-capillary reader, and a micro-haematocrit centrifuge, were manufactured by Vitrex Medical A/S (Herlev, Denmark), International Equipment Company (Needham Heights, MA, USA), and Hawksley and Sons Ltd. (Sussex, England), respectively. For preparing the screen-printed electrodes, the carbon ink (C2030519P4) and silver chloride ink (C2090225P7) were supplied by Gwent group (Torfaen, United Kingdom). An A4 sheet of 180 gsm office paper was available from a local stationery store. The custom-ordered blocking stencils and a rubber squeegee were readily available from the local service provider. For ESM preparation, the chicken eggs were

purchased from a local supermarket and stored at 4 °C before use. The in vitro test for quantitative measurement of HbA1c in whole blood on Roche clinical chemistry analyzer (Tina-quant® HbA1c Gen.2) acquired from Roche (Roche Diagnostics, Switzerland) was employed to validate the method based on the turbidimetric inhibition immunoassay.

4.3.2 Design and fabrication of the 3D-PEID

The 3D-PEID was comprised of a dual screen-printed electrode on a wax-patterned paper coupled with a multilayer of magnetic papers. For preparing the wax-based patterning on a 180 gsm office paper, the designed patterns of hydrophobic barriers as a dark blue-colour on a white background were fabricated based on a slight modification of a wax-printing procedure described previously [138]. Briefly, the wax-patterned paper containing a dual circular and rectangular zone was designed using Adobe illustrator CS6 software and then printed onto the A4 sheet of 180 gsm office paper with a Xerox ColorQube 8570 solid ink printer. The wax-printed paper was transferred to a 150 °C hot plate with the wax side up for 180 seconds and allowed the printed wax to melt and penetrate through the paper to form the blue-colour hydrophobic and insulating barriers. After cooling at room temperature, the wax-printed paper sheet was then ready for printing the three-electrode areas and conductive pads on its hydrophilic zones. According to our in-house screen printing technique, a dual working and counter electrode comprising the conductive pads were screen-printed in the defined hydrophilic areas on the wax-printed paper sheet using carbon ink. After that, to cure the carbon inks, the screen-printed paper was baked in an oven at 65 °C for 30 min before starting the next round of screen-printing process.

A reference electrode with its conductive pad was then screen-printed in the defined hydrophilic zone on the same paper sheet using silver/silver chloride ink before baking again at 65 °C for 30 min. Finally, after allowing the screen-printed paper to cool at room temperature, the dual screen-printed electrode on the wax-patterned paper layer was then stuck onto a customised magnetic paper sheet before assembling the whole system. To complete the proposed 3D-PEID, the dual screen-printed electrode layer adhered to the magnetic paper was covered with a top magnetic-paper layer containing two circular wells, all aligned and assembled with a permanent magnet underneath, as illustrated in Figure 18(A). The wax-patterned paper electrochemical cell was comprised of two paper working zones (4 mm in diameter) surrounded by sharing the same reference (geometric area about 3 mm^2) and counter electrodes (geometric area about 17 mm^2). The wax patterns around the three electrodes constituted an insulator of the electrochemical cell and served as a reservoir with a volume of approximately 60 µL after aligning with a top magnetic-paper layer containing two circular holes. To characterise the surface structure of the screen-printed paper, scanning electron microscope (SEM) images of the proposed device were recorded on a field emission scanning electron microscope (JSM-7610F, JEOL, Tokyo, Japan).

(A)

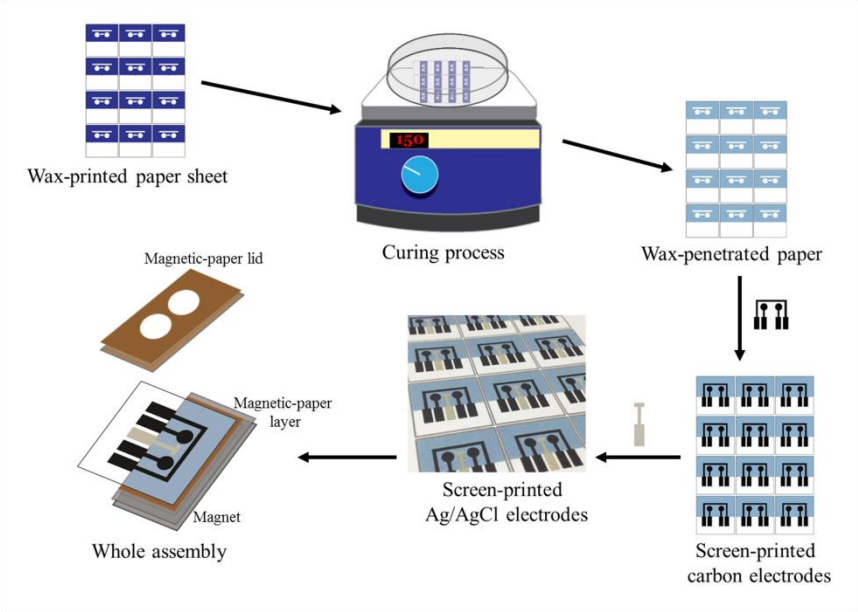

(B)

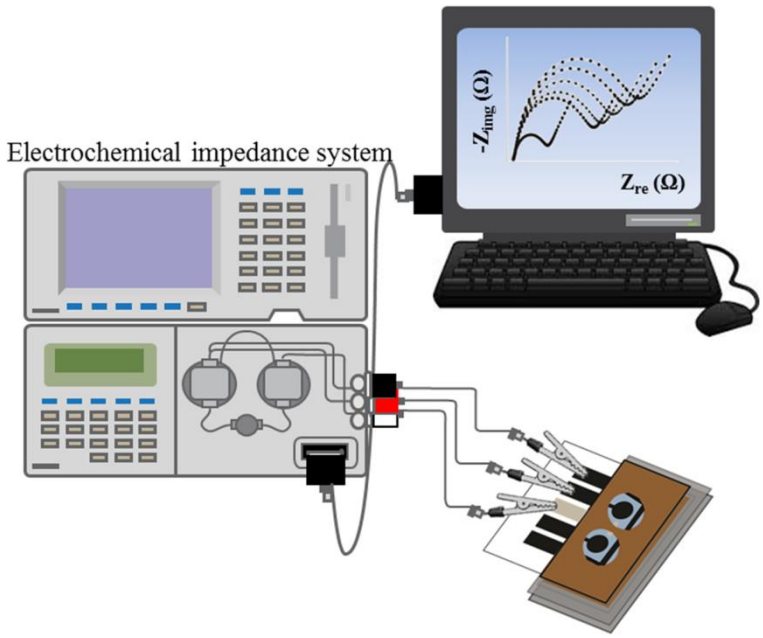

Figure 18. Schematic representation of the proposed 3D-PEID illustrating (A) a process to fabricate the paper-based electrodes and (B) a configuration of the label-free electrochemical impedance system set-up.

4.3.3 ESM preparation

A circular double-layered ESM was prepared according to the procedure described previously [104]. Briefly, after soaking the chicken eggs in absolute acetic acid at 4 °C for 18 h, the membrane was subsequently peeled off and cleansed with a copious amount of ultrapure water before cutting into a circular size (7 mm in diameter). The circular ESMs were then stored in a working buffer for assaying total haemoglobin and HbA1c until further use. To observe the microstructure of the ESM with and without the immobilised haemolysate samples containing the total haemoglobin, a dried circular ESM was stuck onto a piece of glass using a carbon double-sided adhesive tape before placing on a specimen stub and coating with a thin layer of gold before SEM analysis. The SEM images were recorded on a field emission scanning electron microscope (JSM-7610F, JEOL, Tokyo, Japan).

4.3.4 Surface modification with Hp and APBA

An affinity ESM-based impedance sensor was prepared by immobilising Hp or APBA on the surface of the ESM via glutaraldehyde cross-linking. Unless otherwise stated, the membrane was activated with the 25% glutaraldehyde solution for 1 min and washed with 100 mM phosphate buffer solution at pH 7 (PBS), then 10 μg mL^{-1} Hp was applied to the membrane surface and reacted at room temperature for 10 min. The sensing interface was subsequently rinsed with 10 mM ethanolamine, followed by an additional wash before allowing it to react with the various concentrations of total haemoglobin for 5 minutes. The EIS measurement was carried out in a step-wise manner with the electroactive redox probe. The Hp-modified ESMs could be used repeatedly after washing with a regeneration buffer, i.e., 5 M urea

containing 0.15 M sodium chloride at pH 11. For the fabrication of the APBA-modified ESM, the selective binding of HbA1c was performed using a procedure described in our previous work [137], with slight modifications. Briefly, after activating the ESM with the 25% glutaraldehyde solution for 1 min, a 10 mM 4-ethylmorpholine buffer solution containing 0.25 M KCl and 0.1 M NaCl at a pH of 8.5 was used as a working buffer for rinsing the excess aldehyde functional groups. Next, 0.25 mg mL^{-1} of APBA was immobilised on the ESM for 5 min and washed with working buffer. The remaining aldehyde groups were then blocked with 10 mM ethanolamine buffer and washed with working buffer again. Finally, different concentrations of HbA1c were added to the selective sensor and allowed to incubate for 5 min at room temperature, followed by washing with working buffer according to the procedure described above. The APBA-modified ESMs could be regenerated using a 10 mM sodium acetate buffer at pH 5 due to the unstable cis-diol interactions under acidic conditions.

4.3.5 Apparatus set-up for electrochemical impedance measurement

After assembling a multi-layered 3D-PEID, the impedance detection system, i.e., a potentiostat/galvanostat instrument (Autolab PGSTAT30, Eco Chemie, The Netherlands) equipped with the Frequency response analyser software, was then connected to the proposed 3D-PEID using the alligator clips. The configuration of the proposed system is illustrated in Figure 18(B). The whole assembly, including a dual screen-printed electrode layer adhered to a magnetic paper, and a top magnetic-paper layer, was clamped together through a magnetic force. Two pieces of the circular thin-layered ESMs (7 mm in diameter) were carefully placed on the screen-printed

electrodes covering the working, counter, and reference electrodes. After recording the electrochemical impedance spectrum, the impedance data were fitted to an equivalent-circuit model using the NOVA 1.9 software. For selective sensing of total haemoglobin and HbA1c, the EIS measurement was conducted over a wide frequency range from 100 kHz to 10 mHz with an alternating-current amplitude of 10 mV. The redox ions, i.e., a 5 mM $Fe(CN)_6^{3-/4-}$ solution prepared in a working buffer were used as an electroactive probe throughout the experiment.

4.3.6 Ethical conduct of research and sample preparation

Healthy and diabetic volunteers were enrolled in our study of their own volition. All subjects voluntarily gave written informed consent before the start of the study on the development of membrane-based biosensors for diabetes makers, which was approved by the Ethics Review Committee for Research Involving Human Research Subjects, Health Sciences Group, Chulalongkorn University (ECCU) under approval number COA No. 057/2557. Whole blood samples were drawn into vacuum blood collection tubes with tripotassium ethylenediaminetetraacetic acid (K_3EDTA) as an anticoagulant, and the Hct levels were measured using micro-capillary tubes. The plasma was separated from the whole blood and discarded to eliminate other glycated proteins and sugars present in the blood plasma. To remove the plasma completely, the remaining red blood cells were carefully washed thrice with a 0.9% sodium chloride solution. A haemolysing buffer solution prepared according to the previous study [48] was used to lyse the red blood cells prior to the EIS measurement.

4.3.7 Real sample analysis

Unless otherwise stated, after preparing the Hp-modified and APBA-modified ESMs, approximately 40 µL of the haemolysate sample was allowed to incubate for 5 min, then washed with the working buffers for the total and glycated haemoglobin assays before recording the impedance spectra using the electroactive redox probes. The impedance signals on each paper-based sensing electrode were sequentially measured via a one-channel potentiostat instrument. In this study, our proposed multi-layered 3D-PEID performed an independent EIS measurement for each specific analyte by using each modified-ESM location on the surface of each paper-based electrode. By sharing the counter and reference electrodes, each adjacent paper based working electrode could be operated independently to sense the two glycaemic markers.

4.4 Results and Discussion

4.4.1 Surface characterisation of the 3D-PEID

After the curing process, the wax-patterned A4 sheet was prepared for the screen-printing of the three-electrode configuration onto the hydrophilic zones. Fig. 19 shows scanning electron micrographs (Panels A-C) of the porous structures and microfibres of the pure office paper, the boundary of the wax-patterned paper, and the wax-penetrated paper. The melted wax penetrates the pores of the pure office paper and decreases its hydrophilicity remarkably. The functional hydrophobic areas prevent the aqueous solution from wicking and penetrating unwanted zones and act as an insulating region to confine all the reagents and solutions within the defined

working electrode areas. The unprinted-paper zone remained highly hydrophilic and flexible and thus did not affect the screen-printing of the electrodes. The surface morphology of the screen-printed working electrodes is essential for assessing the sensing performance of the electrochemical devices; therefore, we investigated the surface structure of the screen-printed paper-based working electrode. As shown in Fig. 19D, a homogeneous structure was observed on the bare electrode surface, which was particularly helpful in producing paper-based electrodes with a reproducible response. For the preparation of the affinity membrane-based device, an entire sheet of ESM was used as a platform for the selective sensing of either total haemoglobin or HbA1c. Fig. 19E presents the inner surface of the ESM, showing a network-like structure that contains highly cross-linked protein fibres and cavities. The interlacing fibres of the inner layer were uniform and smooth, which was beneficial for protein immobilisation. The surface of the interlacing ESM fibres with immobilised Hp was saturated by haemoglobin after exposure to a red blood cell lysate, as depicted in Fig. 19F. These results indicated that haemoglobin from the red blood cell lysate was successfully immobilised on the surface of the ESM.

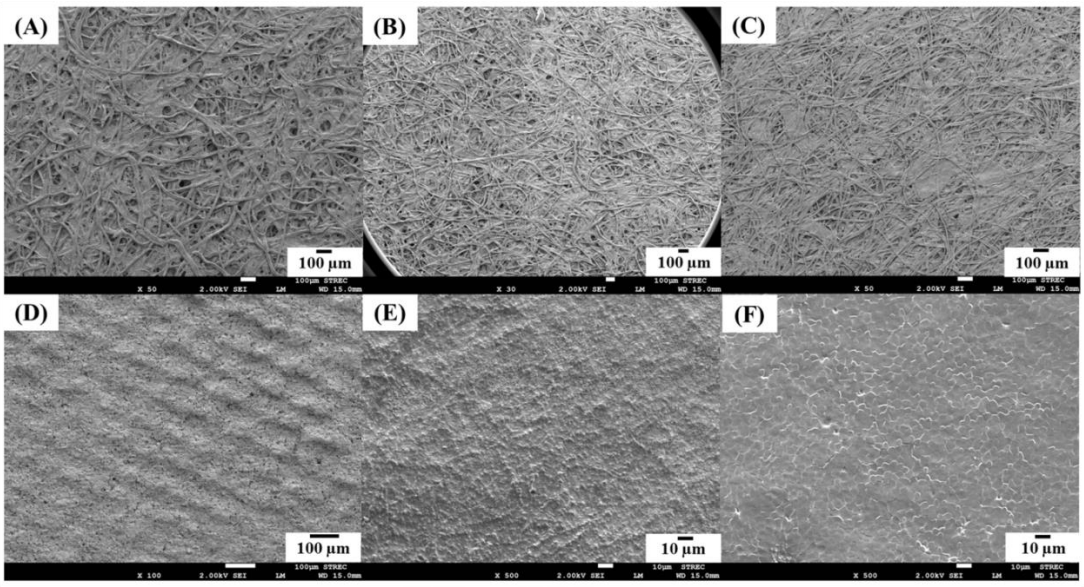

Figure 19. SEM images of (A) pure office paper; (B) the boundary of the wax pattern: left is wax-printed office paper, right is pure office paper; (C) front face of wax-penetrated office paper; (D) screen-printed working electrode; (E) inner surface of the ESM; (F) after exposure to total haemoglobin.

4.4.2 EIS characterisation of the sensing interface

The inner surface of the ESM was subjected to step-wise modifications with the screen-printed working paper electrodes underneath. To investigate the specific binding of the total haemoglobin and HbA1c to the ESM interfaces, EIS measurements were carried out following each step of the surface modification. Nyquist plots acquired in the presence of 5 mM $Fe(CN)_6^{3-/4-}$ at different stages of the modification process are shown in Figs. 20A and B. A semicircular region could be observed at the higher frequencies, corresponding to the charge transfer resistance (Rct) and double layer capacitance, as well as a straight line at the lower frequencies, representing the diffusion-limited process. The spectra obtained with the bare paper-

based electrodes showed a semicircle with a relatively small diameter, which indicated a low Rct of the redox couple. Comparatively, 2-fold increase in the Rct values was observed when the ESMs were placed on the paper-based electrodes, which resulted from the blocking of the diffusion of the redox species to the electrode surface by the interlacing networks of the fibrous ESM. After modification of the ESM with the glutaraldehyde solution, a substantial increase in Rct was observed. The glutaraldehyde-activated ESM was further modified with Hp and APBA before exposure to the various concentrations of total haemoglobin and HbA1c. The results showed that the impedance spectra acquired on electrodes having the Hp-modified and APBA-modified ESM had significantly lower Rct compared to those only having the glutaraldehyde-treated ESM. In the case of APBA modification, the decrease in Rct couldbe at least partly explained by electrostatic attraction of the negatively charged redox probe due to the presence of amino groups of APBA molecules that were actually bound to the glycoproteins of the ESM [137]. On the other hand, the decrease in Rct after immobilisation of Hp cannot be fully explained since the protein acquires negative charge at pH 7 (pI of Hp $\leq$ 6), which rather causes repulsion of the redox probe. To investigate whether the ESM surfaces had successfully immobilised Hp and APBA, control experiments were also performed using an ESM without immobilised Hp and APBA prepared in the same manner. The impedance response to various concentrations of total haemoglobin and HbA1c remained unchanged compared to the baseline signals of the ESMs, as shown in Figs. 21A and B, respectively. These results confirmed the successful immobilisation of Hp and APBA on the ESM surfaces, implying that the changes in impedance were due to the specific

binding of the total haemoglobin and HbA1c to the modified ESMs via non-covalent protein-protein and cis-diol interactions, respectively.

(A)

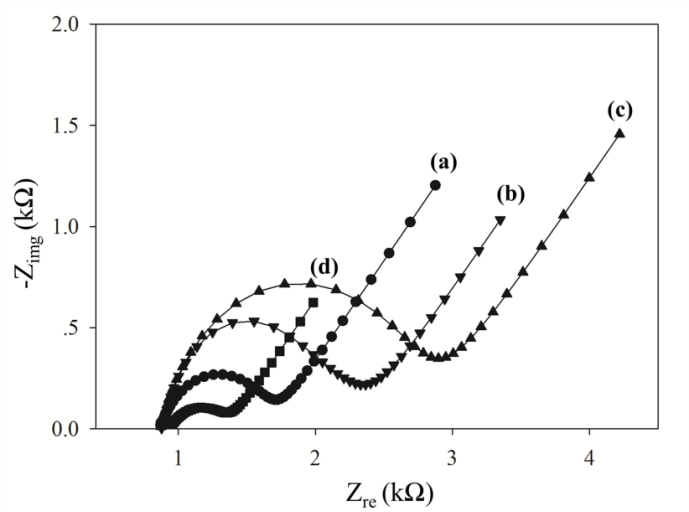

(B)

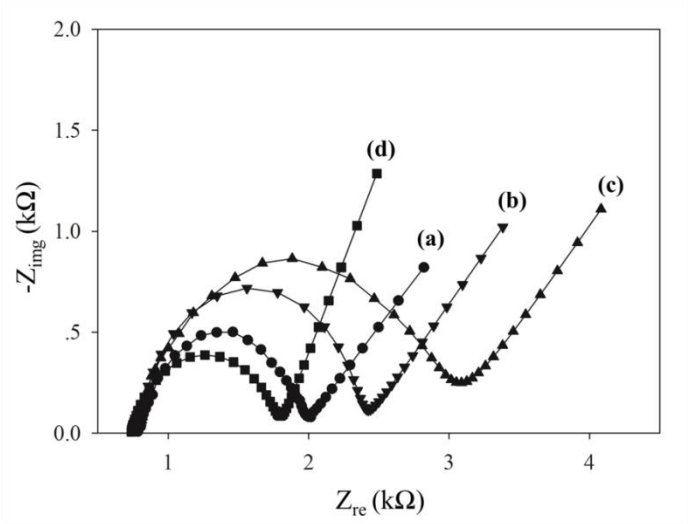

Figure 20. Nyquist plots for (A) total haemoglobin detection, (B) HbA1c detection: the stepwise analysis of the (a) bare paper-based electrodes, (b) ESMs, (c) glutaraldehyde treated-ESMs, and (d) Hp-modified or APBA-modified ESM surfaces in the presence of a 5 mM $Fe(CN)_6^{3-/4-}$ redox probe.

(A)

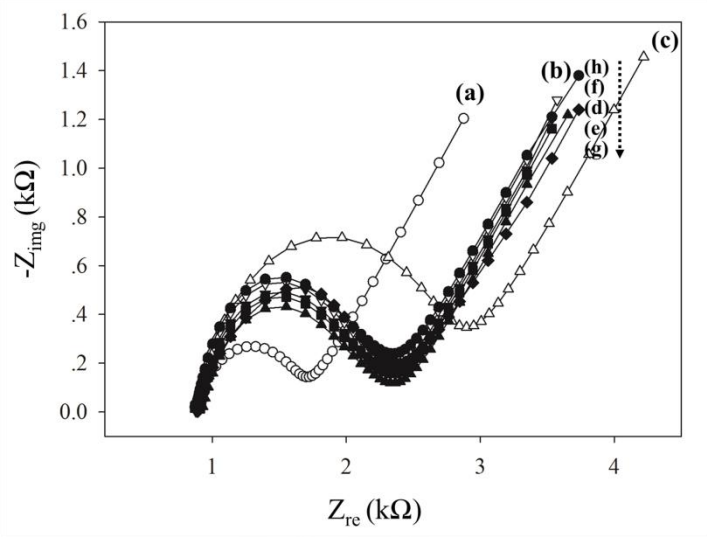

(B)

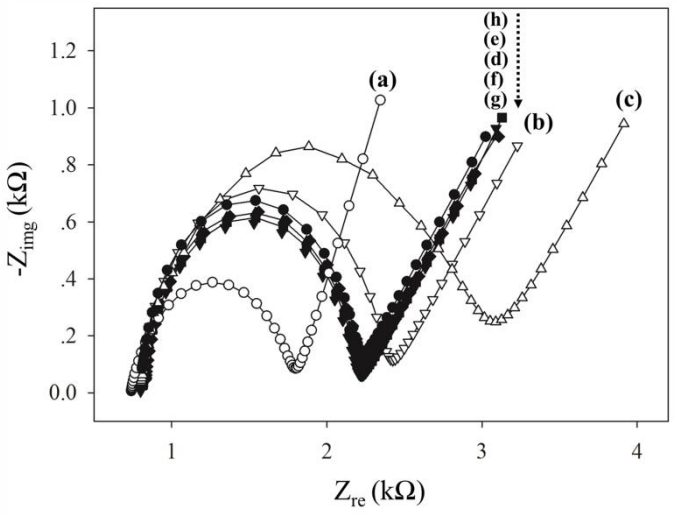

Figure 21. Impedance data obtained from the control experiments using (A) an ESM without immobilised Hp for total haemoglobin detection: (a) bare electrode, (b) ESM, (c) glutaraldehyde-treated ESM, (d) 0.5 g dL^{-1}, (e) 1 g dL^{-1}, (f) 5 g dL^{-1}, (g) 10 g dL^{-1}, (h) 20 g dL^{-1} haemoglobin; and (B) an ESM without immobilised APBA for HbA1c detection: (a) bare electrode, (b) ESM, (c) glutaraldehyde-treated ESM, (d) 2.3% HbA1c, (e) 4.6% HbA1c, (f) 6.3% HbA1c, (g) 10% HbA1c, (h) 14% HbA1c.

4.4.3 Analytical performance

Under optimal conditions, a remarkable increase in impedance was observed with increasing concentrations of total haemoglobin, as depicted in the Nyquist plot of Fig. 22A. The binding interaction between the Hp-modified ESM and the total haemoglobin contents hindered the diffusion of redox species to the surface of paper-based electrode, thus making the redox process more difficult and causing the impedance to increase. Due to the specific binding between the Hp-modified ESM and haemoglobin via non-covalent protein-protein interactions, the Hp-modified ESM was responsive to the various concentrations of total haemoglobin. The substantial increases in impedance signal were directly proportional to haemoglobin levels over the concentration range of 0.5 g dL^{-1} to 20 g dL^{-1}. Moreover, dramatic changes in impedance were noticed at the lower frequency range, as shown in Fig. 22B, thereby demonstrating the sensitive response of the Hp-modified ESM towards haemoglobin. The phase shift increased steadily upon the immobilisation of haemoglobin and subsequent addition of higher haemoglobin concentrations, as shown in Fig. 22C. The experimental impedance data are approximated using the modified Randles' equivalent circuit model shown in Fig. 22D (inset), which includes a series of two constant-phase elements (CPEs) in parallel with two charge-transfer resistances (Rct1, Rct2) and the Warburg impedance (W), along with the ohmic resistance of the electrolyte solution (Rs). The Rct1 and Rct2 correspond to the membrane resistance and charge-transfer kinetics at the paper-based electrode, respectively. This equivalent circuit appears to be the optimal model that matches the experimental impedance spectra with good fitting results, as shown in Fig. 23A. The bulk properties and diffusion features of the redox probe solution, W and Rs, respectively, were not

modified by the stepwise modification process, whereas the CPE and Rct, the dielectric and insulating features at electrode/electrolyte interface, are controlled by the changes occurring at the electrode surface. The capacitance changes are not as sensitive as the charge transfer resistance. According to the impedance values obtained from the fit to this equivalent circuit, an increase in the membrane resistance was observed in the presence of increasing haemoglobin concentrations. The normalised resistances derived from the fitted resistance values were plotted versus the various concentrations of haemoglobin. As illustrated in Fig. 3D, the results showed that the normalised response was linear up to 20 g dL^{-1} of haemoglobin, with a regression equation of $y = 0.0642x + 0.2281$ ($r^2 = 0.989$) and a detection limit (S/N = 3) of 0.08 g dL^{-1}.

(A)

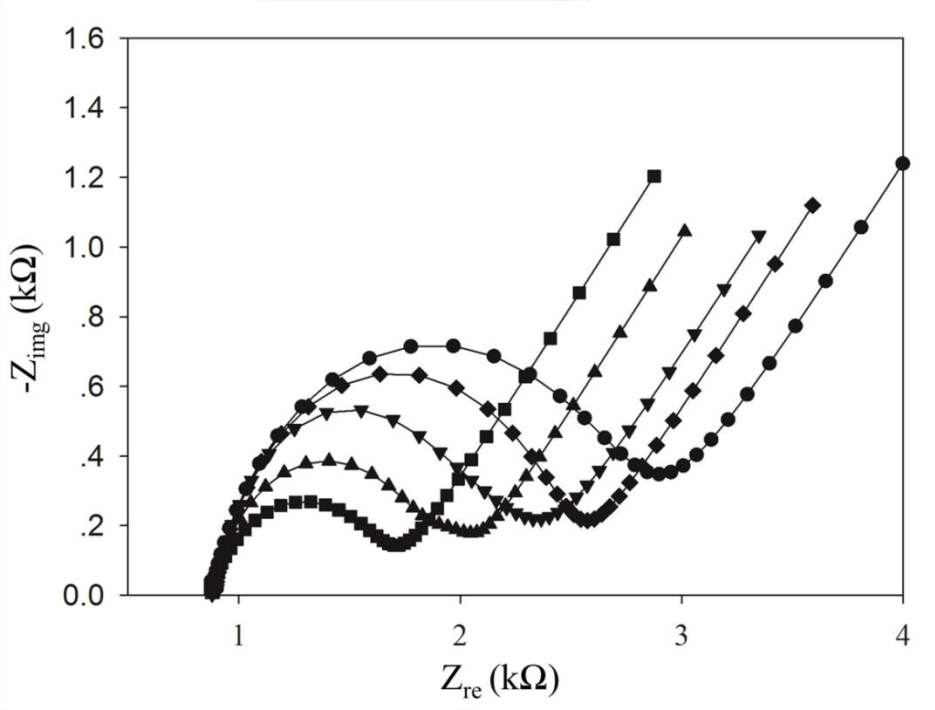

(B)

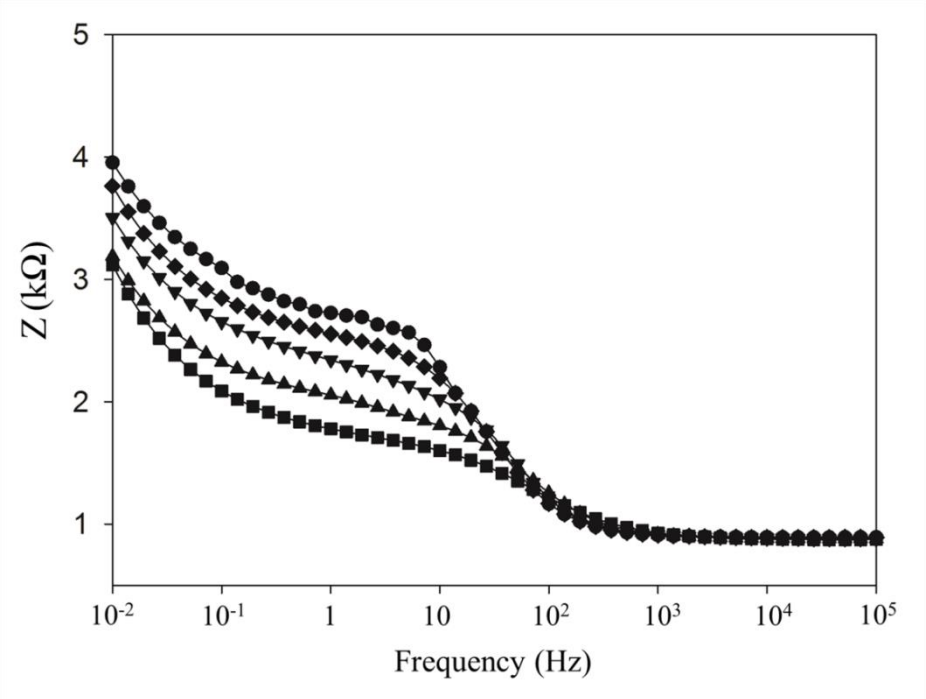
Z (kΩ)
5
4
3
2
1
10-2
10-1
1
10
102
103
104
105
Frequency (Hz)

(C)

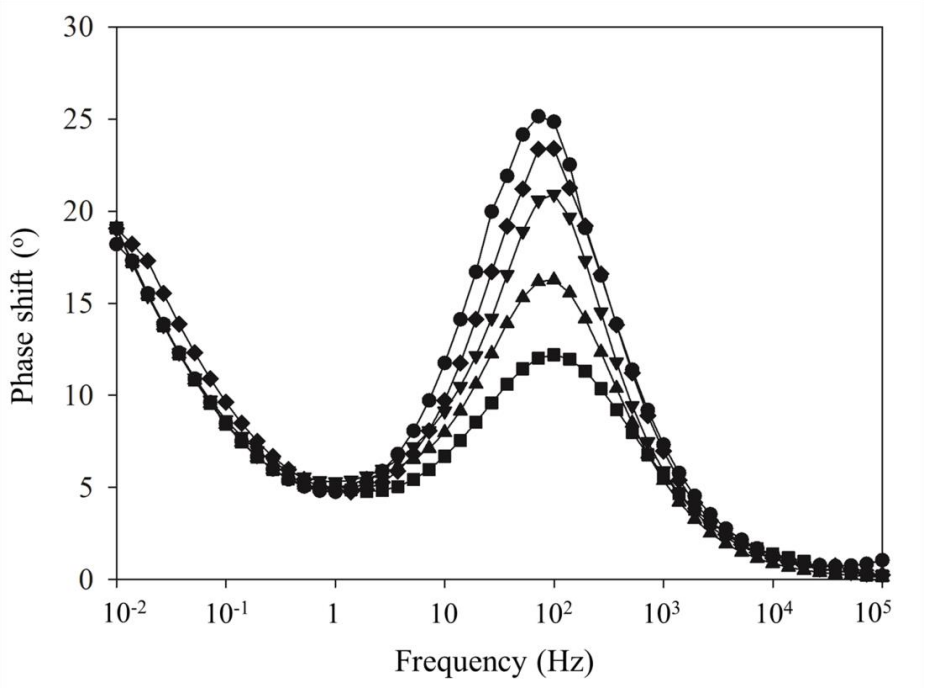
Phase shift (°)
30
25
20
15
10
5
0
10-2
10-1
1
10
102
103
104
105
Frequency (Hz)

(D)

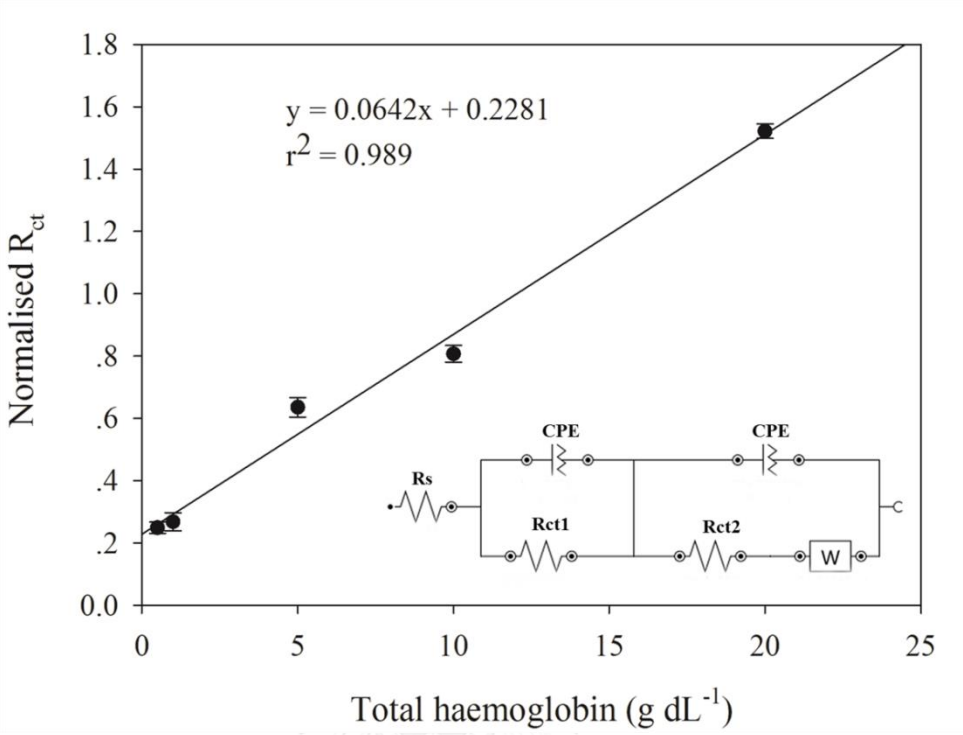

Figure 22. Impedance data obtained from (A) Nyquist plot, (B) Bode-modulus plot of the Hp-modified ESM after it was exposed to various concentrations of total haemoglobin: (■) 0.5 g dL^{-1}, (▲) 1 g dL^{-1}, (▼) 5 g dL^{-1}, (◆) 10 g dL^{-1}, and (●) 20 g dL^{-1}; (C) Bode-phase plot and (D) variation of the normalised Rct with respect to the concentration of total haemoglobin. Inset right: an equivalent circuit for analysing the impedance data; Rs, Rct, CPE, and W represent the solution resistance, charge-transfer resistance, constant-phase element, and Warburg impedance, respectively. The EIS spectra were obtained in 5 mM $Fe(CN)_6^{3-/4-}$ solution prepared in a working buffer at an open circuit voltage from 100 kHz to 10 mHz (ac amplitude, 10 mV).

(A)

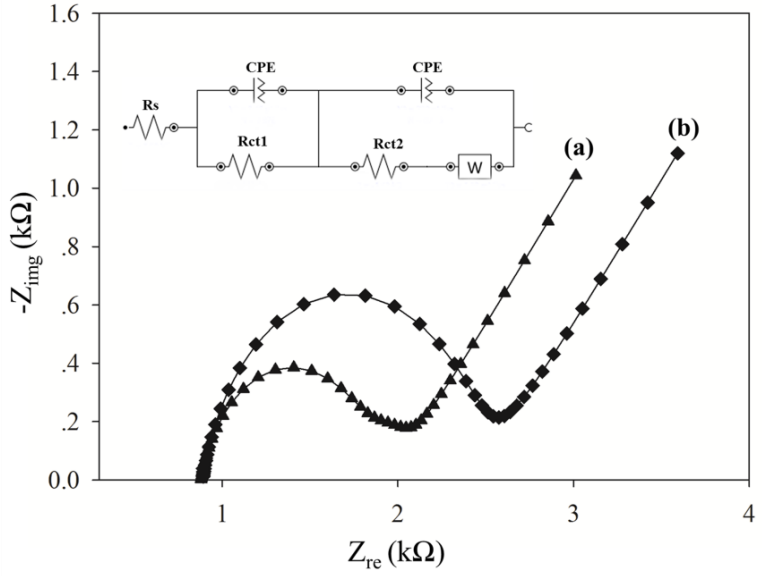

(B)

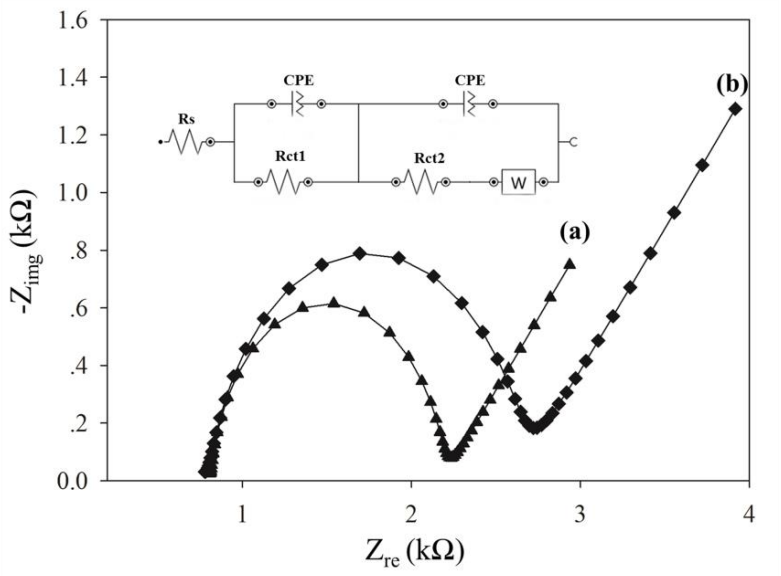

Figure 23. The experimental impedance spectra (scattered points) and the fitted results (solid line): (A) an Hp-modified ESM after exposure to the 2 levels of total haemoglobin concentrations: (a) 1 g dL^{-1}, (b) 10 g dL^{-1} haemoglobin; and (B) APBA-modified ESM after incubation with normal and diabetic concentrations: (a) 4.6% HbA1c, (b) 6.3% HbA1c. Inset: the equivalent circuit for the impedance spectroscopy measurement.

For the HbA1c detection, a substantial increase in impedance with increasing concentrations of HbA1c was observed, as shown in Fig. 24A. The changes in impedance were observed at the lower frequencies; conversely, at higher frequencies, the impedance responses did not depend on the presence of HbA1c and were thus not useful for HbA1c detection, as shown in Fig. 24B. A significant phase shift with increasing concentrations of HbA1c is clearly demonstrated in Fig. 24C. Good fits to normal and diabetic HbA1c concentrations were also obtained over the entire measurement frequency range as shown in Fig. 23B. The APBA-modified ESM was responsive to HbA1c concentrations covering the clinically required range. The good relationship between the normalised Rct and the concentration of HbA1c was observed up to 14% of HbA1c, with a regression equation of $y = 0.0846x + 0.9118$ ($r^2 = 0.997$), as depicted in Fig. 24D. The resulting limit of detection was 0.21% (S/N = 3).

(A)

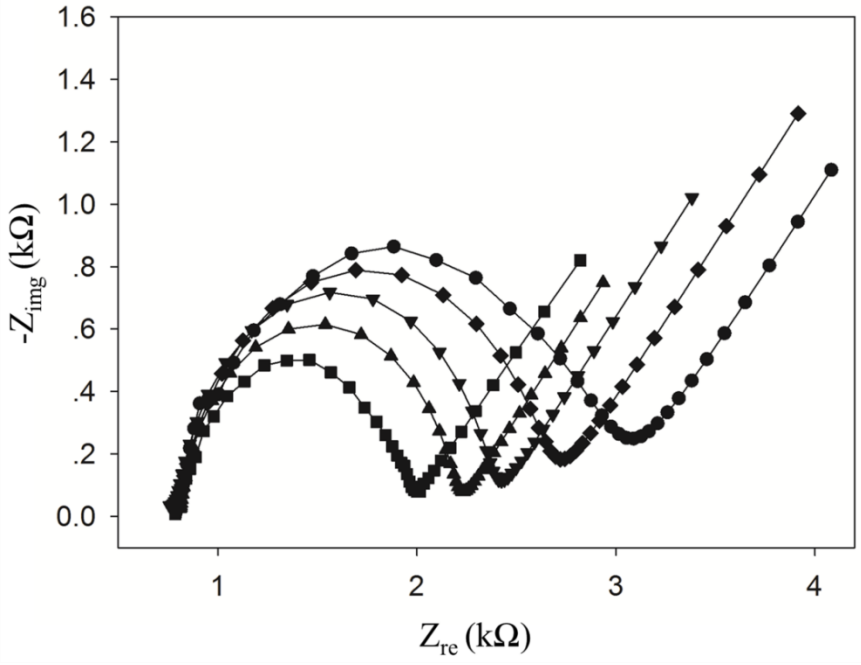

(B)

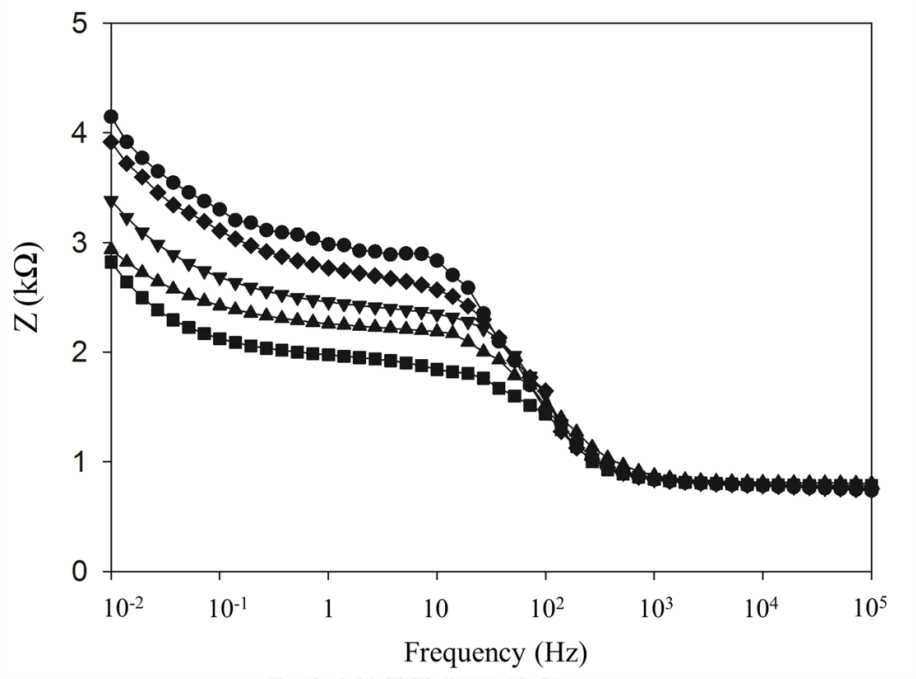
Z (kΩ)
0
1
2
3
4
5
10-2
10-1
1
10
102
103
104
105
Frequency (Hz)

(C)

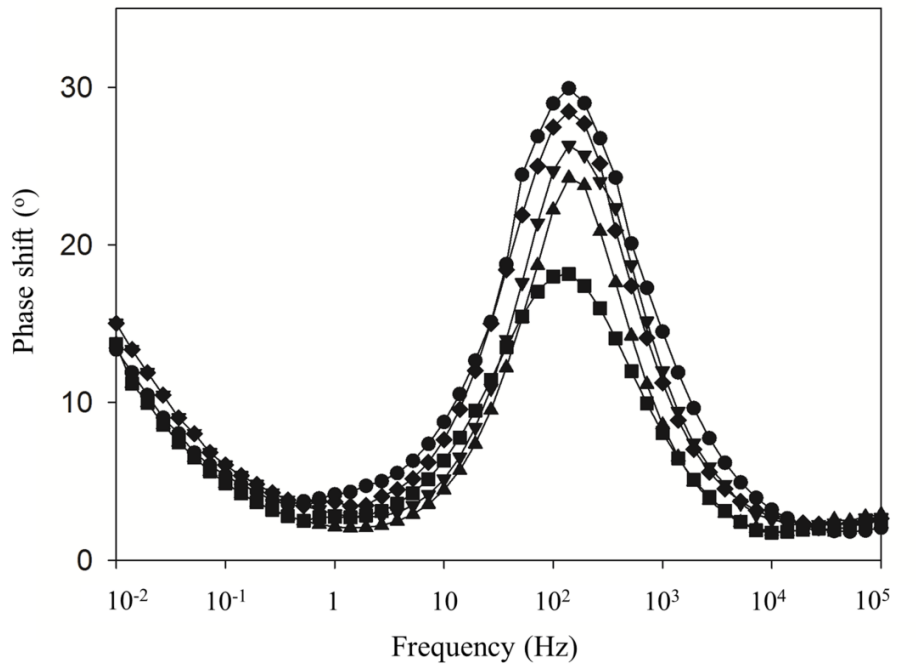
Phase shift (°)
0
10
20
30
10-2
10-1
1
10
102
103
104
105
Frequency (Hz)

(D)

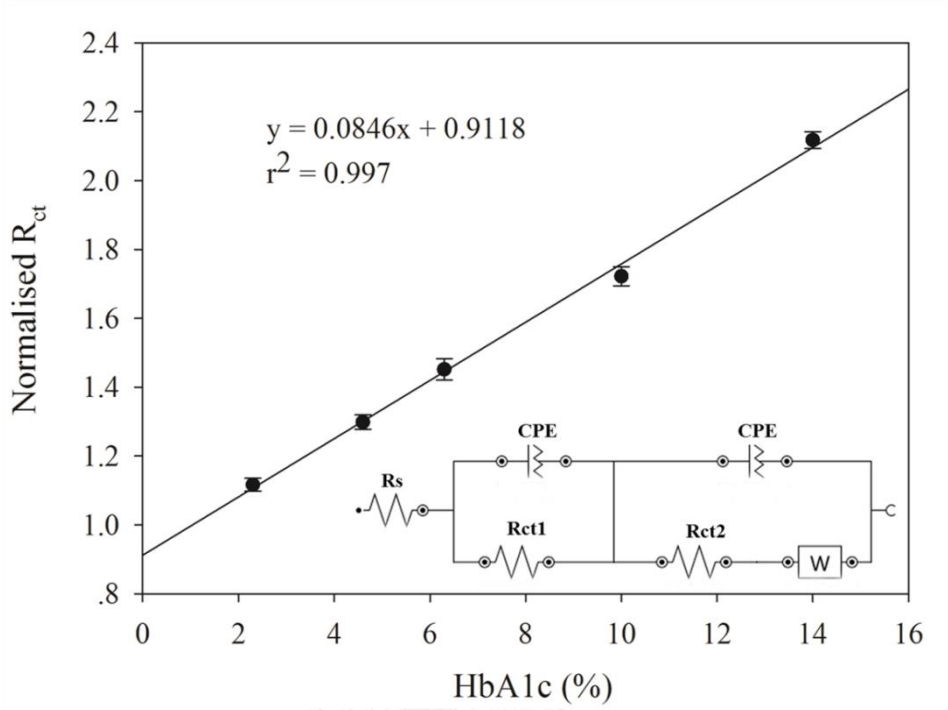

Figure 24. Impedance data obtained from (A) Nyquist plot, (B) Bode-modulus plot of the APBA-modified ESM after it was exposed to various concentrations of HbA1c: (■) 2.3%, (▲) 4.6%, (▼) 6.3%, (◆) 10%, and (●) 14% HbA1c; (C) Bode-phase plot and (D) variation of the normalised Rct with respect to the concentration of HbA1c (%). Inset right: an equivalent circuit for analysing the impedance data. The EIS spectra were obtained in 5 mM $Fe(CN)_6^{3-/4-}$ solution prepared in a working buffer at an open circuit voltage from 100 kHz to 10 mHz (ac amplitude, 10 mV).

The correlation between the haemoglobin concentration and each frequency was investigated to determine the optimal binding frequency at a specific binding constant. The relationship between the impedance derived from the Hp-modified ESM and haemoglobin concentration was compared at each frequency point in the

range from 100 kHz to 10 mHz and further analysed by reaching a compromise between the R-squared value and the correlation's slope, at which the maximised values were selected as the optimum binding target. The R-squared value and the slope from a duplicate measurement on a single paper-based electrode were plotted versus the frequency range, as shown in Fig. 25A. The R-squared value increased from the baseline and reached a maximum value close to 1 before returning to a lower level, whereas the slope gradually decreased until reaching a value close to 0 as the frequency increased. Hence, the optimal frequency of the binding interaction between the Hp-modified ESM and haemoglobin was determined to be 5.18 Hz. The correlation, as shown in Fig. 25B, represents an average impedance value of two different paper-based electrodes at a frequency of 5.18 Hz over a wide concentration range from 0.5 g dL^{-1} to 20 g dL^{-1}, with a regression equation of $y = 0.0500x + 1.8250$ ($r^2 = 0.987$). We further investigated whether the standard curve obtained from an impedance measurement at a specific single-frequency could be used in lieu of that from an impedance measurement recording the entire frequency range. Within the 95% confidence interval, a paired statistical analysis showed no significant differences between the two methods (p-value = 0.001), indicating the potential benefit of using a single frequency value for analysis. The optimal binding frequency for the APBA-modified ESM and HbA1c interaction was also evaluated using two parallel measurements on a single paper-based electrode, as demonstrated in Fig. 25C, and determined to be 9.99 Hz based on the full EIS sweep, at which the R-squared value was close to 1 and the constant slope was approximately zero. Fig. 25D shows a good correlation between the average impedance response at a specific frequency and its associated HbA1c concentration over a clinically relevant range, with a regression

equation of $y = 0.0869x + 1.6527$ ($r^2 = 0.991$). Compared with the results obtained from the impedance measurements recording the whole frequency range of the EIS spectrum, the single-frequency measurements showed no significant differences, at the 95% confidence interval (p-value = 0.001). These findings support the use of a single-frequency as an optimal binding frequency for constructing a calibration curve.

As demonstrated here, our proposed 3D-PEID for measuring multiple diabetes markers not only improves the assay time by using a single specific-frequency measurement, but also offers a great sensitivity to total haemoglobin and HbA1c values within the clinically required ranges, where 13.5–17.5 g dL^{-1} (male), 12.0–16.0 g dL^{-1} (female) of haemoglobin, and 3.8–6.4% of HbA1c are considered the normal reference ranges [84]. Our paper-based device is the first report on the simultaneous detection of total haemoglobin and HbA1c based on a single affinity sensing device covering a broad clinical range [48, 56, 60, 61]. Table 4 provides a brief summary of the current boronate-based electrochemical devices for assaying HbA1c. Thus, our proposed paper-based system provides a sensitive and cost-effective approach for glycaemic monitoring in individuals with diabetes, particularly for developing countries.

(A)

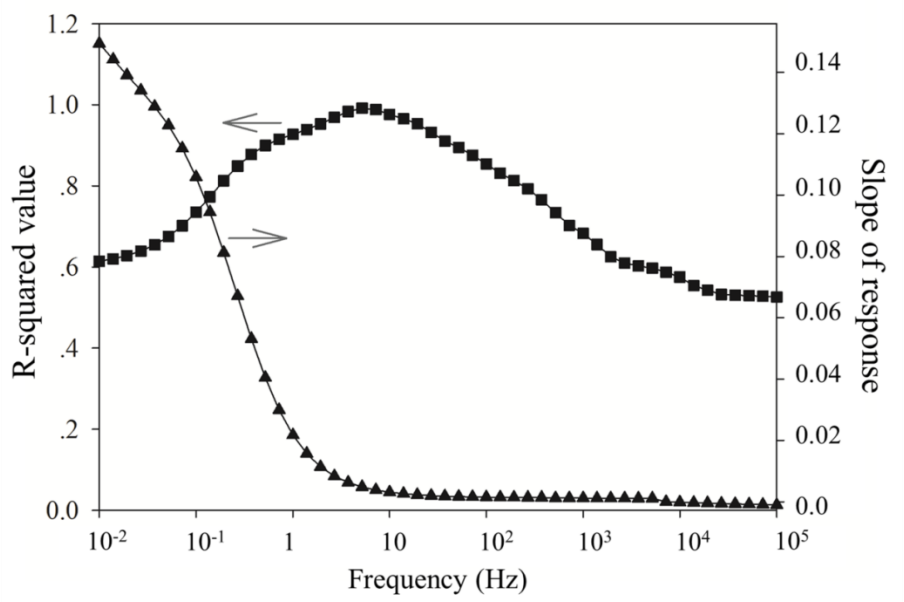
R-squared value
Slope of response
Frequency (Hz)
1.2
1.0
.8
.6
.4
.2
0.0
0.14
0.12
0.10
0.08
0.06
0.04
0.02
0.0
10-2
10-1
1
10
102
103
104
105

(B)

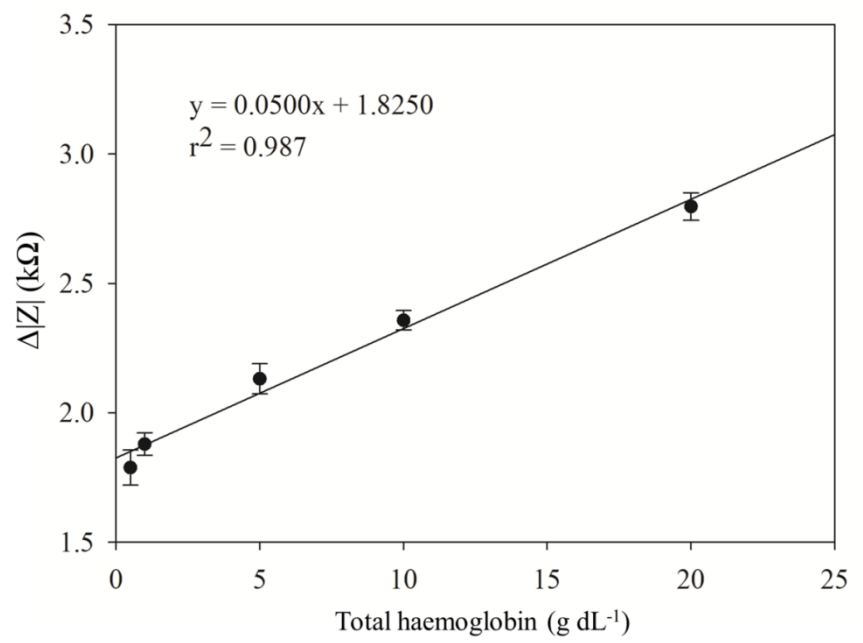
y = 0.0500x + 1.8250
r2 = 0.987
Δ|Z| (kΩ)
Total haemoglobin (g dL-1)
3.5
3.0
2.5
2.0
1.5
0
5
10
15
20
25

(C)

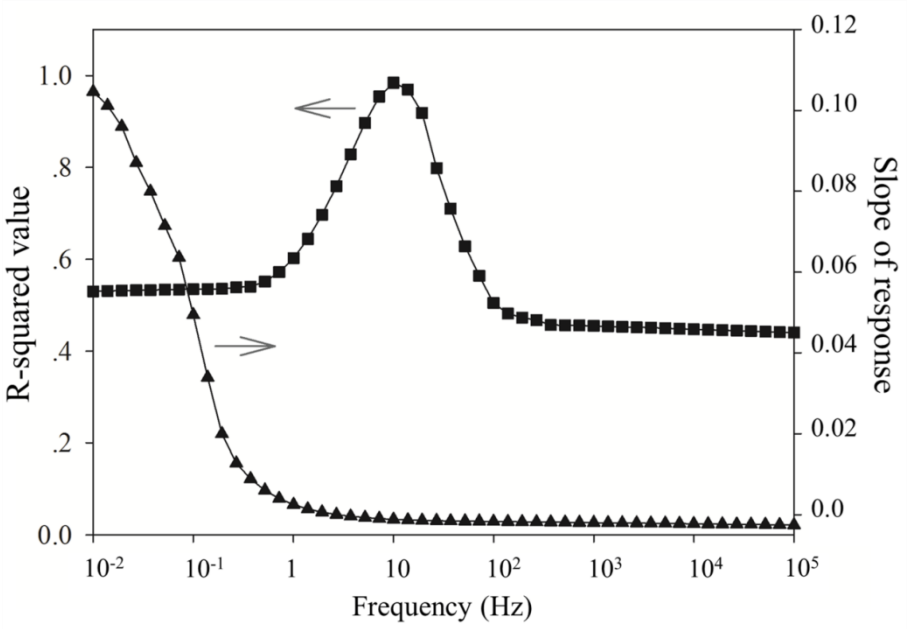

(D)

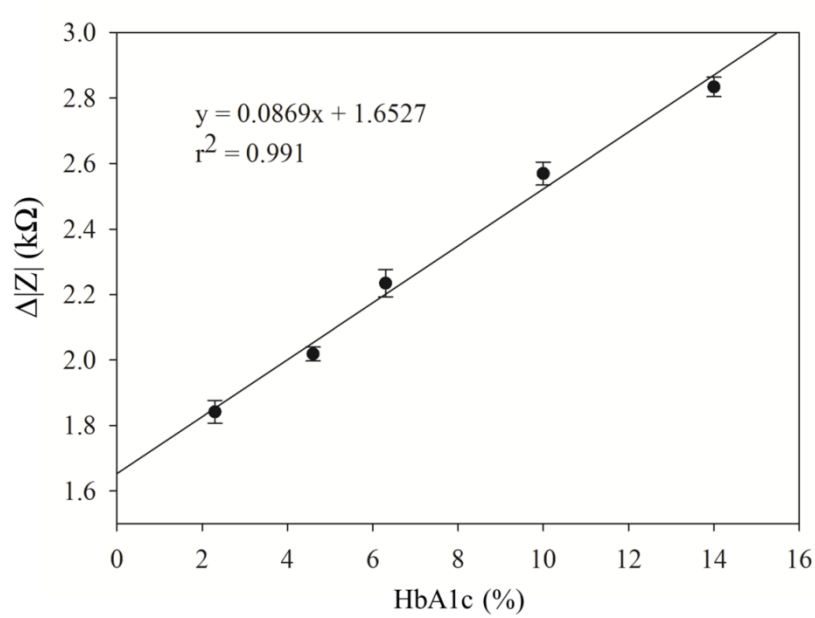

Figure 25. Optimal binding frequency for (A) the Hp-modified ESM and total haemoglobin interaction and (C) the APBA-modified ESM and HbA1c interaction: (■) R-squared value of response versus frequency, (▲) slope of response versus frequency; and (B&D) correlation between the average impedance response at a

specific frequency and its associated total haemoglobin and HbA1c concentration, respectively.

Table 4. Comparison of the analytical characteristics for HbA1c determination using boronate-based electrochemical methods and membrane-immobilised haptoglobin as an affinity matrix for the HbA1c immunosensor.

Approach	Dynamic detection range	Limit of detection	Repeat-ability[b]	Stability	Real sample analysis	Ref.
Cellulose membrane-immobilised haptoglobin as affinity matrix for HbA1c immunosensor	5 – 25% (7.8 – 39 nM)	ND	ND	ND	ND	[44]
Ferroceneboronic acid-based amperometric biosensor (Zirconium dioxide nanoparticle-modified electrodes)	6.8 – 14%	ND	12.7%	ND	Haemolysate	[50]
Flow immunoassay system (boronate-affinity on-chip column)	0 – 500 µg mL^{-1}	ND	ND	ND	Haemolysate	[49]
Thiophene-3-boronic acid monolayer-covered gold	0.2 – 1 µg mL^{-1}	ND	ND	ND	ND	[56]

Approach	Dynamic detection range	Limit of detection	Repeat-ability[b]	Stability	Real sample analysis	Ref.
electrodes						
Voltammetric measurement (poly(amidoamine) G4 dendrimer/formylphenylboronic acid-modified electrodes)	2.5 – 15%	ND	5%	ND	ND	[52]
Voltammetric measurement (cystamine/formylphenylboronic acid-modified electrodes)	4.5 – 15%	ND	ND	ND	Haemolysate	[53]
Thiophene-3-boronic acid-modified gold electrodes integrated into a microfluidic device	10 – 100 μg mL^{-1}	ND	ND	ND	ND	[61]
Thiophene-3-boronic acid-modified ring-shaped interdigitated electrodes	10 – 100 μg mL^{-1}	1 μg mL^{-1}	ND	ND	ND	[60]
Amperometric sensor (poly(terthiophene benzoic acid)/gold nanoparticle-modified electrodes)	0.1 – 1.5% (0.5 – 6%; impedance analysis)	0.052 ± 0.02% (0.27%; impedance analysis)	5.1%	92% of original response after 1 month	Haemolysate	[48]

Approach	Dynamic detection range	Limit of detection	Repeat-ability[b]	Stability	Real sample analysis	Ref.
Potentiometric method	ND	ND	ND	ND	Haemolysate	[54]
Voltammetric measurement (boronic acid-modified pyrroloquinoline quinine/ reduced graphene oxide composites)	9.4 – 65.8 $\mu g\ mL^{-1}$	1.25 $\mu g\ mL^{-1}$	8.5%	95% of original response after 1 month	Haemolysate	[51]
APBA-modified eggshell membranes	2.3 – 14%	0.19%	1.68%, 1.83% within-run CVs and 1.97%, 2.02% run-to-run CVs	69.54% of original response after 4 days	Haemolysate	[137]
3D-PEID for simultaneous detection of total haemoglobin and HbA1c	2.3 – 14%	0.21%	1.84%, 2.18% within-run CVs and 2.11%, 2.41% run-to-run CVs (total haemoglobin) 1.72%, 2.01% within-run CVs and 2.08%,	98.84% of original response after 1 month (Hp-modified ESM) 92.35% of original response after 1 week (APBA-modified ESM)	Haemolysate	Our present work

Approach	Dynamic detection range	Limit of detection	Repeat-ability[b]	Stability	Real sample analysis	Ref.
			2.21% run-to-run CVs (HbA1c)			

ND: not determined; [b] relative standard deviation for repeated measurements.

4.4.4 Regeneration and Reproducibility

The reversibility of the interaction between haemoglobin and HbA1c and their specific recognition elements was also investigated to assess the method's potential for low-cost applications. To evaluate the performance of the regeneration procedure, the regeneration efficiency (RE) was calculated according to the following equation [139]: RE = [1- (RT-B)/T] × 100%, where the RT represents the impedance response obtained after the regeneration cycle, B is the impedance response for the blank, and T is the impedance response before applying any regeneration step. Fig. 26A presents Nyquist plots for the reversible binding interaction of haemoglobin with its interface. The impedance of the Hp-modified ESM in the absence of haemoglobin (curve a) was smaller than that of the Hp-modified ESM in the presence of 1 g dL^{-1} haemoglobin (curve b). After applying the regeneration buffer (5 M urea containing 0.15 M sodium chloride at a pH of 11), the impedance decreased due to the release of the bound haemoglobin from the Hp-modified ESM (curve c). The impedance increased again after exposure to 10 g dL^{-1} of haemoglobin, indicating the rebinding of haemoglobin onto the Hp-modified ESM (curve d). After the second round of regeneration, the regeneration efficiency was 99.14% (curve e). The increase in impedance was then observed after re-incubating with 1 g dL^{-1} of haemoglobin (curve f). The reversible

binding of HbA1c onto the APBA interface was also observed, as shown in Fig. 26B. Compared with the baseline signal of the APBA-modified ESM (curve a), a significant increase in resistance was observed after exposure to 4.6% HbA1c (curve b). After the first round of regeneration using 10 mM sodium acetate buffer at a pH of 5, the impedance decreased after the first rinse (curve c) but remained greater than the initial curve (curve a). The APBA-modified ESM was then re-incubated with 10% HbA1c, resulting in a dramatic increase in resistance (curve d). After applying the subsequent round of regeneration, the impedance significantly decreased (curve e), with a regeneration efficiency of 99.07%. The increase in impedance was observed again after re-incubating with 4.6% HbA1c (curve f). After repeating the same procedure for 10 cycles, the regeneration efficiencies of the Hp-modified ESM and APBA-modified ESM were found to be 90.11% and 89.97%, respectively. These results showed that the proposed 3D-PEID could be used as a reusable sensing platform due to the reversible binding of haemoglobin and HbA1c to their recognition interfaces.

The reproducibility of the proposed device was examined using two levels of haemoglobin and HbA1c, i.e., 10 g dL^{-1} and 20 g $dL^{-1}$of haemoglobin; 4.6% and 10% HbA1c, with measurements performed on the same day and on three consecutive days using the same ESM device. The within-run reproducibility for each concentration (n = 10), expressed as coefficient of variation (CV), was 1.84%, 2.18%, 1.72%, and 2.01% for 10 g dL^{-1} and 20 g dL^{-1} of haemoglobin and 4.6% and 10% HbA1c, respectively. The run-to-run reproducibility for each concentration (n = 30) was 2.11%, 2.41%, 2.08%, and 2.21%, assessed on three consecutive days, for 10 g dL^{-1} and 20 g dL^{-1} of haemoglobin and 4.6% and 10% HbA1c, respectively. The CV

representing the variation between ten independently fabricated paper-based sheets was 1.96% and 2.10%, for 10 g dL^{-1} of haemoglobin and 4.6% HbA1c, respectively. These results indicate that our proposed system provides a great precision for the simultaneous detection of total haemoglobin and HbA1c with an acceptable reproducibility of fabrication.

(A)

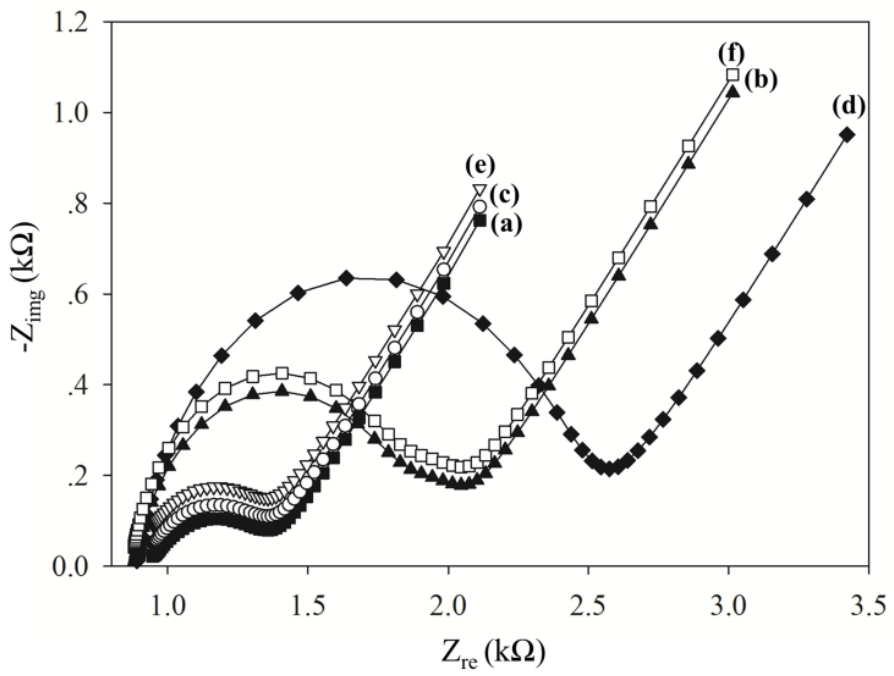

(B)

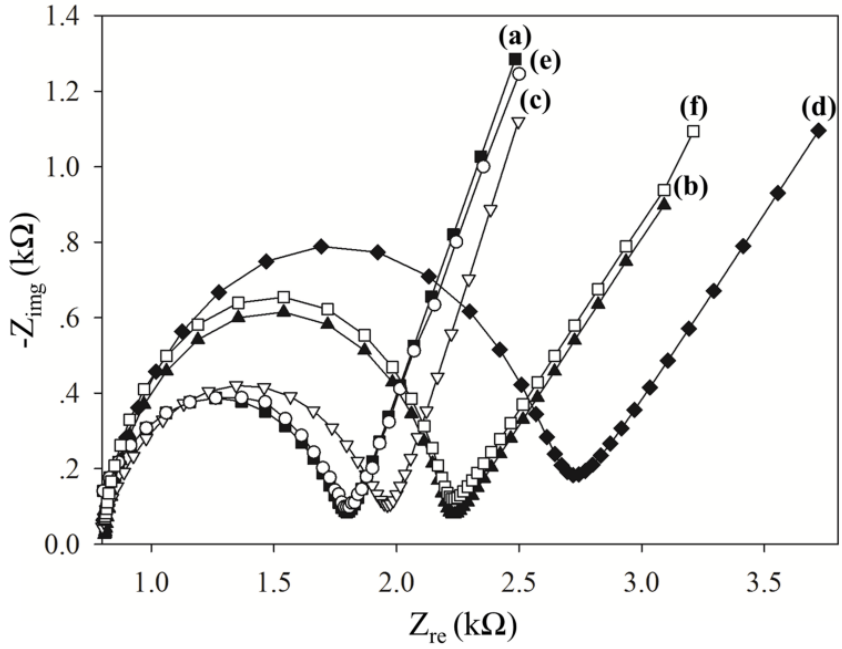

Figure 26. Nyquist plots for (A) step-wise modification of total haemoglobin: (a) an Hp-modified ESM, (b) incubated with 1 g dL^{-1} of haemoglobin, (c) regenerated with 5 M urea containing 0.15 M sodium chloride at pH 11, (d) incubated with 10 g dL^{-1} of haemoglobin, (e) washed with regeneration buffer, (f) re-incubated with 1 g dL^{-1} of haemoglobin; and (B) step-wise modification of HbA1c: (a) an APBA-modified ESM, (b) incubated with 4.6% HbA1c, (c) regenerated with sodium acetate buffer at a pH of 5, (d) incubated with 10% HbA1c, (e) washed with regeneration buffer, (f) re-incubated with 4.6% HbA1c.

The storage stability of the Hp-modified ESM and APBA-modified ESM was evaluated over a period of 4 weeks by storing the membrane in 100 mM phosphate buffer solution (pH 7) at 4 °C. To evaluate the performance of the Hp-modified ESM and APBA-modified ESM, the impedance response was measured after incubation with the same concentration of haemoglobin (10 g dL^{-1}) and HbA1c standard solution

(4.6%), respectively. The results showed the long-term stability of the Hp-modified ESM to be 98.84% over a shelf-life of at least 4 weeks, as shown in Fig. 27A, indicating that the Hp-modified ESM would be suitable for long-distance transport to remote regions, particularly in resource-limited settings. The remarkable stability of the Hp-modified ESM was largely due to the biocompatible microenvironment of the ESM comprising the net-veined structure and the gas-permeable hydrophilicity, which may stabilise the activity of the protein during the long-term storage. For the stability of APBA-modified ESM, as shown in Fig. 27B, the activity of the APBA sensing interface was 92.35% over a one-week period; however, the signal response gradually decreased until reaching an activity of 53.75% after a four-week storage period. The decrease in signal was probably caused by the loss of APBA activity during the prolonged storage period.

(A)

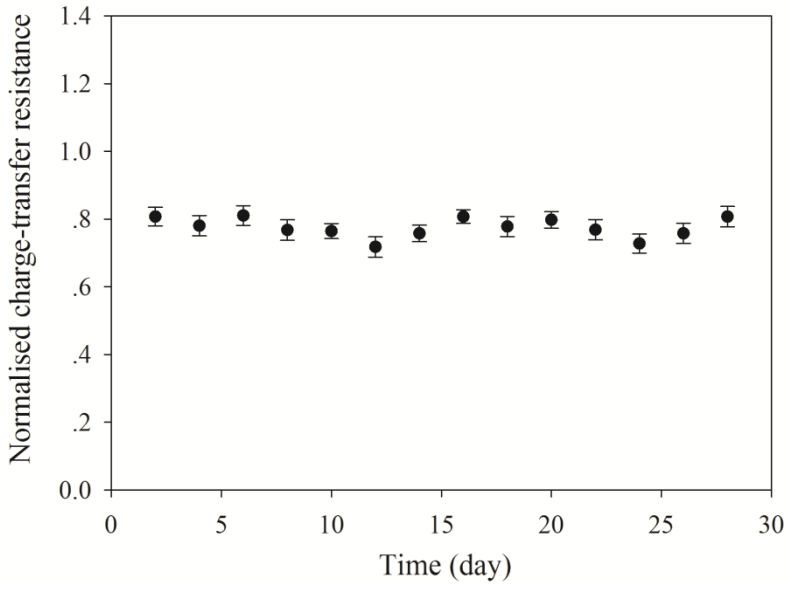

(B)

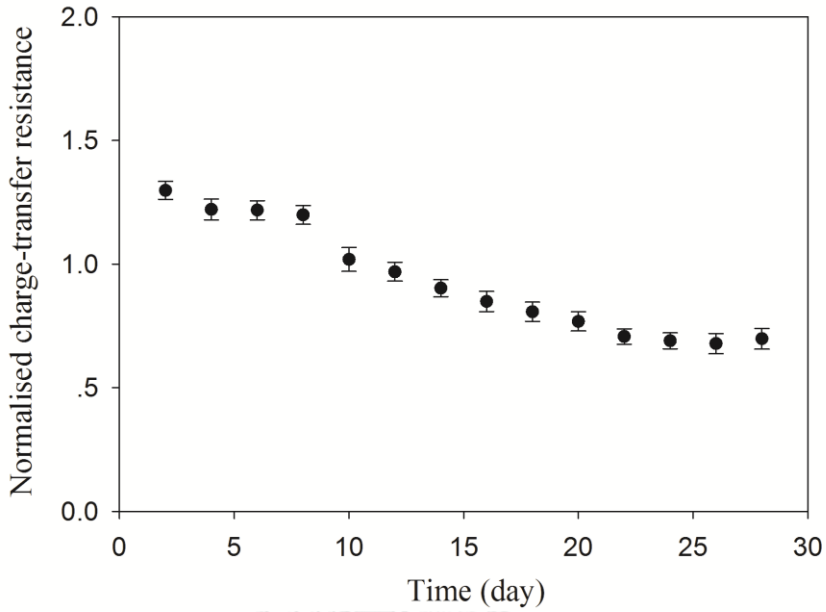

Figure 27. Storage stability of the (A) Hp-modified ESM and (B) APBA-modified ESM keeping in 100 mM phosphate buffer solution (pH 7) over a period of 4 weeks at 4 °C. Each point is the mean value from a duplicate measurement of 10 g dL^{-1} haemoglobin and 4.6% HbA1c; the error bar represents the standard deviation.

4.4.5 Selectivity study

The evaluation of endogenous and exogenous interfering substances present in clinical specimens is essential before the diagnostic system can be implemented clinically. Whole blood specimens contain not only haemoglobin, but also glucose, glycated albumin, and other glycated proteins and sugars found in serum. The boronate recognition group is able to bind to the diol group of any glycated protein or sugar present in the blood matrix. Accordingly, the sample pre-treatment process is crucial to removing the interfering species in the whole blood before being subjected

to the impedance measurement. As stated earlier, in our study, the interfering agents present in plasma were negligible due to the well-prepared treatment of blood samples. Thus, to assess the analytical performance of the proposed system for measuring multiple diabetes markers, human serum albumin and non-glycated haemoglobin (HbAo) were tested as potential interferences in the sensing interfaces. Figs. 28A and B show the Nyquist plots for examining the selectivity of the Hp-modified ESM and APBA-modified ESM for varying levels of human serum albumin and HbAo, respectively. Compared with the signal baseline obtained from the Hp-modified ESM and APBA-modified ESM, the impedance responses remain virtually unchanged by human serum albumin and HbAo over the concentration range of 3–6 g dL^{-1} and 10–20 g dL^{-1}, respectively. These results indicate that the proposed system was highly selective in determining the haemoglobin and HbA1c values in actual specimens, enabling the possibility of using the present method to assess the glycaemic levels in clinical practice. Most importantly, compared with other available methods for HbA1c determination, the boronate affinity assay was less affected by the presence of genetic variants and chemical derivatives of haemoglobin [119, 120]. For the interpretation of the HbA1c results, additional relevant factors, such as severe iron-deficiency anaemia, haemolytic anaemia or any condition that directly affects the erythrocyte lifespan, e.g., renal failure, should be taken into account in practical considerations.

(A)

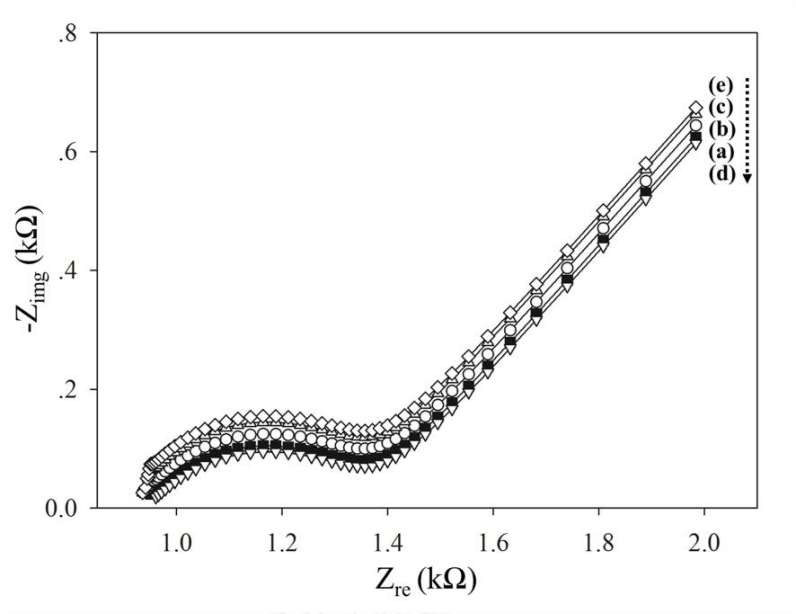

(B)

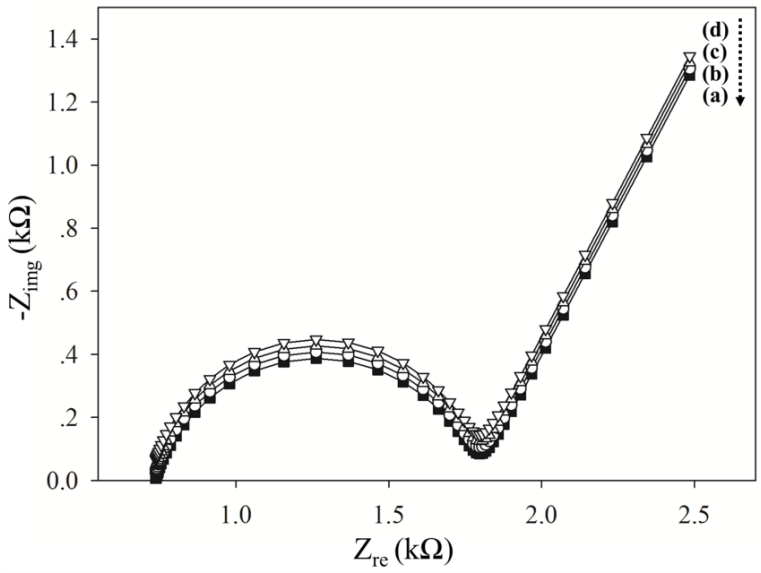

Figure 28. Nyquist plots for investigating the selectivity of (A) Hp-modified ESM immobilised with different concentrations of human serum albumin: (a) 0 g dL^{-1}, (b) 3 g dL^{-1}, (c) 4 g dL^{-1}, (d) 5 g dL^{-1}, and (e) 6 g dL^{-1} of human serum albumin; and (B) APBA-modified ESM immobilised with different concentrations of HbAo: (a) 0 g dL^{-1}, (b) 10 g dL^{-1}, (c) 15 g dL^{-1}, and (d) 20 g dL^{-1} of HbAo.

4.4.6 Real sample analysis and assay comparison

A demonstration of the ability of the diagnostic system to detect the percentage of HbA1c in real human blood samples is essential before it can be implemented clinically. Thus, to further investigate its potential practical application, the effectiveness of the proposed 3D-PEID for measuring the total haemoglobin and HbA1c values was assessed using the real blood samples of healthy and diabetic volunteers, for which the haematocrit values were within the range of 37–48%. Each red blood cell lysate sample was measured individually using our system and with the automated clinical chemistry analyser. The results obtained from the proposed 3D-PEID were compared with those determined with the turbidimetric inhibition immunoassay on an automated large-scale analyser. The agreement and correlation between the two approaches were evaluated via a Bland-Altman bias plot and a Passing-Bablok regression analysis, respectively. As demonstrated in Figs. 29A and C, the data showed acceptable agreement between the results provided by our proposed device and the commercially available kit within an agreement interval of ± 1.96 SD. These results also showed zero bias and a reliable relationship, which indicates that these two approaches could be used interchangeably. Moreover, as shown in Figs. 29B and D, the regression equations according to the Passing-Bablok analysis of the total haemoglobin and HbA1c were $y = 0.9667x + 0.5233$ and $y = 0.9850x + 0.0640$, respectively. These results indicated a good correlation between the two methods throughout the entire measurement range. Within a 95% confidence interval, the values of the y-intercept (0.5233 g dL^{-1}) and the slope (0.9667) were significantly reliable and covered a range of 0.1136–0.8916 g dL^{-1} and 0.9439 to 0.9929, respectively. Additionally, for the determination of HbA1c, the values of the

y-intercept (0.0640 %) and the slope (0.9850) were trustworthy and covered a range of -0.0200–0.4453 % and 0.9277 to 1.0000, respectively. The data presented in this proof-of-concept work demonstrates the validity of the proposed device for the simultaneous detection of total haemoglobin and HbA1c in clinical diagnostics using actual clinical specimens. Our paper-based devices offer the great benefit of an onsite clinical test for monitoring the glycaemic status in individuals with diabetes.

(A)

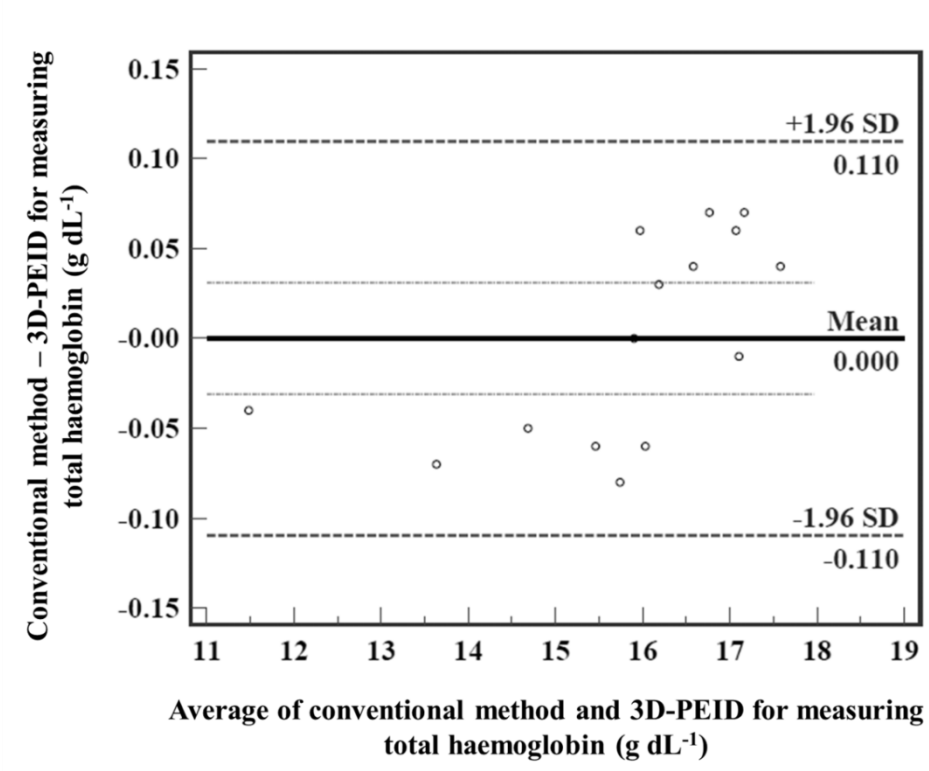

(B)

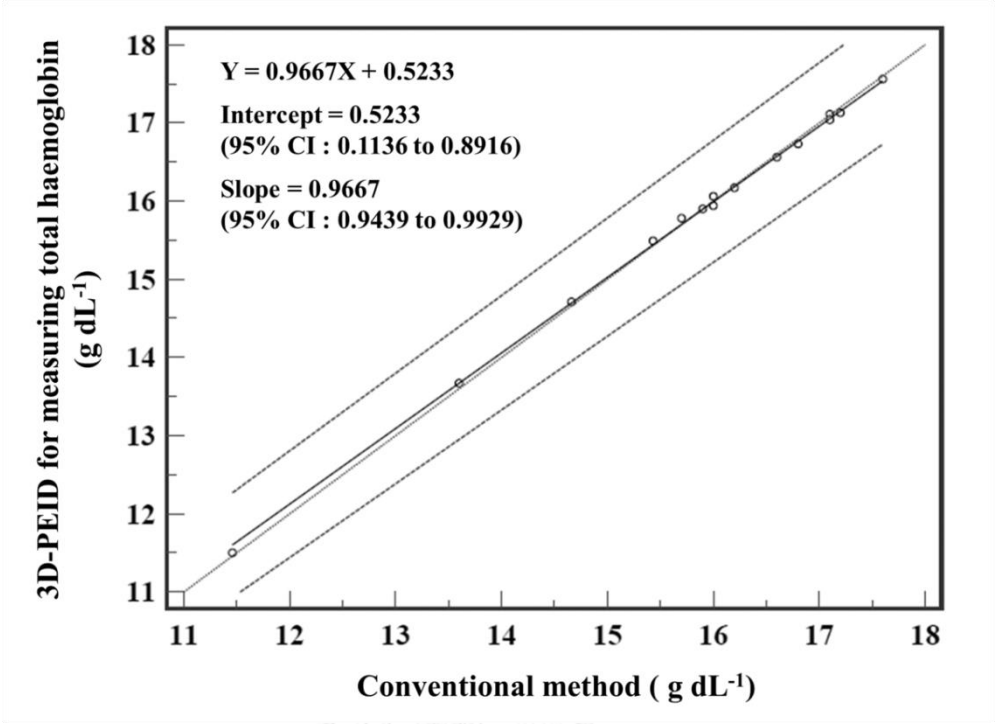
Y = 0.9667X + 0.5233
Intercept = 0.5233
(95% CI : 0.1136 to 0.8916)
Slope = 0.9667
(95% CI : 0.9439 to 0.9929)
3D-PEID for measuring total haemoglobin (g dL-1)
Conventional method (g dL-1)
11
12
13
14
15
16
17
18

(C)

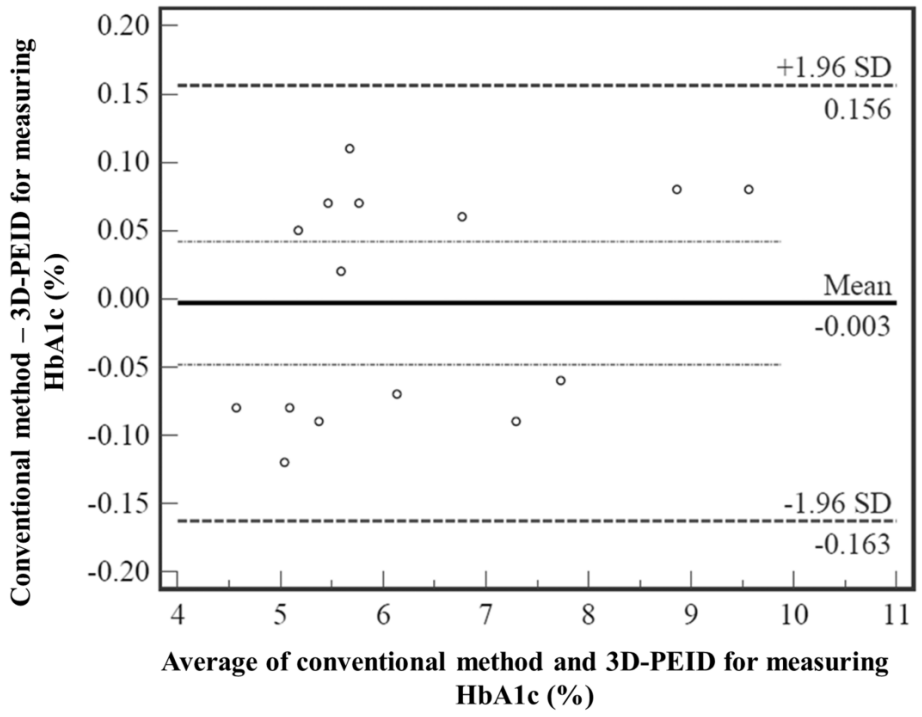
+1.96 SD
0.156
Mean
-0.003
-1.96 SD
-0.163
Conventional method – 3D-PEID for measuring HbA1c (%)
Average of conventional method and 3D-PEID for measuring HbA1c (%)
0.20
0.15
0.10
0.05
0.00
-0.05
-0.10
-0.15
-0.20
4
5
6
7
8
9
10
11

(D)

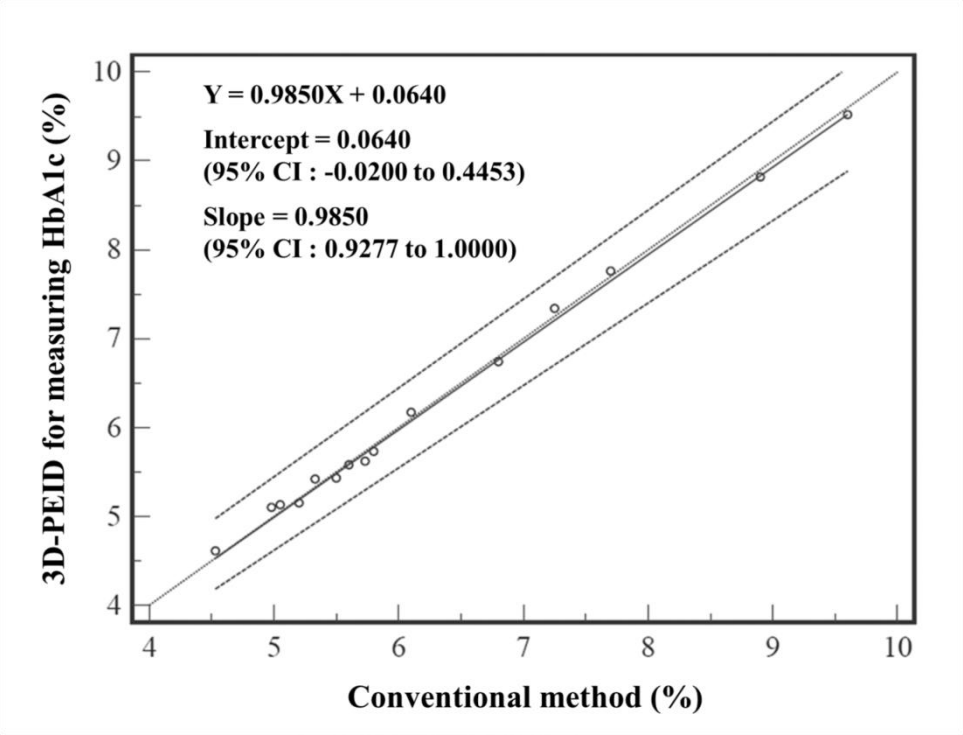

Figure 29. Comparison of the proposed 3D-PEID and the current large-scale method for total haemoglobin and HbA1c measurements using (A&C) a Bland-Altman bias plot and (B&D) Passing-Bablok regression analysis, respectively.

4.5 Conclusions

We have demonstrated a selective 3D-PEID for multiplexed measurement of diabetes markers using a single EIS platform. By monitoring at a single frequency value, the proposed device has a considerable advantage over the conventional EIS measurements in terms of assay time, allowing a decrease in data acquisition time by a factor of 15. However, further improvement on the EIS processing software would be needed to run EIS at the desired frequency value. As demonstrated here, our proposed 3D-PEID not only provides a precise measurement with a wide dynamic

concentration range but also offers a great sensitivity for the total haemoglobin and HbA1c values within the clinically relevant ranges. Such capabilities make this cost-effective device useful for monitoring the glycaemic status in individuals with diabetes. In addition to being a proof-of-concept work, our system performed well compared with the commercial automated method using actual clinical samples, even in specimens obtained from diabetic patients. Conceivably, the successful development of this multiplexed 3D-PEID would be suitable for near-patient monitoring in remote areas. However, POCT systems require not only the production of affordable and portable devices but also the development of the detection instruments to measure the signal into a portable and multi-channel measurement device.

4.6 Acknowledgements

This research was financially supported by the Thailand Research Fund through Research Team Promotion Grant (RTA5780005) and the Ratchadapisek Sompot Endowment Fund of Chulalongkorn University (WCU-58-002-HR). Y.B. acknowledges the Thailand Research Fund through the Royal Golden Jubilee Ph.D. Program (under grant No. PHD/0164/2553) and the Graduate School, Chulalongkorn University for the Tuition Fee Scholarship. Dr. Poomrat Rattanarat is acknowledged for providing excellent technical assistance with the screen-printed fabrication process.

CHAPTER V

SUBMITTED MANUSCRIPT

Boronate-Modified Interdigitated Electrode Array for Selective Impedance-Based Sensing of Glycated Hemoglobin

Yuwadee Boonyasit,[†,‡] Wanida Laiwattanapaisal,[§] Orawon Chailapakul,[#] Jenny Emnéus,[‡] and Arto R. Heiskanen*[,‡,§]

[†] Graduate Program in Clinical Biochemistry and Molecular Medicine, Faculty of Allied Health Sciences, Chulalongkorn University, Bangkok, 10330, Thailand.

[‡] Department of Micro- and Nanotechnology, Technical University of Denmark, Kgs. Lyngby, 2800, Denmark.

[§] Department of Clinical Chemistry, Faculty of Allied Health Sciences, Chulalongkorn University, Bangkok, 10330, Thailand.

[#] Electrochemistry and Optical Spectroscopy Research Unit (EOSRU), Department of Chemistry, Faculty of Science, Chulalongkorn University, Bangkok, 10330, Thailand.

Submitted for publication in *Anal Chem*

5.1 Abstract

An impedance-based label-free affinity sensor was developed for the recognition of glycated hemoglobin (HbA1c). Interdigitated gold microelectrode arrays (IDA) were first modified with a self-assembled monolayer of cysteamine followed by cross-linking with glutaraldehyde and subsequent binding of 3-aminophenylboronic acid (APBA), which selectively binds HbA1c via cis-diol interactions. Impedance sensing was demonstrated to be highly responsive to the clinically relevant HbA1c levels (0.1%-8.36%) with a detection limit of 0.024% (3□). The specificity of the assay was evaluated with non-glycated hemoglobin (HbAo), showing that the impedance response remained unchanged over the concentration range of 10 to 20 g dL-1 HbAo. This demonstrated that the sensor system could be used to specifically distinguish HbA1c from HbAo. Moreover, the binding of HbA1c to the APBA-modified electrodes was reversible, providing a reusable sensing interface as well as showing a stable response after 4 weeks (96% of the initial response). When assaying normal (4.10%) and diabetic (8.36%) HbA1c levels (10 assays per day during a three-day period including a regeneration step after each assay), the overall assay reproducibility, expressed as relative standard error of mean (n = 30), was 1.1%. The performance of the sensor system was also compared with a commercial method (n =15) using patient-derived blood samples. A good agreement (Bland-Altman bias plot) and correlation (Passing-Bablok regression analysis) was demonstrated between the boronate-based affinity sensor and the standard method.

Keywords: Glycated hemoglobin (HbA1c), boronate-modified interdigitated electrode array, electrochemical impedance sensing, diabetes mellitus.

5.2 Introduction

Diabetes is one of the most challenging health problems worldwide and has devastating impact on the quality of life and healthcare expenditures [1]. Glycated hemoglobin (HbA1c) has become a significant index of assessing long-term glycemic control, therapeutic effectiveness, and patient compliance [118]. HbA1c is generated by a non-enzymatic glycation reaction at the N-terminal valine residues in the β-chains of hemoglobin (Hb), corresponding to the 100 to 120-day lifespan of erythrocytes. In clinical practice, the quantification of HbA1c is now an indispensable tool in both routine management and diagnosis of diabetes, including type I and type II diabetes. HbA1c measurements are also used to achieve stringent control in pregnant diabetic individuals, thereby, minimizing the perinatal risk of congenital malformations, overweight infants, as well as complications of pregnancy [140]. The American Diabetes Association (ADA) recommends the HbA1c level be maintained below 7%, and using HbA1c testing for diagnosis of diabetes [5].

Current methods to detect HbA1c include electrophoresis [88], ion-exchange chromatography [141], boronate affinity chromatography [37], mass spectrometry [33-35], immunoassays [43-45, 91], piezoelectric sensors [39-41], chemiluminescence [42], surface plasmon resonance [58], and surface-enhanced resonance Raman spectroscopy [59]. However, most of these techniques require sophisticated instrumentation with multiple operational steps at high cost, and fail to meet the clinical demand of portability. Consequently, development of selective, sensitive, trustworthy, and portable devices for measurement of HbA1c is needed. Electrochemical affinity sensors have considerable potential for developing portable analytical devices due to their sensitivity, low cost, simplicity, and possibility for

miniaturization [62]. Since the boronate groups are able to form selective and reversible bonds with the cis-diol groups in different glycated biomolecules under alkaline conditions [63], boronate ligands are now frequently used for developing affinity-based sensing interfaces to capture glycosylated biomolecules, e.g., HbA1c [40], saccharides [40, 142], bacteria [143], nucleotides [144], DNA aptamers [145], cancer cells [146], and antibodies [147, 148].

Table 5 compares different electrochemical boronate-based methods, their mode of operation, linear range and limit of detection (LOD) for determination of HbA1c. Majority of the published approaches are still based on different voltammetric techniques, although during the recent years contributions using electrochemical impedance spectroscopy (EIS) have increased in number. EIS offers great potential for developing label-free sensors as has been widely presented for applications relying on recognition by antibodies and DNA [149]. EIS provides important insights into the signal transduction and processes occurring at the electrode interface, reflecting the physical and chemical structure in the amplitude and phase of the response [150]. EIS-based HbA1c sensors mainly rely on a self-assembled monolayer (SAM) of thiophene-3-boronic acid (T3BA) [56, 60, 61]. The response of different EIS-based sensors is primarily related to the changes in the charge transfer resistance using hexacyanoferrate as the redox indicator, although some sensors have also relied on the capacitive behavior of the electrode interface [60, 61]. Their linear range has yet to meet the clinical range of HbA1c in real blood samples and the ability to detect HbA1c in actual clinical specimens has yet to be demonstrated. Although good selectivity and a wide linear range for HbA1c detection were previously achieved on boronate-modified eggshell membranes, the stability of the proposed system needs to

be improved [137, 151]. In general, sensitivity, selectivity, reproducibility, and long-term stability of HbA1c sensors need to be improved to meet the clinical requirements. Effective comparison of analytical performance shown by different electrochemical HbA1c sensors is, however, difficult since different units are used to express the linear range and LOD. According to the clinical interpretation norms, HbA1c levels should be reported as mmol mol^{-1} or % of total Hb [152].

In this study, a boronate affinity sensor array was developed for selective label-free EIS detection of HbA1c over the clinically relevant concentration range. Electrode chips, having 12 individually addressable three-electrode systems comprising interdigitated working electrodes (Figure 30) [153], were fabricated and modified with 3-aminophenylboronic acid (APBA). To our knowledge, the presented sensor system is the first one capable of assessing HbA1c levels covering the whole clinically required range with the necessary sensitivity, reproducibility, and excellent operational and storage stability. The sensor system was able to distinguish HbA1c from non-glycated hemoglobin (HbAo) with a low detection limit and demonstrate an excellent agreement with a standard method. Moreover, HbA1c binding to the APBA-modified electrodes was reversible, thereby, providing a reusable sensing system. Our sensor demonstrates great improvement in HbA1c assays, having the potential for integration into a microfluidic array system [154] for diabetes diagnosis and management.

Table 5. Analytical characteristics of electrochemical boronate-based HbA1c sensors

Approach (recognition element/ electrode/ redox indicator/ label)	Linear range[a]	LOD[a]	Reproducibility[b]	Stability[c] (%, Period)	Real samples	Ref.
Electrochemical Impedance Spectroscopy (EIS)						
T3BA[d]/ Au disk/ HCF[d]/ None	0.1-1 µg/mL	ND[e]	ND[e]	ND[e]	ND[e]	[56]
T3BA[d]/ Au thin film/ None/ None	10-100 µg/mL	ND[e]	ND[e]	ND[e]	ND[e]	[61]
T3BA[d]/ Au thin film/ None/ None	10-100 µg/mL	1 µg/mL	ND[e]	ND[e]	ND[e]	[60]
APBA[d]-modified ESM[d]/ Screen printed Au/ HCF[d]/ None	2.3-14%	0.19%	RSD[b] 2.0% (n = 30)	70%, 4 days	Hemolysate	[137]
APBA[d]-modified ESM[d]/ Screen printed carbon/ HCF[d]/ None	2.3-14%	0.21%	RSD[d] 2.15% (n = 30)	92%, 1 week	Hemolysate	[151]
APBA[d] / Au thin film / HCF[d] / None	0.10-8.36%	0.024%	RSE[b] 1.1% (n = 30 assays each with 12 measurements)	96%, 28 days	Hemolysate	This work
Electrochemistry others (technique)						
FcBA[d]/ PG[d]-ZrO_2NP/ Fc[d]/ None (SWV[d])	6.8-14%	ND[e]	RSD[b] 12.7% (n = 3)	ND[e]	Hemolysate	[50]
FcBA[d]/ Au thin film/ FcM[d]/ GOx[d] (CV[d])	2.5-15%	ND[e]	RSD[b] 5% (n = 3)	ND[e]	ND[e]	[52]
FPBA[d]/ Au thin film/ FcM[d]/ GOx[d] (CV[d])	4.5-15%	ND[e]	ND[e]	ND[e]	Hemolysate	[53]
APBA[d]/ Screen printed carbon-AuNP/ H_2O_2/ None (CAm[d])	0.1-1.5%	0.052%	RSD[b] 5.1% (n = 5)	92%, 1 month	Hemolysate	[48]
PBA[d]/ GC[d]/ ARS[d]/ None (Pm[d])	ND[e]	ND[e]	ND[e]	ND[e]	Hemolysate	[54]
APBA[d]/ GC[d] disk-graphene oxide/ Immobilized PQQ[d]/ None (DPV[d])	9.4-65.8 µg/mL	1.25 µg/mL	RSD[b] 8.5% (n = 6)	95%, 1 month	Hemolysate	[51]

[a] Linear range and limit of detection (LOD) are usually given in either µg/mL or % HbA1c of the total Hb contents. [b] The published evaluations of sensor reproducibility (expressed as relative standard deviation, RSD, or relative standard error of mean, RSE) are based on repeated determination of the same concentration of HbA1c using one or multiple electrodes. [c] The stability % refers to the initial response obtained with the tested sensor. [d] Abbreviations: APBA (aminophenylboronic acid); ARS

(alizarin red); CAm (chronoamperometry); CV (cyclic voltammetry); DPV (differential pulse voltammetry); ESM (eggshell membrane), Fc (ferrocene); FcBA (ferroceneboronic acid); FcM (ferrocenemethanol); FPBA (formylphenylboronic acid); GC (glassy carbon); GOx (glucose oxidase); HCF (hexacyanoferrate); PBA (phenylboronic acid); Pm (potentiometry); PG (pyrolytic graphite); PQQ (pyrroloquinoline quinone); SWV (square wave voltammetry); T3BA (thiophene-3-boronic acid). [e] ND – not determined.

5.3 Experimental Section

5.3.1 Reagents and chemicals

All reagents and chemicals used were of analytical grade and used as received. A Lyphochek® HbA1c linearity set, Lyphochek® diabetes controls, and in2itTM (II) A1c test kits were acquired from BioRad Laboratories (Hercules, CA, USA). 3-Aminophenylboronic acid (APBA), 4-ethylmorpholine, sodium chloride, potassium chloride, ethylenediaminetetraacetic acid tripotassium salt dihydrate (K_3EDTA), potassium hexacyanoferrateII ($[Fe(CN)_6]^{4-}$), potassium hexacyanoferrateIII ($[Fe(CN)_6]^{3-}$), glutaraldehyde (25% solution in water, specially purified for use as an electron microscopy fixative), sodium acetate trihydrate, glacial acetic acid, potassium cyanide, potassium phosphate monobasic, sodium phosphate monobasic, sodium phosphate dibasic, potassium hydroxide, hydrogen peroxide (30% solution in water), 96% ethanol, acetone, cysteamine hydrochloride, Brij® 35 (polyoxyethylene (23) lauryl ether; 30% solution in water], and non-glycated hemoglobin (HbAo) were obtained from Sigma-Aldrich Corporation (St. Louis, MO, USA). All aqueous

solutions were prepared in ultrapure water (resistivity 18.2 Mohm cm) from a Milli-Q® water purification system (Millipore Corporation, Billerica, MA, USA). A cyanmethemoglobin standard solution was available from R.C.M. Supplies Co., Ltd. (Bangkok, Thailand). Micro-haematocrit tubes were from Vitrex Medical A/S, Herlev, Denmark, and VACUETTE® vacuum tubes were from Greiner Bio-One GmbH, Kremsmünster, Austria. AZ® 5214E positive photoresist was acquired from MicroChemicals GmbH, Ulm, Germany.

5.3.2 Fabrication of IDA chips

The microelectrode chips were fabricated using UV photolithography with a lift-off process on single-side polished 4-inch silicon wafers having a 500-nm thermally grown (1050 °C) insulating silicon dioxide layer [153]. Briefly, positive photoresist (1.5 μm) was spin coated on silicon wafers and subjected to image reversal process. After development, 150 nm deep undercuts were formed by 100 s isotropic etching in buffered hydrofluoric acid (BHF) to eliminate formation of lift-off ears at the edges of the gold patterns. A titanium (10 nm) and gold (150 nm) film were deposited by electron beam evaporation. After lift-off under ultrasonication in acetone finalizing the metal patterning, a 500-nm silicon nitride passivation layer was deposited by plasma-enhanced chemical vapor deposition and patterned by UV photolithography using another lithographic mask followed by reactive ion etching to expose the active electrode areas and contact pads. The photoresist was removed by ultrasonication in acetone followed by rinsing with ethanol and then deionized water. The layout of the chip with 12 identical three-electrode systems is depicted in Figure

30a. Each measurement site (inset) consists of an interdigitated working electrode (ID-WE; 500-µm digits, 10-µm width/gap), counter electrode (CE; Ø 700 µm), and reference electrode (RE; Ø 50 µm).

5.3.3 Electrode preparation and surface modifications

Before using the IDA chips for experiments, they underwent an initial cleaning by 10-min ultrasonication in acetone, followed by an intermediary rinsing with ethanol and finally with water. For experiments, each chip was placed in a setup fabricated from 5-mm poly(methyl methacrylate) (PMMA) as illustrated in Figure 30b. A PMMA plate (1) served as a support for the chip (2) and a patterned lid (3) defined a well (10×10 mm^2) for liquid handling. The lid was sealed on the chip using a poly-dimethylsiloxane (PDMS) gasket (4). The assembly was fastened together with screws. After assembling the system, the electrodes were cleaned chemically (25% v/v H_2O_2 and 50 mM KOH) followed by electrochemical cleaning (a potential sweep: -200 to -1200 mV in 50 mM KOH) [155]. First, the electrodes were modified with a cysteamine (200 mM; 1 h) self-assembled monolayer (SAM) followed by glutaraldehyde and then APBA to create the final boronate affinity layer. Glutaraldehyde served as a homo-bifunctional cross-linker between the amine moieties of APBA and cysteamine. After each electrode modification step, the chip surface was rinsed thoroughly with water. The influence of the modification steps was characterized by EIS using 5 mM ($[Fe(CN)_6]^{3-/4-}$) prepared in 10 mM 4-ethylmorpholine buffer (pH 8.5) containing 250 mM KCl and 100 mM NaCl. As shown in Figure 30b and c, during impedance measurements the setup had a tailor-

made printed circuit board (PCB) (5) with spring-loaded pins (Figure 30c, inset) to provide electric connections to the electrodes through the patterned holes in the lid (3).

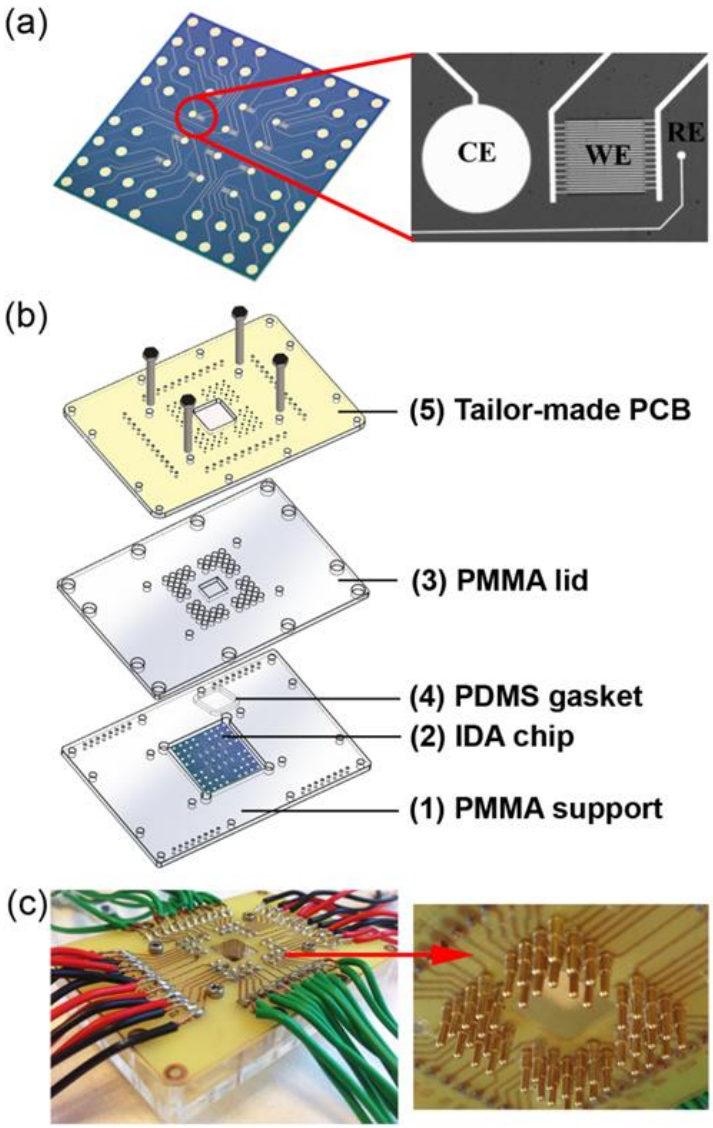

Figure 30. (a) Layout of the IDA chip with 12 measurement sites each having a 3-electrode configuration (inset: a microscopic image of one measurement site with a counter electrode (CE), interdigitated working electrode (IDE-WE), and reference electrode (RE)). (b) Measurement setup: (1) A 5-mm PMMA plate as a support for an IDA chip (2); a 5-mm PMMA lid (3), defining the electrochemical cell (10 × 10

mm^2); a PDMS gasket (4) for sealing around the center of the IDA chip; a tailor-made PCB (5) for electrical connections to the individually addressable electrodes. The entire setup is tightened with screws. (c) A photo of the assembled setup with the mounted PCB (inset: magnification of the spring-loaded pins).

5.3.4 Label-free EIS detection of HbA1c

A Reference 600 potentiostat from Gamry Instruments (Warminster, PA, USA) was employed for impedance measurements using the setup described above. The impedance spectra were acquired using Gamry Framework software (Version 6.11) over the frequency range between 100 kHz and 0.1 Hz using a sinusoidal potential of 10 mV_{rms}. The measurements were performed using 120 µL an electrolyte solution composed of 5 mM $[Fe(CN)_6]^{3-/4-}$, 250 mM KCl, and 100 mM NaCl buffered with 10 mM 4-ethylmorpholine (pH 8.5) according to a previously published protocol [56]. Prior to acquiring impedance spectra, the incubation with HbA1c standards or hemolysate samples was done using the volume of 85 µL followed by a thorough rinsing with the measurement buffer. By using a regeneration buffer (10 mM sodium acetate; pH 5 adjusted using acetic acid), the APBA-modified microelectrode surface could be used repeatedly since the binding of diol groups to boronate is unstable under acidic conditions [50].

5.3.5 Sample preparation

For investigations involving human subjects, the appropriate institutional review board approval was obtained by the Ethics Review Committee for Research Involving Human Research Subjects, Health Sciences Group, Chulalongkorn University (ECCU) under the approval number COA No. 057/2557. A written consent was obtained from each of the participants. In this study, healthy and diabetic volunteers, as defined by the American Diabetes Association criteria [5], were enrolled of their own volition.

Whole blood samples were collected into vacuum tubes containing K_3EDTA as an anti-coagulant. Hematocrit values (Hct) were determined using micro-haematocrit tubes, a micro-haematocrit centrifuge (Hawksley and Sons Ltd., Lancing, UK), and a micro-capillary reader (International Equipment Company, Needham Heights, MA, USA). Before separating the plasma from the cells, total Hb levels were determined by spectrophotometry at 540 nm using an in-house Drabkin's reagent (200 mg $K_3[Fe(CN)_6]$, 50 mg KCN, and 140 mg KH_2PO_4 in 1000 ml of water) having 0.03% Brij® 35. During the assays, Drabkin's reagent and cyanmethemoglobin were used as the blank and standard, respectively. To prepare hemolysates, the remaining red blood cells were washed three times with physiological saline (0.9% NaCl) and lysed by addition of hemolyzing buffer (26 mM NaH_2PO_4, 7.4 mM Na_2HPO_4, and 13.5 mM KCN). During experimental procedures utilizing KCN, sufficient protection is required to avoid the toxic effects, especially possible inhalation of the fumes. The work should be performed in a ventilated area.

5.3.6 Data handling and analysis

The sensor system contained 12 individually addressable three-electrode systems, providing 12 impedance spectra for each assay. The EIS data were fitted to Randles equivalent circuit model, modified with a constant phase element (CPE), using Gamry Echem Analyst software (Version 6.11). The obtained charge transfer resistance (Rct) values were used throughout the study. To compare the performance of different microelectrodes at equivalent conditions, the Rct values were normalized using equation NRct = [Rct(i)-Rct(0)]/Rct(0), where the Rct(0) and Rct(i) are the charge transfer resistance of an APBA-modified electrode before and after exposure to HbA1c, respectively. To determine the assay reproducibility, 10 assays per day were performed during a three-day period using standard solutions containing normal (4.10%) and high (8.36%) level of HbA1c.

The regeneration efficiency (RE) was calculated according to equation RE = [1-(RT-B)/T] x 100% [139], where RT is the impedance after the regeneration cycle, B is the baseline impedance for the APBA-modified sensor, and T is the impedance before applying any regeneration step. The performance of the sensor system was also evaluated by the Bland-Altman bias plot and a Passing-Bablok regression analysis using MedCalc software (version 9.6.2.0) from MedCalc Software bvba (Ostend, Belgium). Specifically, the results obtained from our proposed sensor system were compared to those determined with the commercial in2itTM (II) A1c test kits.

As HbA1c concentrations are often reported in different units, the International Federation of Clinical Chemistry (IFCC) and different national diabetes control programs, such as National Glycohemoglobin Standardization Program

(NGSP) in the USA, have agreed on a consensus statement that HbA1c results be reported in SI units, i.e., mmol mol^{-1} (IFCC) or % (NGSP) [152]. Calibration material certified by the NGSP was used throughout our experiments, and importantly, the hemolysate standard solution was used to calibrate the automated commercial instrument. Hence, the calibration was representative for clinical samples.

5.4 Results and Discussion

5.4.1 Optimization and characterization of the HbA1c sensor

5.4.1.1 Surface modifications and EIS characterization

EIS is an effective way to probe the interface properties of chemically modified electrodes as well as for label-free sensing of an analyte. We characterized the different steps of surface modification and their influence on the sensor performance in order to optimize the used concentrations and immobilization time. Impedance measurements were performed after each surface modification step and HbA1c binding assay. Figure 31a and 31b show the modification strategy to construct the APBA affinity surface and subsequently achieve the binding of HbA1c, respectively.

Figure 32a shows Nyquist plots for the redox process of $[Fe(CN)_6]^{3-/4-}$ before and after electrode cleaning, as well as after cysteamine, glutaraldehyde, and APBA modification. Compared with the Nyquist plot acquired using a chemically cleaned electrode (curve 1), a significant decrease in Rct was observed when the electrochemical surface cleaning was performed (curve 2). As shown in the inset, a considerable decrease in the diameter of the semicircle, i.e. decrease in Rct, was

observed (curve 3) upon applying the positively charged cysteamine SAM. This indicates increased electron transfer kinetics of the negatively charged $[Fe(CN)_6]^{3-/4-}$ redox couple due to the influence of the positive surface charge [155, 156]. After applying glutaraldehyde, the semi-circle was broadened indicating an increased Rct (curve 4). This can be attributed to decreased accessibility of $[Fe(CN)_6]^{3-/4-}$ to the electrode surface due to the decreased positive surface charge and steric hindrance caused by the glutaraldehyde. APBA modification of the glutaraldehyde activated electrode resulted in a further increase in Rct, confirming that boronate groups were successfully immobilized on the electrode surface (curve 5). The observed increase in the Rct was largely due to the electrostatic repulsion between the negative charge of $[Fe(CN)_6]^{3-/4-}$ and the negatively charged surface of the APBA-modified electrode under alkaline conditions.

Figure 32b shows Nyquist plots acquired after incubation with standard solutions containing 4.10% (normal level) and 8.36% (diabetic level) of HbA1c. Both HbA1c concentrations caused a significant increase in the diameter of the Nyquist plot in comparison with the one acquired after APBA modification (curve 5, Figure 32a). This is due to the binding of HbA1c to APBA that increasingly hinders the access of $[Fe(CN)_6]^{3-/4-}$ to the electrode surface.

To provide quantitative information on the effect of different electrode modifications and HbA1c concentrations, the acquired Nyquist plots were fitted to Randles equivalent circuit model modified with a CPE (Figure 32b, inset). The solid lines in Figure 32b show the fitting of Nyquist plots acquired after incubation with HbA1c standard solutions (4.10% and 8.36%), indicating that the equivalent circuit

model describes well the data down to the lowest frequencies. In this model, Rs and Rct correspond to the resistance of the electrolyte solution and the charge transfer kinetics at the electrode, respectively. The CPE, parallel with the Rct and the Warburg impedance (W), accounts for non-Faradaic processes related to the double layer capacitance and possible surface inhomogeneity. W describes the diffusion impedance due to mass transfer of $[Fe(CN)_6]^{3-/4-}$ to the electrode. Ideally, Rs and W are not affected by modifications occurring at the electrode surface, whereas both Rct and CPE are altered by electrode modifications. The impedance of CPE is defined as $ZCPE = [Q(j\omega)^{\alpha}]^{-1}$, where ω is the angular frequency, exponent α can vary from 0 to 1, and factor Q describes a pure capacitor or resistor when α is equal to 1 or 0, respectively [157]. Table 6 summarizes the determined values of Rct and ZCPE (Q and α) as well as the effective equivalent capacitance (C_{eff}) derived from the ZCPE. In the case of the different electrode modification steps, the value of C_{eff} decreases as a consequence of successive modifications. This is in accordance with the view that chemical electrode modifications behave as capacitors in series with the double layer capacitance of a bare electrode [155]. APBA modification, on the other hand, makes an exception, showing an increase in capacitance of the electrode interface. Incubation with HbA1c standard solutions leads to a significant increase in Rct with concentration. However, the trend in C_{eff} is not clear, which may be attributed to the influence of the sample matrix in the HbA1c standards. Hence, for quantitative determination of HbA1c concentration in real samples, Rct provides higher sensitivity and clearer trend.

(a)

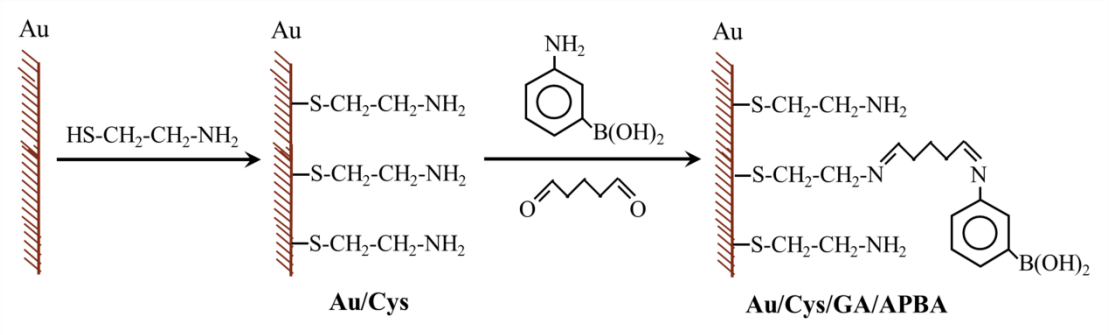

(b)

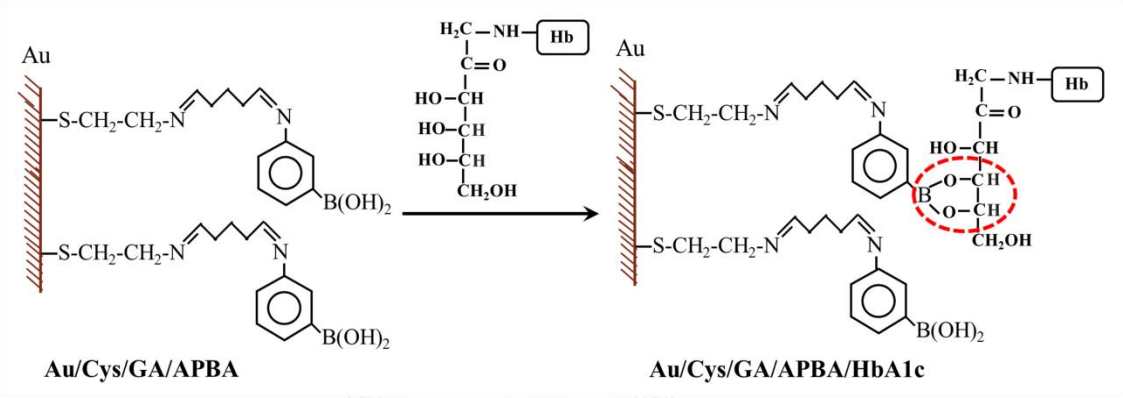

Figure 31. Illustration of electrode modification strategy and boronate-based recognition of HbA1c

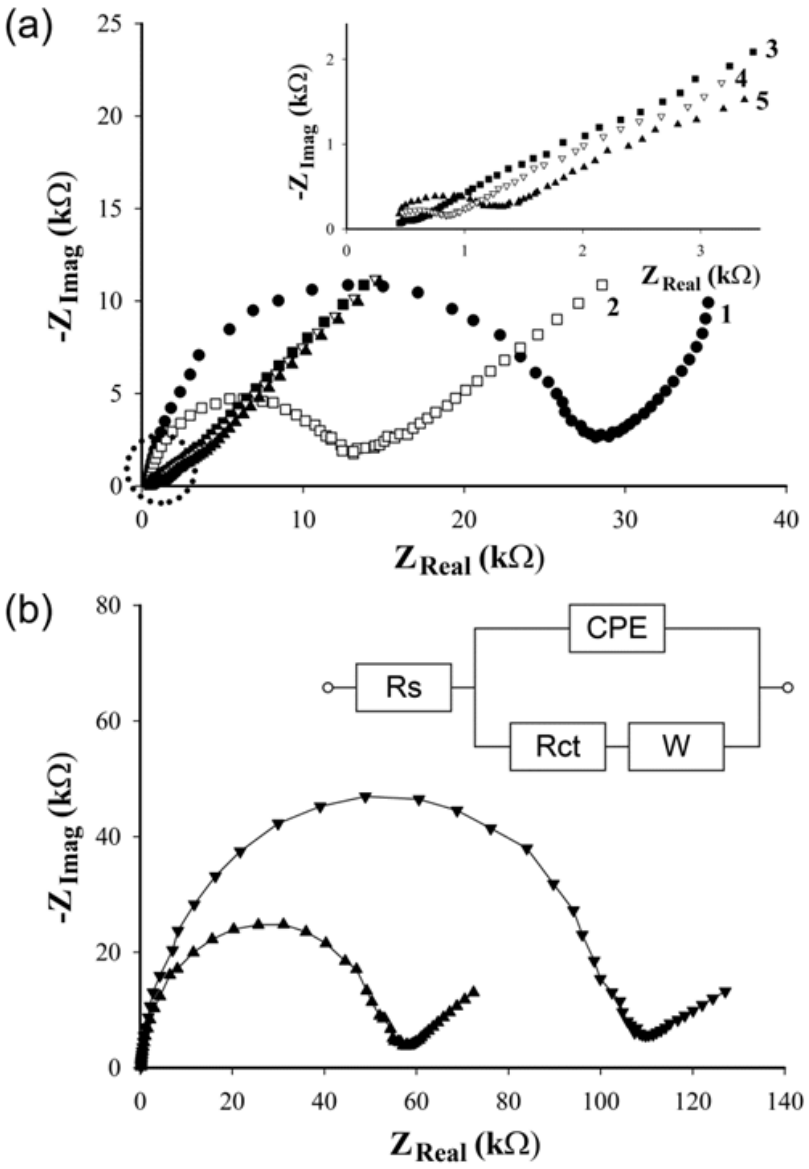

Figure 32. Characteristic Nyquist plots after (a) chemical (1) and electrochemical (2) electrode cleaning as well as surface modification steps (inset: close-up view after (3) cysteamine SAM, (4) glutaraldehyde activation, and (5) APBA modification), and (b) incubation with 4.10% (▲) and 8.36% (▼) HbA1c standard solution. The solid lines represent curve fitting to the equivalent circuit in the inset (the details can be found in the text). 5 mM $[Fe(CN)_6]^{3-/4-}$ was used as the redox indicator.

Table 6. Characteristic values of equivalent circuit parameters: charge transfer resistance (Rct) and constant phase element impedance (Z_{CPE} expressed as Q and α) after different electrode modifications and incubation with various concentrations of HbA1c as well as the calculated effective capacitance (C_{eff}) based on Z_{CPE}.

Treatment	**Rct (kΩ)[c]**	**Q (nS s^{α})[c]**	**α[c]**	**C_{eff} (nF)[d]**
Chemical cleaning[a]	26.12	43.17	0.903	20.65
Electrochemical cleaning[a]	16.01	18.65	0.899	7.70
Cysteamine modification[a]	0.61	18.21	0.705	5.34
Glutaraldehyde activation[a]	0.81	14.57	0.690	3.33
APBA-modification[a]	1.51	38.35	0.817	4.49
0.10% HbA1c[b]	2.68	13.21	0.934	6.48
0.20% HbA1c[b]	7.19	19.77	0.935	10.40
0.40% HbA1c[b]	13.49	13.70	0.937	7.70
2.02% HbA1c[b]	26.89	12.05	0.942	7.30
2.57% HbA1c[b]	30.36	12.33	0.940	7.40
4.10% HbA1c[b]	48.46	19.52	0.945	13.07
8.36% HbA1c[b]	103.20	19.77	0.944	13.62

[a] The values of the parameters correspond to the Nyquist plots shown in Figure 32a of the article.

[b] The values of the parameters correspond to the Nyquist plots shown in Figure 3a of the article.

[c] During the nonlinear regression analysis of the impedance spectra, the value of solution resistance (Rs) has been 210 Ω.

[d] The calculation of C_{eff} was done according to the approach presented by Hsu and Mansfeld (Corrosion 2001, 57, 747-748) [158].

5.4.1.2 Effect of pH, glutaraldehyde/APBA concentration, and incubation time

Phenylboronic acid, having pK_a of 8.7-8.9 [159], is known to be anionic at alkaline conditions [142]. Near the pK_a, it has a tetrahedral form, specifically able to bind diol groups of glycated proteins [160]. At pH 8.5, the NRct values of the sensor were higher than at pH 7 (control), indicating that boronate-diol affinity was stronger at alkaline conditions (Figure 33). This agrees with previous findings [41]. Thus, pH 8.5 was used in all subsequent experiments.

Different glutaraldehyde concentrations were evaluated for sensor preparation using two clinically relevant levels of HbA1c (4.1% and 8.36%). The Rct increased with increasing concentration until 5%, above which the values remained constant (Figure 34a). This concentration was, therefore, used in all subsequent experiments. As the sensitivity for HbA1c recognition relies on the density of surface bound boronate groups, different concentrations of APBA were investigated. The Rct increased with increasing APBA concentration, reaching a maximum at around 20 mM, which indicates that the surface is becoming fully saturated with APBA groups (Figure 34b). 20 mM APBA was used for preparation of the APBA modifications in all subsequent experiments.

As both the number of boronate functional groups and HbA1c molecules on the surface of the electrode affect the sensitivity of the sensor, the effect of immobilization and incubation time on the determined Rct values was studied in two steps. First, the time for immobilizing 20 mM APBA on an electrode surface was investigated for two different HbA1c concentrations (4.10% and 8.36%). Then, the incubation time of HbA1c was studied using a boronate sensing surface prepared based on the optimized immobilization time. The Rct increased steadily with the

APBA immobilization time from 5 to 30 minutes (Figure 35a), reaching a maximum after about 20 minutes for both the high and low HbA1c level. This immobilization time was used to prepare the boronate sensing surfaces for further experiments. Similarly, the Rct increased with increasing HbA1c incubation time (Figure 35b), approaching a maximum after 15 minutes for both the high and low HbA1c level. In order to minimize the assay time, the optimal incubation time was chosen to be 15 min.

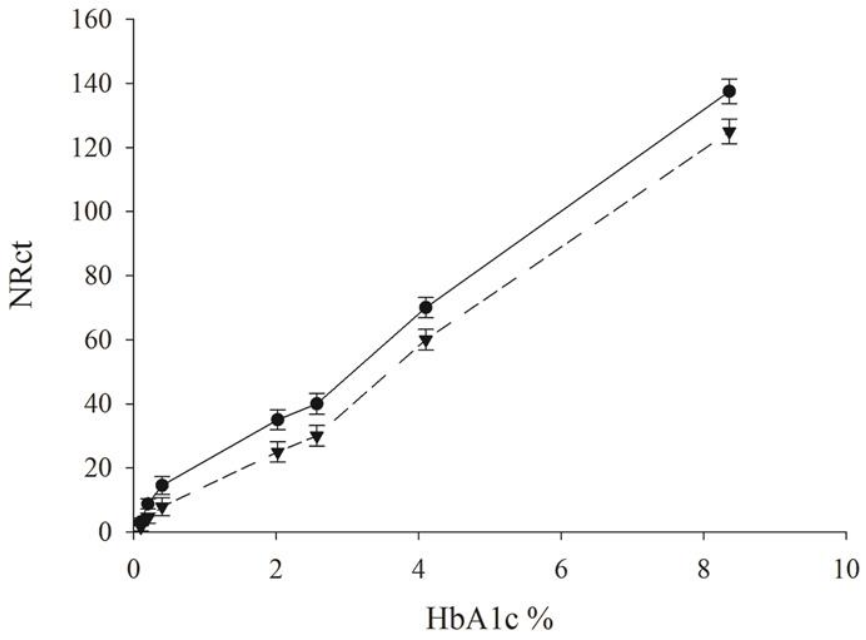

Figure 33. Comparison of HbA1c binding on APBA-modified electrodes under neutral (▼ - pH 7) and alkaline (● - pH 8.5) conditions after incubation with 0.10%, 0.20%, 0.40%, 2.02%, 2.57%, 4.10%, and 8.36% HbA1c. The response for each HbA1c concentration is expressed as normalized charge transfer resistance (average ± standard deviation, n = 2).

(a)

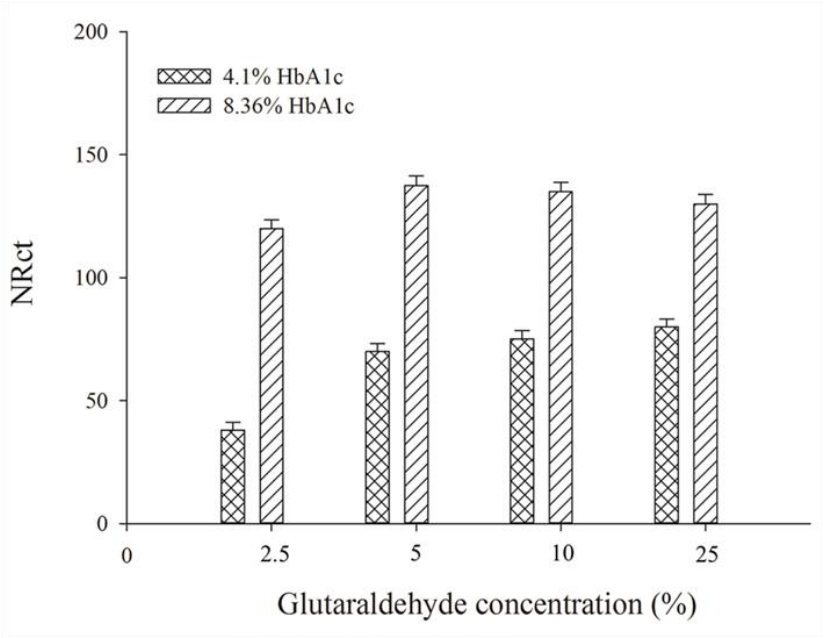

(b)

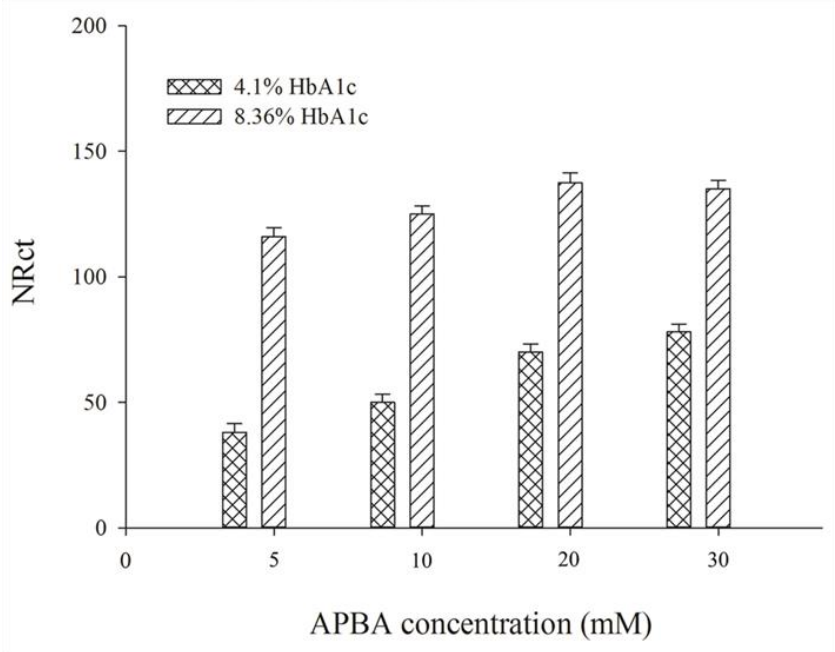

Figure 34. Optimization of (a) glutaraldehyde and (b) APBA concentration using normal (4.1%) and diabetic (8.36%) HbA1c level. The response for each modification and HbA1c concentration is expressed as normalized charge transfer resistance (average ± standard deviation, n = 2).

(a)

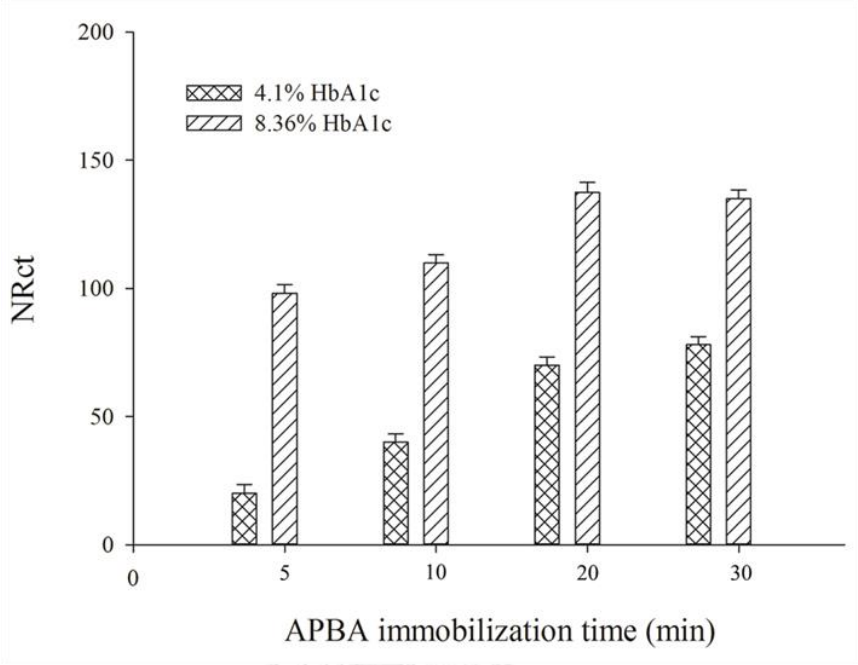

(b)

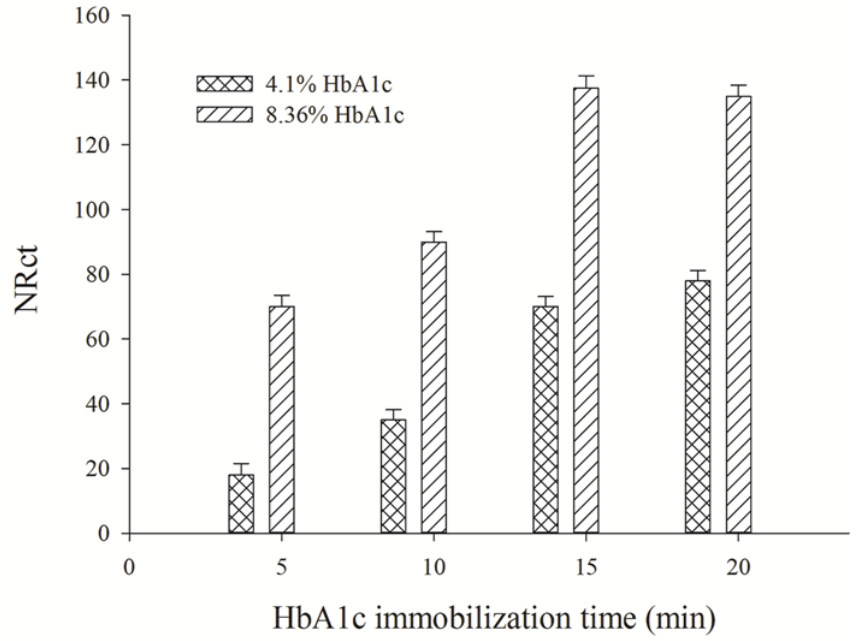

Figure 35. Optimization of time for (a) APBA immobilization and (b) HbA1c incubation using normal (4.1%) and diabetic (8.36%) HbA1c level. The response for each time and HbA1c concentration is expressed as normalized charge transfer resistance (average ± standard deviation, n = 2).

5.4.2 Analytical sensor characteristics and application

5.4.2.1 Calibration, regeneration, reproducibility, selectivity, and stability

For calibration, duplicate measurements were performed at each HbA1c concentration using one IDA chip. The increase in Rct with increasing HbA1c concentration is clearly demonstrated by the Nyquist plots of Figure 36a representing one sensor (the Rct values are shown in Table 6). The normalized Rct was plotted vs. HbA1c concentration (Figure 36b and inset), revealing that the response was linear up to 8.36% with LOD of 0.024% (3σ). The IDA-sensor system offers higher sensitivity than that described by Kim et al. [53] and our previous work [137]. Compared with other label-free electrochemical approaches (Table 5) [56, 60, 61], the system provides better sensitivity and a wider linear range for assaying HbA1c, and meets the requirement of clinical HbA1c detection. In comparison with the piezoelectric sensor having a similar recognition layer [40], the sensitivity of our sensor was very high, probably due to a greater boronate density. Control experiments (electrodes with only glutaraldehyde or cysteamine modification) demonstrated that the aldehyde functionalities of glutaraldehyde bound the amino groups of HbA1c independent of concentration, whereas cysteamine did not show any interaction with HbA1c (Figure 37). These results confirm that the Rct changes (Figure 36a) were due to binding of HbA1c to APBA via cis-diol interactions.

To determine the reversibility of HbA1c binding to APBA, electrode regeneration was investigated. Table 7 presents Rct data for the binding interaction on one electrode. 0.1% and 0.20% HbA1c caused an increase in Rct similarly as shown in Figure 36a. After regeneration using 10 mM sodium acetate (pH 5) for 30 minutes,

the Rct returned in both cases to the original value due to the release of HbA1c. The RE was 99.25% and 99.03% after the first and second regeneration cycle, respectively. After the second regeneration cycle, incubation with 0.1% HbA1c still caused a similar Rct increase as was initially observed for that concentration. The results indicate that the HbA1c-APBA interaction was reversible, facilitating construction of a reusable HbA1c assay system.

The reproducibility of the sensor was tested in determination of both normal (4.10%) and diabetic (8.36%) HbA1c levels using a separate IDA chip for each concentration. 10 measurement cycles per chip, each followed by a regeneration step, were run on each day during three consecutive days. Each measurement cycle comprised 12 acquired impedance spectra using all the individually addressable measurement sites on each chip. Variation in measurements between individual electrodes, expressed as relative standard deviation (RSD), was 4.0%. Considering the 10 measurement cycles per day during three days (n = 30), the overall assay reproducibility for each concentration, expressed as relative standard error of mean (RSE), was 1.1%. Using 12 measurement sites per chip, the proposed sensor provides reproducibility for HbA1c assays that meets the recommended intralaboratory variability of less than 2% [118]. Tests on several chips indicated that during continued assays, including a regeneration step after each measurement cycle, the functionality of some electrodes may be affected. Due to this, although the chips are reusable, the recommendable approach is to use one chip for a complete assay that comprises calibration and analysis of the blood sample of one patient.

Since APBA is able to covalently bind to a diol group of any glycated protein, the selectivity for HbA1c in relation to non-glycated haemoglobin (HbAo) was tested as a potential interference. Figure 38 shows Nyquist plots for assaying HbAo covering the concentration range that represents normal variation between individuals. Upon introduction of HbAo, the Rct virtually remained unchanged over the concentration range from 10 to 20 g dL^{-1} in comparison with the Rct of the APBA-modified electrode in the absence of HbAo. This result demonstrated the ability of the sensor to distinguish between HbA1c and HbAo, indicating its applicability for determination of clinically relevant HbA1c levels in the blood of diabetic individuals. In our study, red blood cells were separated from plasma by centrifugation followed by careful washing with physiological saline. Thus, other interfering agents present in plasma, such as glycated albumin and glucose, were eliminated.

The stability of the sensor system was investigated over a period of 4 weeks. Between measurements, the whole chip (12 on-chip APBA-modified electrodes) was stored in Milli-Q water at room temperature. In order to evaluate the activity of the individual sensors, the impedance response was determined every second day using 4.10% HbA1c standard solution. Figure 36c shows that there was virtually no decrease in the response during the entire 4-week period, which is an improvement compared to previously published boronate-based sensors. After 4 weeks, the sensor had retained 96% of its initial response to HbA1c.

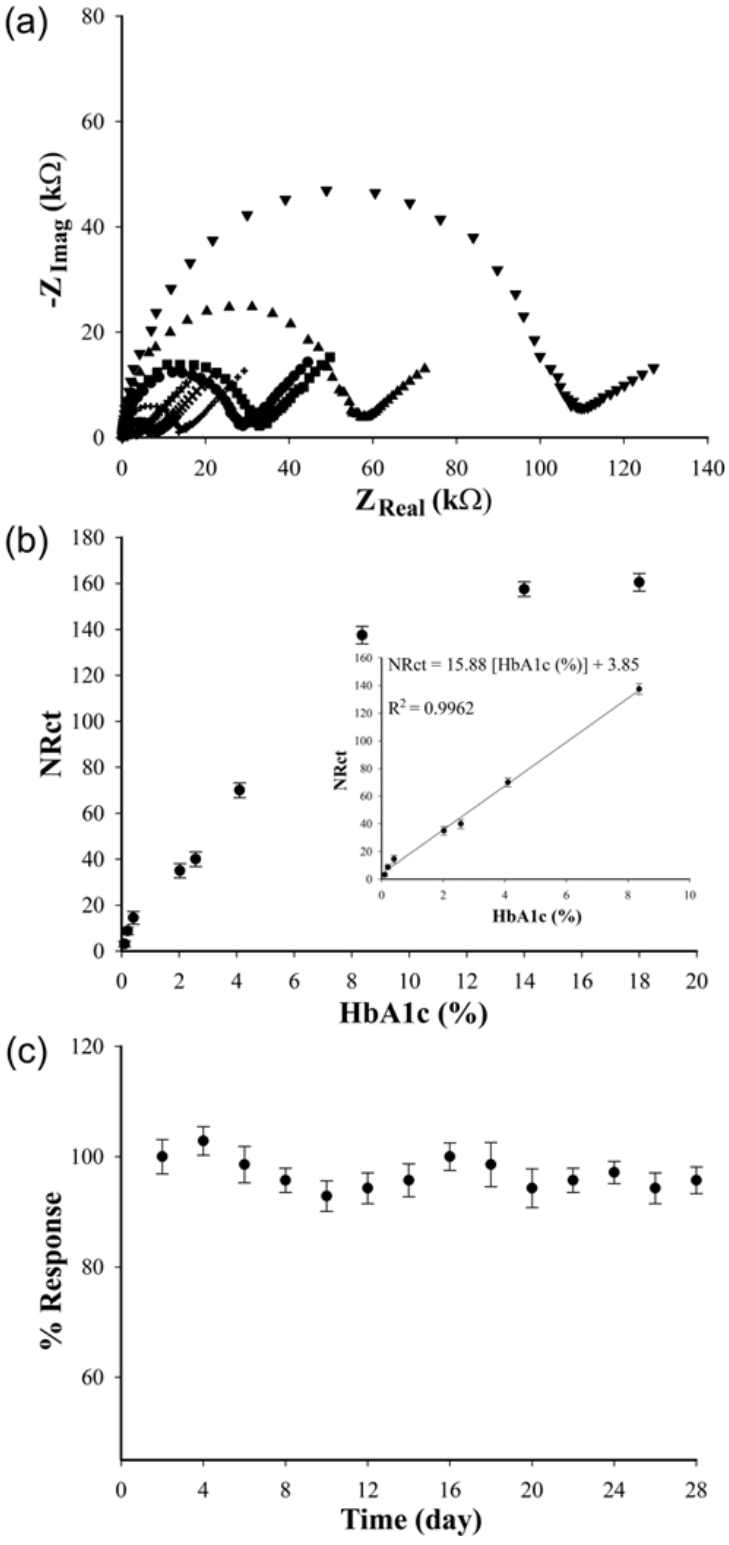

Figure 36. (a) Characteristic Nyquist plots acquired using an APBA-modified electrode before and after incubation with (★) 0.10%, (✕) 0.20%, (✚) 0.40%, (●)

2.02%, (■) 2.57%, (▲) 4.10%, and (▼) 8.36% HbA1c. (b) Variation of normalized Rct (NRct) with HbA1c concentration using an IDA-sensor chip (inset: close-up view showing the range of linearity). (c) Storage stability (% of the initial NRct) of the IDA-sensor chip over a period of 4 weeks determined by assaying 4.10% HbA1c. Each data point (b and c) represents the mean ± standard deviation of duplicate measurements using all the IDE-WEs of the chip (n = 24). 5 mM $[Fe(CN)_6]^{3-/4-}$ was used as the redox indicator.

(a)

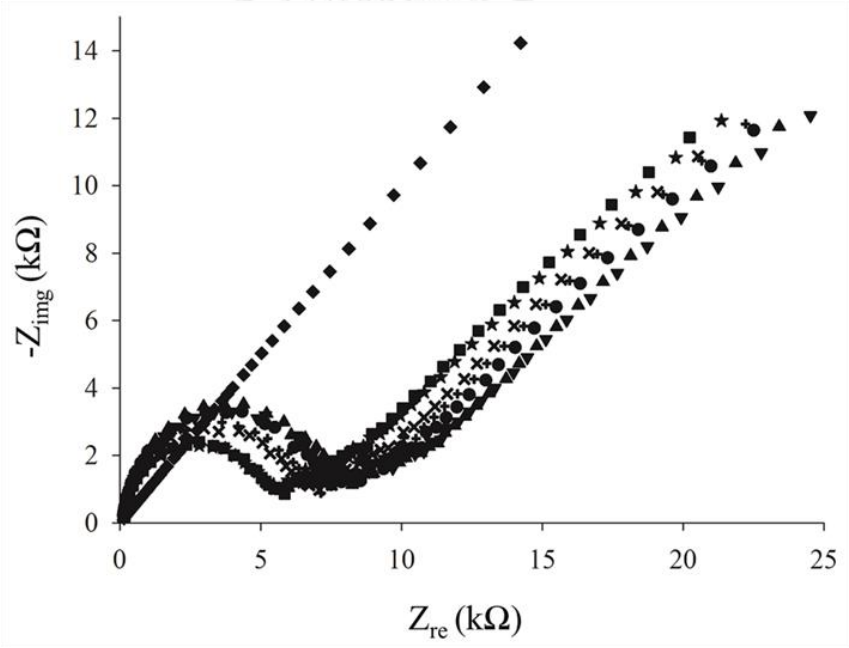

(b)

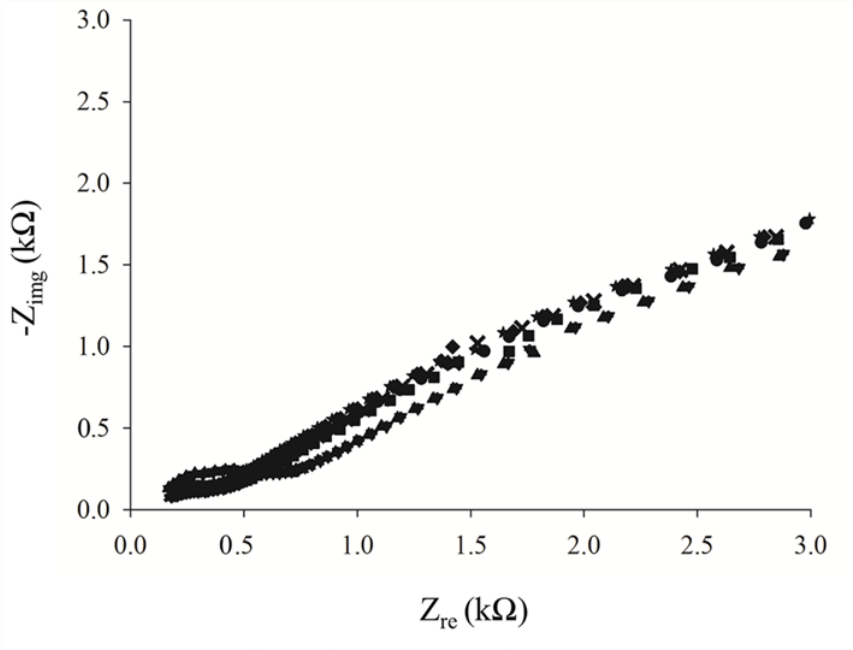

Figure 37. Characteristic Nyquist plots for a (a) glutaraldehyde activated and (b) cysteamine-modified electrode before and after incubation with (◆) 0%, (★) 0.10%, (✕) 0.20%, (✚) 0.40%, (●) 2.02%, (■) 2.57%, (▲) 4.10%, and (▼) 8.36% HbA1c standard solution. The increase in Rct due to covalent binding of HbA1c to glutaraldehyde is practically independent of HbA1c concentration, whereas no significant increase in Rct is observed on a cysteamine-modified electrode due to lack of any interaction between cysteamine and HbA1c.

Table 7. Evaluation of regeneration efficiency (RE) on an APBA-modified electrode

Treatment	Rct[a] (kΩ)	RE[b] (%)
APBA-modification	1.51 ± 0.12	
Incubation with 0.10% HbA1c[c]	2.67 ± 0.26	
Regeneration[d]	1.53 ± 0.15	99.25
Incubation with 0.20% HbA1c[c]	7.18 ± 0.53	
Regeneration[d]	1.58 ± 0.13	99.03
Incubation with 0.10% HbA1c[c]	2.60 ± 0.30	

[a] The Rct values represent mean ± standard deviation of duplicate measurements.

[b] The regeneration efficiency was determined as described in section "Data handling and analysis".

[c] The chip was incubated with HbA1c for 15 min.

[d] The chip was regenerated for 30 min using 10 mM sodium acetate buffer (pH 5).

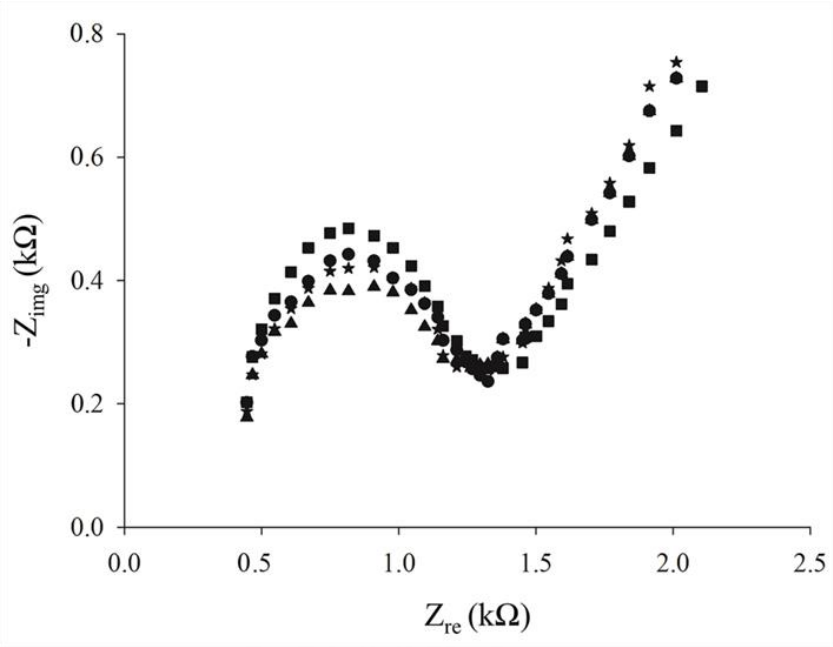

Figure 38. Characteristic Nyquist plots for an APBA-modified electrode before (▲) and after incubation with (■) 10, (★) 15, and (●) 20 g dL^{-1} HbAo.

5.4.2.2 Real sample analysis and assay comparison

To evaluate the sensor reliability, HbA1c was quantitated in 15 hemolysate samples from healthy and diabetic volunteers. The aim was a detailed assessment of the agreement with a standard method and possible bias in the target clinical range. The quantified hematocrit and total Hb content varied between 35-47% and 12-17 g dL^{-1}, respectively. The agreement and correlation between the two methods were investigated using the Bland-Altman bias plot and the Passing-Bablok regression analysis, respectively. The results revealed an excellent agreement between our sensor and the standard method (Figure 39a) with an agreement interval of ± 1.96 SD. Virtually no bias was found between the methods, implying that they could be interchangeable. Based on the Passing-Bablok regression analysis, the equation and

95% confidence limits of its slope and y-intercept (Figure 39b) indicate a good linearity (cusum linearity test, $p > 0.10$) and correlation between the methods. The results validate our IDA-sensor system using actual clinical samples, demonstrating its potential as a fast, easy to use, robust and inexpensive approach for monitoring of glycemic status of diabetes patients.

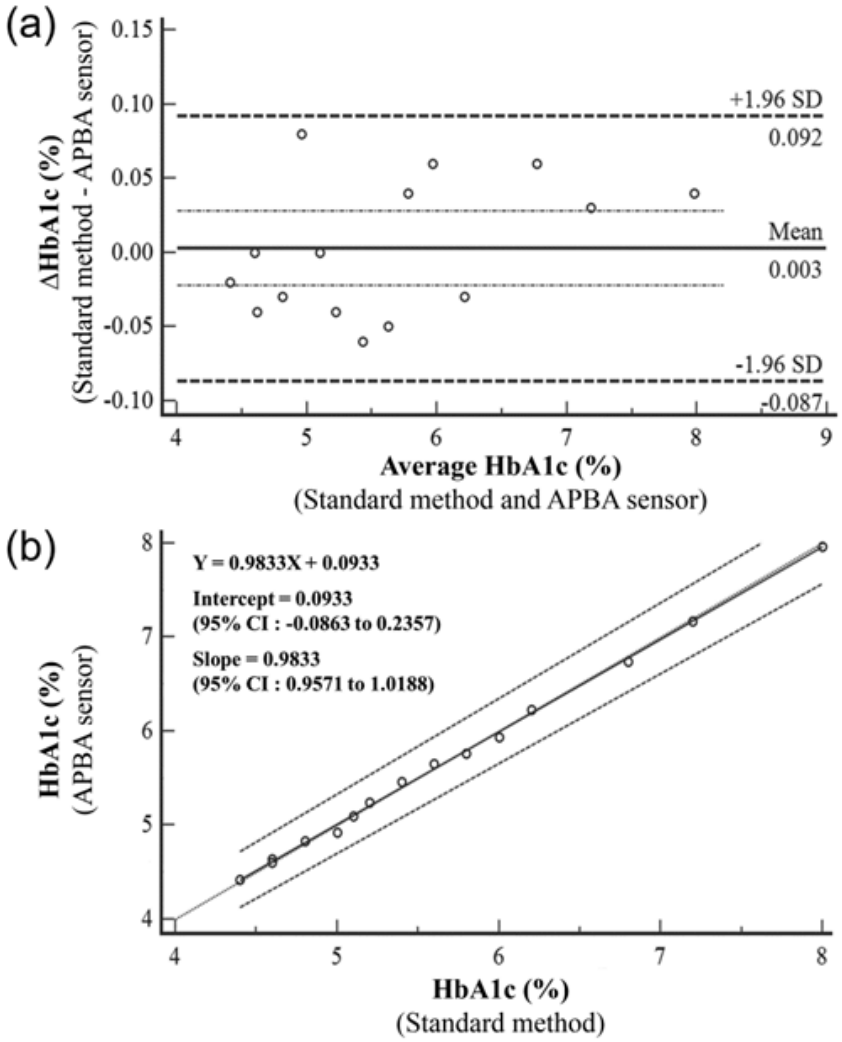

Figure 39. Comparison of HbA1c sensing between the IDA-sensor chip of Figure 3 and a standard method using hemolysate samples: (a) Bland-Altman bias plot (solid line: mean difference; dashed lines: limits of agreement), and (b) Passing-Bablok

regression analysis (solid line: regression line (cusum linearity test, $p > 0.10$); dashed lines: 95% confidence interval of the regression line). 5 mM $[Fe(CN)_6]^{3-/4-}$ was used as the redox indicator.

5.5 Conclusions

The proposed boronate-based affinity sensor was remarkably selective in determining HbA1c levels using label-free impedance detection. The results showed that the boronate-modified IDA microelectrodes were highly responsive to a wide range of HbA1c levels and provided bias-free determination of HbA1c in patient-derived blood samples with excellent correlation with a standard method. This indicated that the presented affinity sensor has the potential for continuous monitoring of glycemic status in diabetic patients. Without the use of biomolecular recognition elements (e.g. antibodies) and detection labels, the proposed affinity sensor has the merit of great simplicity and robustness. As a future perspective, our affinity sensor can also be applicable to determining other diabetes markers, e.g., glycated albumin. Furthermore, as demonstrated, mass fabrication of the IDA chips provides a highly reproducible sensor system, offering a possibility to integrate it into mass fabricated microfluidic devices for automated fluid handling.

5.6 Acknowledgement

Y.B. acknowledges the Thailand Research Fund through the Royal Golden Jubilee Ph.D. Program (Grant No. PHD/0164/2553) and the Graduate School, Chulalongkorn University, for the Tuition Fee Scholarship.

CHAPTER VI

MANUSCRIPT IN PREPARATION

Development of a multiplexed microfluidic platform for measuring multiple diabetes makers: the promise of an automated impedimetric assay on microfluidics using a unique single-frequency value

Yuwadee Boonyasit[1], Orawon Chailapakul[2], Arto R. Heiskanen[3,*], Wanida Laiwattanapaisal[4,*], and Jenny Emnéus[3,*]

[1] Graduate Program in Clinical Biochemistry and Molecular Medicine, Faculty of Allied Health Sciences, Chulalongkorn University, Bangkok, 10330, Thailand.

[2] Electrochemistry and Optical Spectroscopy Research Unit (EOSRU), Department of Chemistry, Faculty of Science, Chulalongkorn University, Bangkok, 10330, Thailand.

[3] Department of Micro- and Nanotechnology, Technical University of Denmark, Kgs. Lyngby, 2800, Denmark.

[4] Department of Clinical Chemistry, Faculty of Allied Health Sciences, Chulalongkorn University, Bangkok, 10330, Thailand.

Manuscript in publication

6.1 Experimental Section

6.1.1 Chemicals and materials

For preparing all the microfluidic components of the platform, polycarbonate (PC) (Bayer MaterialScience AG, Leverkusen, Germany), poly(methyl methacrylate) (PMMA) (Röchling Technische Teile KG, Mainburg, Germany), polydimethylsiloxane (PDMS) (Dow Corning, Wiesbaden, Germany), and silicon adhesive (INT TA106) (Intertronics, Oxfordshire, UK) were used, as previously presented elsewhere [161]. Electric connections were made of spring-loaded pin arrays (811-S1-NNN-10-015101) (PreciDip SA, Delémont, Switzerland). The stainless-steel balls (1/16 inch) were purchased from VXB Bearings (Anaheim, California). The other chemical used in photolithography processes were employed according to the recommendation of the suppliers (Danchip, Technical University of Denmark).

6.1.2 Instrumentation

All the procedures for fabricating the microfluidic platform and the instruments used in this study were in accordance with our previous works [154, 161]. Each polymeric component was designed by using AutoCAD® 2013 software (Autodesk Inc., San Rafael, CA, USA) and machined by micromilling using a Mini-Mill/3Pro system (Minitech Machinery Corporation, Norcross, GA, USA) executing G-code generated by EZ-CAM17 Express software (EZCAM Solutions, Inc., New York, NY, USA). The UV activation and heat/pressure-assisted bonding technique were employed using a 5000-EC Series UV Curing Flood Lamp System (Dymax

Corporation, Torrington, CT, USA), and a PW20 hydraulic press (Paul-Otto Weber GmbH, Remshalden, Germany), respectively. For cutting a double-sided silicone adhesive, the carbon dioxide laser cutting was done with an Epilog Laser Mini 18 (Epilog Laser, Golden, CO, USA). Micropumps were operated with Lego® Interactive Servo Motors (Lego System A/S, Billund, Denmark) that were controlled by an NXT Intelligent Brick (Lego System A/S, Billund, Denmark) executing a LabView-based script. A potentiostat/galvanostat instrument (Autolab PGSTAT30, Eco Chemie, The Netherlands) equipped with the Frequency response analyser software was used to perform the impedance measurement throughout this study.

The instruments used for measuring the haematocrit (Hct) values, including micro-haematocrit tubes, a micro-capillary reader, and a micro-haematocrit centrifuge, were manufactured by Vitrex Medical A/S (Herlev, Denmark), International Equipment Company (Needham Heights, MA, USA), and Hawksley and Sons Ltd. (Sussex, England), respectively.

6.1.3 Design and fabrication of microfluidic system

The fabrication and integration of the microfluidic platform involved the various modules with different functions including the microfluidic motherboard housing all the necessary multi-modules (1), inlet and waste outlet reservoir modules (2), two 4-channel miniaturised peristaltic pumps (3), two miniaturised valves (4), microfluidic chip integrated with microelectrode arrays (5), and interconnections (6), as shown in Figure 40(A). After drawing the designs, all the plastic components were constructed by micromilling technique. The upper part of inlet and outlet reservoirs, the rotor beds, peristaltic micropump housing, and the microfluidic motherboard were

made of 10 mm, 10 mm, 5.8 mm, and 4 mm thick PC, respectively, whereas the lower part of inlet and outlet reservoirs, the upper part of microfluidic chip, the middle and lower parts of microfluidic chip, and the other micromilled components were fabricated of 2 mm, 2 mm, 1.5 mm, and 5 mm thick PMMA. Prior to thermal and pressure-assisted bonding (20 minutes at 85 °C/4.4 MPa), each individual micromilled PMMA components were gently cleaned with 96% ethanol and followed by ultrasonication in Mill-Q water before exposure to 1-minute UV activation.

The microfluidic chip, comprised of a 2 mm thick PMMA lid and two 1.5 mm thick PMMA layers with microfluidic channels, was interfaced to a microelectrode array chip placing in a 5 mm PMMA holder through a 50-µm-thick double-sided silicon adhesive layer, as schematically shown in Figure 40(B). The microelectrode array chip, each consisting of a working (WE), counter (CE), and reference (RE) electrode, contains 12 identical three electrode systems, which can be potentiostated individually. The IDA chip, comprised of a meshing set of microband array electrodes, constitutes the gold interdigitated WE with 500 µm long fingers and 10 µm width and gap. Both the CEs and Res are gold disks with 700 µm and 50 µm diameters, respectively. Prior to integration, the microelectrode array chip was chemically cleaned by using a mixture of H_2O_2 (25% v/v) and KOH (5 M) followed by electrochemical cleaning using a potential sweep from -200 to -1200 mV in 50 mM KOH, as previously described [155]. The individually addressable microelectrode arrays afford the great opportunity for integration into a multiplexed microfluidic platform, which is of considerable importance for detection of many other biomolecules associated with the metabolic biomarkers. In this study, the microfluidic channels were designed specifically to determine two independent

samples measured simultaneously for both the total and glycated haemoglobin levels in the actual specimens. The fully integrated multiplexed microfluidic platform equipped with the electronic connections through a spider-like printed circuit board (PCB), as shown in Figure 40(C), was capable of acquiring the impedance signal responses through the spring loaded pins underneath a custom designed PCB. The two 4-channel peristaltic micropumps and microvalves were operated by the Lego® Motors connected to the brick units (Lego System A/S, Billund, Denmark) under control of the custom-made LabView-based software. For recording the whole impedance spectrum, a potentiostat/galvanostat instrument (Autolab PGSTAT30, Eco Chemie, The Netherlands) equipped with the Frequency response analyser software was connected to the custom-made PCB and the data acquisition was done through an appropriate equivalent-circuit model using the NOVA 1.9 software. The unique feature of optimal binding frequency that specific to each binding interaction was also investigated, in order to circumvent the particular problem of time-intensive procedure.

(A)

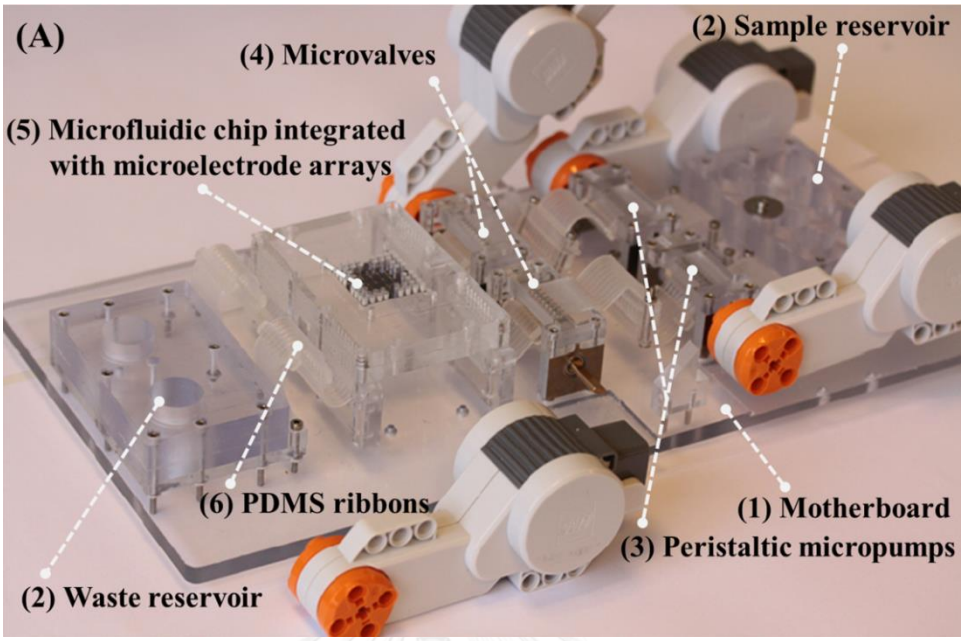
(A)
(4) Microvalves
(2) Sample reservoir
(5) Microfluidic chip integrated with microelectrode arrays
(6) PDMS ribbons
(1) Motherboard
(3) Peristaltic micropumps
(2) Waste reservoir

(B)

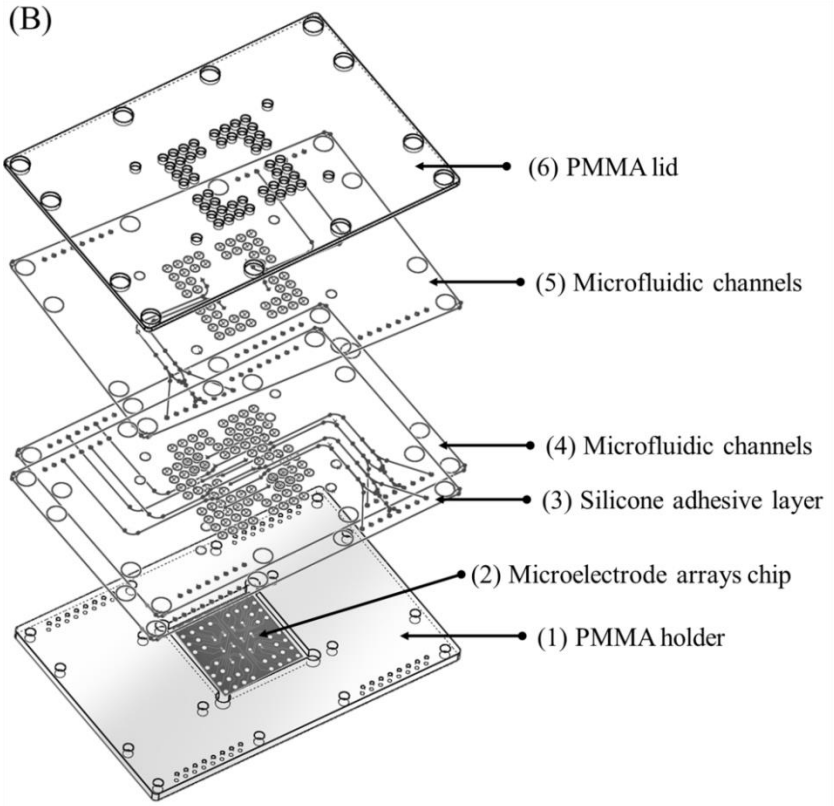
(B)
(6) PMMA lid
(5) Microfluidic channels
(4) Microfluidic channels
(3) Silicone adhesive layer
(2) Microelectrode arrays chip
(1) PMMA holder

(C)

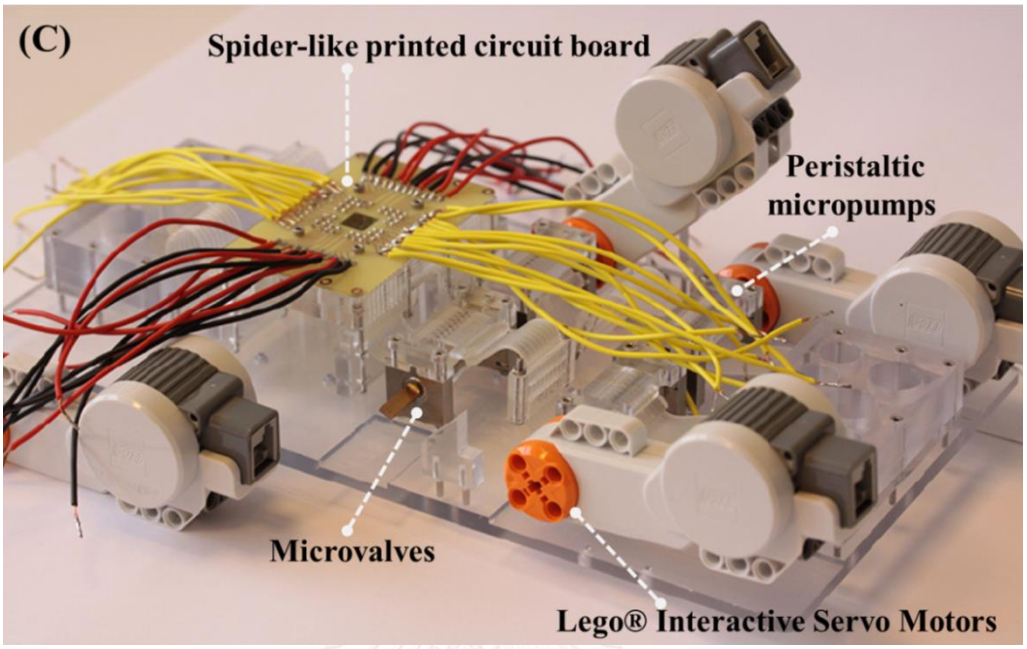

Figure 40. Photographs of the fully integrated multiplexed microfluidic platform: (A) a multipliable platform involving the various modules with different functions: (1) microfluidic motherboard housing all the necessary components, (2) inlet and waste outlet reservoir modules, (3) two 4-channel peristaltic micropumps, (4) two microvalves, (5) microfluidic chip integrated with microelectrode arrays, and (6) PDMS ribbons. (B) A schematic diagram of the assembly of a microfluidic chip comprising: the 5 mm thick PMMA holder (1) integrated with microelectrode array chip (2), (3) a 50-µm-thick double-sided silicone adhesive layer, (4) a 1.5 mm thick PMMA with microfluidic channels thermally bonded with a 1.5 mm thick PMMA with microfluidic channels (5), and (6) a 2 mm thick PMMA lid. (C) A photograph of a microfluidic platform equipped with the electronic connections through a spider-like PCB.

6.2 Results and Discussion

6.2.1 Microfluidic platform with integrated microelectrode arrays

The ultimate aim in designing the presented microfluidic system was to facilitate the development of a single multiplexed microfluidic device for impedimetric assaying of multiple diabetes markers using a unique single-frequency value. The construction of the multiplexed microfluidic platform comprising the multi-functional modules for simultaneous detection of total and glycated haemoglobin has been accomplished through polymeric prototyping techniques, for example micromilling and UV assisted thermal/pressure bonding. Almost all the microfluidic components were made from polymeric materials, i.e. PMMA, PDMS and PC, and thus facilitated the development of a simple, reproducible and user friendly system. The overall structure of the proposed platform is shown in Figure 45. An assembled microfluidic platform comprised of (1) a microfluidic reservoir chip for collecting the two independent samples (S1, S2), chemicals used for on-line surface modifications (M1, M2), and electroactive redox probes (P) during the impedimetric measurements, (2) 4-channel miniaturised peristaltic micropumps for automated fluid operations, (3) 4-channel microvalves for routing each solution to the microfluidic chip with integrated microelectrode arrays, (4) 4-chamber microfluidic chip integrated with 12-microelectrode arrays, and (5) microfluidic reservoir chip for waste collection during experiments.

The inlet reservoir chip was specifically designed to contain seven chambers for keeping each solution separately. The reagents used for the on-line surface modification process to obtain the Hp-modified and APBA-modified IDA sensors were stored in M1 and M2 chamber, respectively, whereas the two independent

haemolysate samples were kept in S1 and S2 chamber, respectively. In this manner, the multiplex analysis was provided in that one sample could be analysed for both the total and glycated haemoglobin values and, moreover, the two independent samples could be measured simultaneously. The electroactive redox probes, 5 mM $Fe(CN)_6^{3-/4-}$, were kept in P chamber and used throughout the EIS measurements. To control the flow of fluid during the experiments, the multi-channel peristaltic micropumps, comprising of a multi-roller, an 8-channel PDMS ribbon, and a rigid rotor bed, connected to an inlet reservoir chip were used to sequentially deliver each reagent solution into the specifically designed microfluidic chip integrated with 12-microelectrode arrays. The ball joint interconnection block at the end of the PDMS ribbons could perfectly fit into the eight-hole pattern present in the inlet reservoir chip, thus offering the leakage-proof [162]. The peristaltic micropumps were operated by the Lego® motors attached to a brass shaft and the fluidic operations were automated using a programmed LabView-based script stored in the Lego® NXT Intelligent Brick, as stated earlier [161, 163].

In addition, the mechanical actuated valve system also plays an important role in delivering the reagent solution to the microfluidic chip. The valve modules, consisting of a brass shaft stacked with eight PMMA discs, an 8-channel PDMS ribbon, and two rigid supports, allowed the possibility of routing the solution to the microfluidic chip. In this case, only four PMMA discs were designed to have a semi-circular recess on the edge, thereby enabling a four-active-channel valve. The PDMS ribbon was sandwiched between the two rigid PMMA supports, in which the 1/16 inch stainless-steel balls could move up and down inside the lower PMMA support. The lower PMMA support was positioned on the top side of the shaft stacked with

eight PMMA discs. After fastening all the components together, the rotation of shaft with respect to the position of recess on the disc significantly affects the PDMS channels. When the steel ball is positioned on the edge of disc, the ball presses the PDMS channel against the upper PMMA support resulting in a closing of the channel. On the contrary, the channels are opened when the ball is positioned on the semi-circular recess on the edge of the disc, allowing the routing of fluid through the PDMS channel.

The designed three-layer microfluidic chip, having two PMMA layers with microfluidic channels and a PMMA lid, was thermally bonded together before integrating with the 12-microelectrode array chip positioned on the top of a 5 mm PMMA holder using a 50-µm-thick silicon double-sided adhesive tape cut with laser ablation. The assembled microfluidic chip integrated with the microelectrode array contained four chambers for assaying the total haemoglobin values in parallel with HbA1c from two independent samples. Each analyte could be assayed in triplicate due to the three identical three electrode systems in each chamber. The entirely assembled microfluidic platform equipped with a custom designed PCB was electrically contacted to the potentiostat through the spring-loaded pin array. The impedance signal responses were recorded and also observed to determine the optimal binding frequency that was specific to each binding interaction. Each analyte could be detected specifically using a single frequency value or a limited frequency range for analysis, making this automated microfluidic platform suitable for the multiplexed impedimetric assay on a single device.

The modular structure of the proposed microfluidic system provides potential benefits of simplicity, economic integration, portability, full automation, simultaneous

multiple analytes detection, and simple maintenance. For the sake of simplicity in field analysis, the constructed pumping and valving makes the proposed microfluidic platform capable of controlling reagent flow in each channel independently and functioning as a fully automatic system. The optimal frequency of the binding interaction between the target analyte and its molecular recognition element was also investigated at a specific single-frequency value, thereby overcoming a particular time-consuming procedure. The miniaturised microfluidic system also provides the ability to reduce the reagent consumption and chemical waste products, thus contributing to low operational costs and corresponding closely to the concept of green chemistry, respectively.

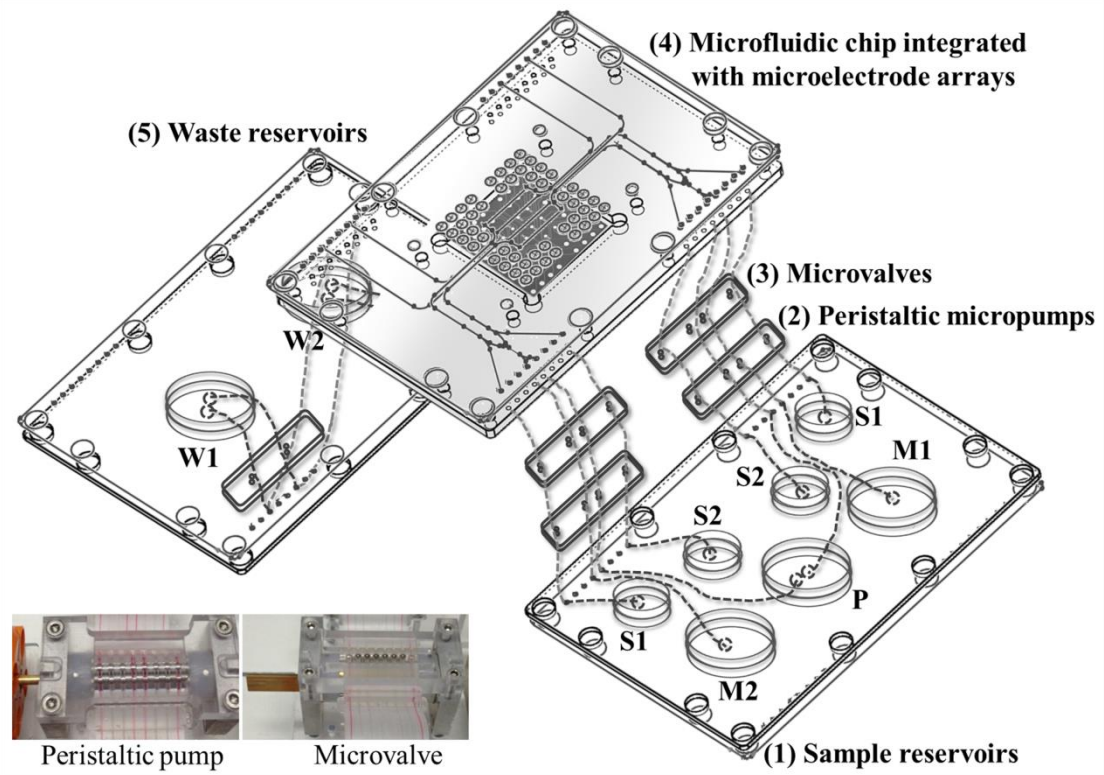

Figure 41. Schematic representation of the multiplexed microfluidic platform comprising various interconnecting individual modules with different functions: (1) reagent reservoirs for samples (S1, S2), chemicals used for on-line modification process (M1, M2), and electroactive redox probes (P), (2) 4-channel peristaltic micropumps for sequentially delivering each solution into the microfluidic chip, (3) 4-channel microvalves for controlling the flow of fluid operated by Lego® servo motors, (4) microfluidic channels integrated with 12-microelectrode array chip, and (5) microfluidic reservoir chip for waste collection during assays (W1, W2).

CHAPTER VII

CONCLUSIONS

7.1 Conclusion

Herein, affinity membrane-based sensors and a multiplex microfluidic platform for measuring diabetic markers were developed as alternative approaches to glycaemic monitoring in clinical practice. The proposed µPADs provide considerable improvement in both simplicity and speed and exhibit sufficient sensitivity. The corrected fructosamine values for serum albumin were acquired simultaneously. The proposed µPADs made great strides in providing a reliable marker for glycaemic control in diabetes associated with chronic kidney disease, particularly for dialysis patients. Moreover, the proposed boronate-based sensors were remarkably selective in determining HbA1c levels using label-free impedance detection. The APBA-modified ESMs and IDA chips were highly responsive to a wide range of HbA1c levels, indicating that these methods are suitable for clinical monitoring of glycaemic control. The APBA-modified ESMs also provide a cost-effective sensor for the diagnosis of diabetes, whereas the IDA chips are suitable for mass production and can be further integrated into a microfluidic system. These proposed methods have the potential for continuously monitoring glycaemic levels in diabetic patients and can be applicable to determining the presence other glycated proteins, e.g., glycated albumin, found in plasma.

A selective 3D-PEID for multiplexed measurement of diabetes markers was demonstrated using a single paper-based platform. The proposed 3D-PEID not only

provides a precise measurement with a wide dynamic concentration range, but also offers great sensitivity to determine the total haemoglobin and HbA1c values within the clinically relevant ranges. Such capabilities make this cost-effective device useful for monitoring the glycaemic status in individuals with diabetes. Besides this, the multiplexed microfluidic platform integrated with 12-microelectrode array chip was also developed for simultaneous impedimetric detection of total haemoglobin and HbA1c contents. This proof-of-concept prototype has very great merit in various aspects, including cost-effective device, portability, automated operation, simple fabrication and integration, interchangeability, and robust analysis tool. The self-contained electrochemical device integrated with a programmable fluid handling makes the present platform a fully automated measurement system. The constructed system also demonstrates significant potential for minimising the overall reagent quantities, resulting in a substantial reduction in the amount of chemical waste products.

7.2 Executive Summary

7.2.1 A microfluidic paper-based analytical device for the assay of albumin-corrected fructosamine values from whole blood samples

The proposed µPAD has the potential to continuously monitor glycaemic levels in low-resource settings. The characteristics of the proposed device are listed below:

1. The applicability of µPADs for acquiring albumin-corrected fructosamine values is clearly demonstrated with a short analysis time and an acceptable limit of detection.

2. When assessing the spiked serum albumin concentrations of 0.25 and 1 g dL^{-1}, the within-run coefficients of variation (CVs) were 2.43% and 2.19%, and the run-to-run CVs were 4.26% and 3.98%, respectively.
3. When evaluating the spiked primary standard fructosamine concentrations of 0.25 and 1 mM, the within-run reproducibility was 2.23% and 2.08% CVs, and the run-to-run reproducibility was 3.84% and 3.6% CVs.
4. The other endogenous substances found in whole blood samples, including haemoglobin (100 mg dL^{-1}), bilirubin (1.5 mg dL^{-1}), ɣ-globulin (2000 mg dL^{-1}), glucose (1000 mg dL^{-1}), ascorbic acid (5 mg dL^{-1}), and uric acid (10 mg dL^{-1}) were acceptable.
5. Good agreement between the proposed system and conventional laboratory large-scale methods was observed for HbA1c analysis in real blood samples.

7.2.2 Selective label-free electrochemical impedance measurement of glycated haemoglobin on 3-aminophenylboronic acid-modified eggshell membranes

A novel ESM-based analytical device was proposed as a low-cost biosensor for quantitative measurement of HbA1c. The characteristics of this sensing platform, which is ideal for point-of-care diagnostics, are summarised below:

1. The proposed device provides clinical applicability as an affinity membrane-based biosensor for the identification of HbA1c over a clinically relevant range (2.3%-14%) with a detection limit of 0.19%.
2. When assaying normal and abnormal HbA1c levels, the within-run coefficients of variation were 1.68% and 1.83%, respectively, and the run-to-run coefficients of variation were 1.97% and 2.02%, respectively.

3. Compared with a currently used commercial method (n =15), the results demonstrated excellent agreement between the techniques, demonstrating the clinical applicability of this sensor for monitoring glycaemic control.

7.2.3 A multiplexed three-dimensional paper-based electrochemical impedance device for simultaneous label-free affinity sensing of total and glycated haemoglobin: the potential of using a specific single-frequency value for analysis

A novel 3D-PEID was first introduced for measuring the multiple diabetes markers. The characteristics of the paper-based device are summarised below:

1. The Hp-modified and APBA-modified ESMs were highly responsive to a clinically relevant range of total haemoglobin (0.5-20 g dL^{-1}; r^2 =0.989) and HbA1c (2.3%-14%; r^2 =0.997) levels with a detection limit of 0.08 g dL^{-1} and 0.21%, respectively.
2. The optimal binding frequencies of total haemoglobin and HbA1c to their specific recognition elements were 5.18 Hz and 9.99 Hz, respectively.
3. The within-run coefficients of variation were 1.84%, 2.18%, 1.72%, and 2.01%, whereas the run-to-run CVs were 2.11%, 2.41%, 2.08%, and 2.21%, when assaying two levels of haemoglobin and HbA1c, respectively.
4. The CVs for the total haemoglobin and HbA1c levels measured on ten independently fabricated paper-based sheets were 1.96% and 2.10%, respectively.
5. The long-term stability of the Hp-modified and APBA-modified ESMs were 98.84% and 92.35%, respectively.

6. Compared with the commercial automated method, the results demonstrated excellent agreement between the techniques.

7.2.4 Boronate-modified interdigitated electrode array for selective impedance-based sensing of glycated haemoglobin

The APBA-modified IDA chips have the potential for monitoring glycaemic levels in diabetic patients. The characteristics of the proposed APBA-modified IDA sensor are listed below:

1. The boronate-modified electrode was highly responsive to the clinically relevant range of HbA1c levels (0.1%-8.36%) with a detection limit of 0.024% (3σ).
2. The specificity of the assay was evaluated with non-glycated haemoglobin (HbAo), showing that the impedance response remained unchanged over the concentration range of 10 to 20 g dL^{-1} HbAo. This demonstrated that the sensor system could be used to specifically distinguish HbA1c from HbAo.
3. When assaying normal and diabetic HbA1c levels, the overall assay reproducibility, expressed as relative standard error of mean, was 1.1%.
4. The performance of the sensor system was also compared with a commercial method (n =15) using patient-derived blood samples.

7.2.5 Development of a multiplexed microfluidic platform for measuring multiple diabetes makers: the promise of an automated impedimetric assay on microfluidics using a unique single-frequency value

1. The individually addressable microelectrode arrays afford a great opportunity for integration into a multiplexed microfluidic device for sensing multiple diabetes makers.
2. The automated peristaltic micropumps and microvalves were capable of routing the reagent solutions to each microchannel properly.

7.3 Limitations of the Study

Although the affinity membrane-based analytical device using a specific single-frequency value is used to circumvent the time-intensive procedure of acquiring entire impedance spectra, the further improvement on the processing software is still needed to be set to run EIS at the desired frequency value. Not only the production of affordable and portable devices is required for POCT system, but also the detection instrument to measure the signal should be developed into a portable and multi-channel measurement device.

7.4 Future Perspective

The development of μPADs towards clinical applicability has significant advantages over conventional laboratory-based bioassays, including small sample volumes, speed, simplicity, low-cost, instrument-free analysis, quantitative assessment, portability, and the simultaneous analysis of multiple biomarkers.

Additionally, paper-based assays have great merit in green chemistry, as the amount of hazardous waste is reduced and can be disposed of safely via incineration. The implementation of μPAD in medical diagnostics is needed for near-patient monitoring in remote areas and in resource-limited settings. Such a device provides considerable potential for off-site diagnostician in telemedicine. For diabetic patients, telemedicine can reduce the clinical visits and healthcare costs, allowing for inexpensive and continuous monitoring of their glycaemic levels.

Unless otherwise stated, the availability of a selective label free electrochemical sensing platform provides a more economical, accurate, reproducible, and reliable assay for monitoring and assessing the glycaemic levels in diabetic patients. The affinity ESM has contributed substantially to the field of method development and its application in medicinal diagnostics. For diagnostic purpose, such device is something of novelty due to its notable feature of selective binding via cis-diols interaction and also covering the HbA1c values at a clinically relevant range. The reproducibility and ease of fabrication of the affinity ESM-based sensor spur the experimentation in the field of electrochemistry, especially for the diagnosis of diabetes. The low cost of this sensing platform makes the proposed membrane-based sensor ideal for point-of-care diagnostics. Indeed, a trustworthy and low cost sensing platform makes it useful for assessing glycaemic levels in resource-limited settings.

So far no previous reports exist regarding the simultaneous measurement of total haemoglobin and HbA1c on a single affinity sensing device. As an alternative to traditional approaches, the paper-based assay allows for a distinct possibility that multiple analytes can be measured simultaneously in a single device. The multiplexed measurement of a panel of biomarkers has attracted a considerable interest due to its

potential for monitoring the patient compliance, evaluating the effectiveness of therapy, and early screening for the diseases. Such a multipliable platform offers a promising potential for ubiquitous healthcare monitoring in resource-limited regions, as it can reduce the number of clinical visits and the healthcare costs. The impedimetric assays on the 3D-PEID coupled with a specific single-frequency value for analysis offer not only the simplicity, low-cost, portability, and rapidity, but also provide the great opportunities for measuring the multiple diabetes markers with the high precision. Each analyte target could be detected by monitoring their optimal binding frequency specific to that reaction using a single 3D-PEID platform.

Moreover, the IDA chip consists of 12 individually addressable integrated three-microelectrode systems, thereby enabling the possibility for simultaneously sensing multiple analytes in a single chip using each microelectrode in the array. A mass fabrication of the IDA chips provides a highly reproducible sensor system, offering a possibility to integrate it into mass fabricated microfluidic devices for automated fluid handling. Additionally, the presented microfluidic platform can be tailored specifically to suit the particular needs for the multiplexed analysis of various significant biomarkers, such as cardiac biomarkers, cancer biomarkers, and many other metabolic biomarkers. The microfluidic system can be also redesigned to increase the sample throughput and the assembled 4-channel microvalve can be further specially adapted for many other applications. Furthermore, each analyte can be measured in triplicate due to the three individually addressable microelectrode arrays in the designed chamber. The two independent hemolysate samples can be analysed simultaneously using the automatic pumping and valving operations during the assays and each target analyte can be detected by monitoring the optimal binding

frequency specific to that binding interaction. Indeed, each biomarker and its molecular recognition would have the unique binding frequency, thus the EIS shows great promise as a tool for simultaneous multimarker detection using a specific single-frequency value.

REFERENCES

[1] World Health Organization. Use of glycated haemoglobin (HbA1c) in diagnosis of diabetes mellitus: abbreviated report of a WHO consultation. (2011).

[2] Shafi, T., Sozio, S.M., Plantinga, L.C., Jaar, B.G., Kim, E.T., Parekh, R.S., Steffes, M.W., Powe, N.R., Coresh, J., Selvin, E. Serum fructosamine and glycated albumin and risk of mortality and clinical outcomes in hemodialysis patients. Diabetes Care, (2012): 1-12.

[3] Mittman, N., Desiraju, B., Fazil, I., Kapupara, H., Chattopadhyay, J., Jani, C.M., Avram, M.M. Serum fructosamine versus glycosylated hemoglobin as an index of glycemic control, hospitalization, and infection in diabetic hemodialysis patients. Kidney Int. Suppl., 117 (2010): S41-S45.

[4] Coronel, F., Macia, M., Cidoncha, A., Sanchez, A., Tornero, F., Barrientos, A.,Valor, R. Fructosamine levels in CAPD: its value as glycemic index. Adv. Perit. Dial., 7 (1991): 253-256.

[5] American Diabetes Association. Standards of medical care in diabetes—2013. Diabetes Care, 36 (2013): S11-S66.

[6] Lamb, E., Venton, T., Cattell, W., Dawnay, A. Serum glycated albumin and fructosamine in renal dialysis patients. Nephron, 64 (1993): 82-88.

[7] Schleicher, E., Wieland, O. Specific quantitation by HPLC of protein (lysine) bound glucose in human serum albumin and other glycosylated proteins. Clin. Chem. Lab. Med., 19 (1981): 81-88.

[8] Schleicher, E., Scheller, L., Wieland, O. Quantitation of lysine-bound glucose of normal and diabetic erythrocyte membranes by HPLC analysis of furosine [ε-N (L-furoylmethyl)-L-lysine]. Biochem. Biophys. Res. Commun., 99 (1981): 1011-1019.

[9] Brownlee, M., Vlassara, H., Cerami, A. Measurement of glycosylated amino acids and peptides from urine of diabetic patients using affinity chromatography. Diabetes, 29 (1980): 1044-1047.

[10] Burd, J.F., Neyer, G. (1997) Electrochemical determination of fructosamine. 5,639,672

[11] Moore, J., Outlaw, M., Barnes, A., Turner, R. Glycosylated plasma protein measurement by a semi-automated method. Ann. Clin. Biochem., 23 (1986): 198-203.

[12] Baker, J.R. (1987) Methods of determiningfructosamine levels in blood samples. 4,642,295

[13] Baker, J., Metcalf, P., Scragg, R., Johnson, R. Fructosamine Test-Plus, a modified fructosamine assay evaluated. Clin. Chem., 37 (1991): 552-556.

[14] Vorberg, E. (1999) Kit for fructosamine determination. 5,866,352

[15] Vella, S.J., Beattie, P., Cademartiri, R., Laromaine, A., Martinez, A.W., Phillips, S.T., Mirica, K.A., Whitesides, G.M. Measuring markers of liver function using a micropatterned paper device designed for blood from a fingerstick. Anal. Chem., 84 (2012): 2883-2891.

[16] Pollock, N.R., Rolland, J.P., Kumar, S., Beattie, P.D., Jain, S., Noubary, F., Wong, V.L., Pohlmann, R.A., Ryan, U.S., Whitesides, G.M. A

paper-based multiplexed transaminase test for low-cost, point-of-care liver function testing. Sci. Transl. Med., 4 (2012): 1-10.

[17] Boonyasit, Y., Laiwattanapaisal, W. A microfluidic paper-based analytical device for the assay of albumin-corrected fructosamine values from whole blood samples. Bioanalysis, 7 (2015): 79-90.

[18] Yamaguchi, M., Kambe, S., Eto, T., Yamakoshi, M., Kouzuma, T., Suzuki, N. Point of care testing system via enzymatic method for the rapid, efficient assay of glycated albumin. Biosens. Bioelectron., 21 (2005): 426-432.

[19] Martinez, A.W., Phillips, S.T., Carrilho, E., Thomas III, S.W., Sindi, H., Whitesides, G.M. Simple telemedicine for developing regions: camera phones and paper-based microfluidic devices for real-time, off-site diagnosis. Anal. Chem., 80 (2008): 3699-3707.

[20] Martinez, A.W., Phillips, S.T., Butte, M.J., Whitesides, G.M. Patterned paper as a platform for inexpensive, low-volume, portable bioassays. Angew. Chem. Int. Ed., 46 (2007): 1318-1320.

[21] Dungchai, W., Chailapakul, O., Henry, C.S. Use of multiple colorimetric indicators for paper-based microfluidic devices. Anal. Chim. Acta, 674 (2010): 227-233.

[22] Wu, Y., Xue, P., Kang, Y., Hui, K.M. Paper-Based Microfluidic Electrochemical Immunodevice Integrated with Nanobioprobes onto Graphene Film for Ultrasensitive Multiplexed Detection of Cancer Biomarkers. Anal. Chem., 85 (2013): 8661-8668.

[23] Wang, P., Ge, L., Yan, M., Song, X., Ge, S., Yu, J. Paper-based three-dimensional electrochemical immunodevice based on multi-walled carbon nanotubes functionalized paper for sensitive point-of-care testing. Biosens. Bioelectron., 32 (2012): 238-243.

[24] Zang, D., Ge, L., Yan, M., Song, X.,Yu, J. Electrochemical immunoassay on a 3D microfluidic paper-based device. Chem. Commun., 48 (2012): 4683-4685.

[25] Ge, S., Ge, L., Yan, M., Song, X., Yu, J., Huang, J. A disposable paper-based electrochemical sensor with an addressable electrode array for cancer screening. Chem. Commun., 48 (2012): 9397-9399.

[26] Li, L., Li, W., Yang, H., Ma, C., Yu, J., Yan, M., Song, X. Sensitive origami dual-analyte electrochemical immunodevice based on polyaniline/Au-paper electrode and multi-labeled 3D graphene sheets. Electrochim. Acta, 120 (2014): 102-109.

[27] Li, W., Li, L., Li, M., Yu, J., Ge, S., Yan, M., Song, X. Development of a 3D origami multiplex electrochemical immunodevice using a nanoporous silver-paper electrode and metal ion functionalized nanoporous gold–chitosan. Chem. Commun., 49 (2013): 9540-9542.

[28] Ge, L., Wang, S., Song, X., Ge, S., Yu, J. 3D origami-based multifunction-integrated immunodevice: low-cost and multiplexed sandwich chemiluminescence immunoassay on microfluidic paper-based analytical device. Lab Chip, 12 (2012): 3150-3158.

[29] Ge, L., Yan, J., Song, X., Yan, M., Ge, S., Yu, J. Three-dimensional paper-based electrochemiluminescence immunodevice for multiplexed

measurement of biomarkers and point-of-care testing. Biomaterials, 33 (2012): 1024-1031.

[30] Yetisen, A.K., Akram, M.S., Lowe, C.R. Paper-based microfluidic point-of-care diagnostic devices. Lab Chip, 13 (2013): 2210-2251.

[31] Lisowski, P., Zarzycki, P.K. Microfluidic Paper-Based Analytical Devices (μPADs) and Micro Total Analysis Systems (μTAS): Development, Applications and Future Trends. Chromatographia, 76 (2013): 1201-1214.

[32] Martinez, A.W. Microfluidic paper-based analytical devices: from POCKET to paper-based ELISA. Bioanalysis, 3 (2011): 2589-2592.

[33] del Castillo, E., Montes-Bayón, M., Añón, E., Sanz-Medel, A. Quantitative targeted biomarker assay for glycated haemoglobin by multidimensional LC using mass spectrometric detection. J. Proteomics, 74 (2011): 35-43.

[34] Roberts, N.B., Amara, A.B., Morris, M., Green, B.N. Long-term evaluation of electrospray ionization mass spectrometric analysis of glycated hemoglobin. Clin. Chem., 47 (2001): 316-321.

[35] Jeppsson, J.O., Kobold, U., Barr, J., Finke, A., Hoelzel, W., Hoshino, T., Miedema, K., Mosca, A., Mauri, P., Paroni, R. Approved IFCC reference method for the measurement of HbA1c in human blood. Clin. Chem. Lab. Med., 40 (2002): 78-89.

[36] Eckerbom, S., Bergqvist, Y., Jeppsson, J.O. Improved method for analysis of glycated haemoglobin by ion exchange chromatography. Ann. Clin. Biochem., 31 (1994): 355-360.

[37] Frantzen, F., Grimsrud, K., Heggli, D.E., Sundrehagen, E. Protein-boronic acid conjugates and their binding to low-molecular-mass cis-diols and glycated hemoglobin. J. Chromatogr. B, 670 (1995): 37-45.

[38] Mullins, R., Austin, G. Sensitivity of isoelectric focusing, ion exchange, and affinity chromatography to labile glycated hemoglobin. Clin. Chem., 32 (1986): 1460-1463.

[39] Halámek, J., Wollenberger, U., Stöcklein, W., Scheller, F. Development of a biosensor for glycated hemoglobin. Electrochim. Acta, 53 (2007): 1127-1133.

[40] Přibyl, J., Skládal, P. Quartz crystal biosensor for detection of sugars and glycated hemoglobin. Anal. Chim. Acta, 530 (2005): 75-84.

[41] Přibyl, J., Skládal, P. Development of a combined setup for simultaneous detection of total and glycated haemoglobin content in blood samples. Biosens. Bioelectron., 21 (2006): 1952-1959.

[42] Adamczyk, M., Chen, Y.Y., Johnson, D.D., Mattingly, P.G., Moore, J.A., Pan, Y., Reddy, R.E. Chemiluminescent acridinium-9-carboxamide boronic acid probes: Application to a homogeneous glycated hemoglobin assay. Bioorg. Med. Chem. Lett., 16 (2006): 1324-1328.

[43] Chen, H.H., Wu, C.H., Tsai, M.L., Huang, Y.J., Chen, S.H. Detection of Total and A1c-Glycosylated Hemoglobin in Human Whole Blood Using Sandwich Immunoassays on Polydimethylsiloxane-Based Antibody Microarrays. Anal. Chem., 84 (2012): 8635-8641.

[44] Stöllner, D., Stöcklein, W., Scheller, F., Warsinke, A. Membrane-immobilized haptoglobin as affinity matrix for a hemoglobin-A1c immunosensor. Anal. Chim. Acta, 470 (2002): 111-119.

[45] Liu, G., Khor, S.M., Iyengar, S.G., Gooding, J.J. Development of an electrochemical immunosensor for the detection of HbA1c in serum. Analyst, 137 (2012): 829-832.

[46] RamanáSuri, C. Zeta potential based colorimetric immunoassay for the direct detection of diabetic marker HbA1c using gold nanoprobes. Chem. Commun., 46 (2010): 5755-5757.

[47] Szymezak, J., Leroy, N., Lavalard, E., Gillery, P. Evaluation of the DCA Vantage analyzer for HbA1c assay. Clin. Chem. Lab. Med., 46 (2008): 1195-1198.

[48] Kim, D.-M., Shim, Y.B. Disposable Amperometric Glycated Hemoglobin Sensor for the Finger Prick Blood Test. Anal. Chem., 85 (2013): 6536-6543.

[49] Tanaka, T., Tsukube, S., Izawa, K., Okochi, M., Lim, T.K., Watanabe, S., Harada, M., Matsunaga, T. Electrochemical detection of HbA1c, a maker for diabetes, using a flow immunoassay system. Biosens. Bioelectron., 22 (2007): 2051-2056.

[50] Liu, S., Wollenberger, U., Katterle, M., Scheller, F.W. Ferroceneboronic acid-based amperometric biosensor for glycated hemoglobin. Sens. Actuator-B Chem., 113 (2006): 623-629.

[51] Zhou, Y., Dong, H., Liu, L., Hao, Y., Chang, Z., Xu, M. Fabrication of electrochemical interface based on boronic acid-modified pyrroloquinoline quinine/reduced graphene oxide composites for voltammetric determination of glycated hemoglobin. Biosens. Bioelectron., 64 (2015): 442-448.

[52] Song, S.Y., Yoon, H.C. Boronic acid-modified thin film interface for specific binding of glycated hemoglobin (HbA 1c) and electrochemical biosensing. Sens. Actuator-B Chem., 140 (2009): 233-239.

[53] Song, S.Y., Han, Y.D., Park, Y.M., Jeong, C.Y., Yang, Y.J., Kim, M.S., Ku, Y., Yoon, H.C. Bioelectrocatalytic detection of glycated hemoglobin (HbA 1c) based on the competitive binding of target and signaling glycoproteins to a boronate-modified surface. Biosens. Bioelectron., 35 (2012): 355-362.

[54] Liu, H., Crooks, R.M. Determination of percent hemoglobin A1c using a potentiometric method. Anal. Chem., 85 (2012): 1834-1839.

[55] Hsieh, K.M., Lan, K.C., Hu, W.L., Chen, M.K., Jang, L.S., Wang, M.H. Glycated hemoglobin (HbA 1c) affinity biosensors with ring-shaped interdigital electrodes on impedance measurement. Biosens. Bioelectron., 49 (2013): 450-456.

[56] Park, J.Y., Chang, B.Y., Nam, H., Park, S.M. Selective electrochemical sensing of glycated hemoglobin (HbA1c) on thiophene-3-boronic acid self-assembled monolayer covered gold electrodes. Anal. Chem., 80 (2008): 8035-8044.

[57] Chuang, Y.C., Lan, K.C., Hsieh, K.M., Jang, L.S., Chen, M.K. Detection of glycated hemoglobin (HbA 1c) based on impedance

measurement with parallel electrodes integrated into a microfluidic device. Sens. Actuator-B Chem., 171 (2012): 1222-1230.

[58] Liu, J.T., Chen, L.Y., Shih, M.C., Chang, Y., Chen, W.Y. The investigation of recognition interaction between phenylboronate monolayer and glycated hemoglobin using surface plasmon resonance. Anal. Biochem., 375 (2008): 90-96.

[59] Syamala Kiran, M., Itoh, T., Yoshida, K.-i., Kawashima, N., Biju, V., Ishikawa, M. Selective detection of HbA1c using surface enhanced resonance Raman spectroscopy. Anal. Chem., 82 (2010): 1342-1348.

[60] Hsieh, K.M., Lan, K.C., Hu, W.L., Chen, M.K., Jang, L.S., Wang, M.H. Glycated hemoglobin (HbA_{1c}) affinity biosensors with ring-shaped interdigital electrodes on impedance measurement. Biosens. Bioelectron., 49 (2013): 450-456.

[61] Chuang, Y.C., Lan, K.C., Hsieh, K.M., Jang, L.S., Chen, M.K. Detection of glycated hemoglobin (HbA_{1c}) based on impedance measurement with parallel electrodes integrated into a microfluidic device. Sens. Actuator-B Chem., 171 (2012): 1222-1230.

[62] Pundir, C.S., Chawla, S. Determination of glycated hemoglobin with special emphasis on biosensing methods. Anal. Biochem., 444 (2014): 47-56.

[63] Stolowitz, M.L., Ahlem, C., Hughes, K.A., Kaiser, R.J., Kesicki, E.A., Li, G., Lund, K.P., Torkelson, S.M., Wiley, J.P. Phenylboronic acid-salicylhydroxamic acid bioconjugates. 1. A novel boronic acid complex for protein immobilization. Bioconjugate Chem., 12 (2001): 229-239.

[64] Tsai, W., Yang, J., Lai, C., Cheng, Y., Lin, C., Yeh, C. Characterization and adsorption properties of eggshells and eggshell membrane. Bioresour. Technol., 97 (2006): 488-493.

[65] Danaei, G., Finucane, M.M., Lu, Y., Singh, G.M., Cowan, M.J., Paciorek, C.J., Lin, J.K., Farzadfar, F., Khang, Y.H., Stevens, G.A. National, regional, and global trends in fasting plasma glucose and diabetes prevalence since 1980: systematic analysis of health examination surveys and epidemiological studies with 370 country-years and 2· 7 million participants. Lancet, 378 (2011): 31-40.

[66] Collins, A.J., Foley, R.N., Chavers, B., Gilbertson, D., Herzog, C., Johansen, K., Kasiske, B., Kutner, N., Liu, J., St Peter, W. United States Renal Data System 2011 Annual Data Report: Atlas of chronic kidney disease & end-stage renal disease in the United States. Am. J. Kidney Dis., 59 (2012): e1-420.

[67] Foley, R.N., Collins, A.J. The USRDS: What You Need to Know about What It Can and Can't Tell Us about ESRD. Clin. J. Am. Soc. Nephrol., 8 (2013): 845-851.

[68] McMurray, S.D., Johnson, G., Davis, S., McDougall, K. Diabetes education and care management significantly improve patient outcomes in the dialysis unit. Am. J. Kidney Dis., 40 (2002): 566-575.

[69] Hovind, P., Rossing, P., Tarnow, L., Smidt, U.M., Parving, H.H. Progression of diabetic nephropathy. Kidney Int., 59 (2001): 702-709.

[70] Goldstein, D.E., Little, R.R., Lorenz, R.A., Malone, J.I., Nathan, D., Peterson, C.M., Sacks, D.B. Tests of glycemia in diabetes. Diabetes Care, 27 (2004): 1761-1773.

[71] Chen, H.S., Wu, T.E., Lin, H.D., Jap, T.S., Hsiao, L.C., Lee, S.H., Lin, S.H. Hemoglobin A1c and fructosamine for assessing glycemic control in diabetic patients with CKD stages 3 and 4. Am. J. Kidney Dis., 55 (2010): 867.

[72] Martinez, A.W., Phillips, S.T., Butte, M.J., Whitesides, G.M. Patterned paper as a platform for inexpensive, low-volume, portable bioassays. Angew. Chem. Int. Ed., 46 (2007): 1318-1320.

[73] Klasner, S.A., Price, A.K., Hoeman, K.W., Wilson, R.S., Bell, K.J., Culbertson, C.T. Paper-based microfluidic devices for analysis of clinically relevant analytes present in urine and saliva. Anal. Bioanal. Chem., 397 (2010): 1821-1829.

[74] Bhakta, S.A., Borba, R., Taba Jr, M., Garcia, C.D., Carrilho, E. Determination of nitrite in saliva using microfluidic paper-based analytical devices. Anal. Chim. Acta, 809 (2014) 117-122.

[75] Li, X., Tian, J., Shen, W. Quantitative biomarker assay with microfluidic paper-based analytical devices. Anal. Bioanal. Chem., 396 (2010): 495-501.

[76] Kruse-Jarres, J., Jarausch, J., Lehmann, P., Vogt, B., Rietz, P. A new colorimetric method for the determination of fructosamine. Lab. Med., 13 (1989): 245-253.

[77] Songjaroen, T., Dungchai, W., Chailapakul, O., Henry, C.S., Laiwattanapaisal, W. Blood separation on microfluidic paper-based analytical devices. Lab Chip, 12 (2012): 3392-3398.

[78] Songjaroen, T., Dungchai, W., Chailapakul, O., Laiwattanapaisal, W. Novel, simple and low-cost alternative method for fabrication of paper-based microfluidics by wax dipping. Talanta, 85 (2011): 2587-2593.

[79] Doumas, B.T., Ard Watson, W., Biggs, H.G. Albumin standards and the measurement of serum albumin with bromcresol green. Clin. Chim. Acta, 31 (1971): 87-96.

[80] Executive Summary: Standards of Medical Care in Diabetes—2013. Diabetes Care, 36 (2013): S4-S10.

[81] Sakamoto, H., Kagaku, D.K. (1996) Multilayer analytical element for assaying fructosamine. 5,565,170

[82] Burd, J.F., Hoblitzell, T. (1995) Multi-layer devices and methods of assaying for fructosamine 5,470,752

[83] [83] Brun, J.F., Aloulou, I., Varlet-Marie, E. Type 2 diabetics with higher plasma viscosity exhibit a higher blood pressure. Clin. Hemorheol. Microcirc., 30 (2004): 365-372.

[84] Kratz, A., Ferraro, M., Sluss, P.M., Lewandrowski, K.B. Laboratory reference values. N. Engl. J. Med., 351 (2004): 1548-1564.

[85] Ricos, C., Garcia-Lario, J., Alvarez, V., Cava, F., Domenech, M., Hernandez, A., Jimenez, C., Minchinela, J., Perich, C., Simon, M. Biological variation database, and quality specifications for imprecision, bias and total

error (desirable and minimum). The 2004 update. (2009) See http://www.westgard.com/biodatabase-2014-update.htm

[86] Brownlee, M. Biochemistry and molecular cell biology of diabetic complications. Nature, 414 (2001): 813-820.

[87] Baynes, J.W., Thorpe, S.R. Role of oxidative stress in diabetic complications: a new perspective on an old paradigm. Diabetes, 48 (1999): 1-9.

[88] Weykamp, C., Penders, T., Siebelder, C., Muskiet, F., Van der Slik, W. Interference of carbamylated and acetylated hemoglobins in assays of glycohemoglobin by HPLC, electrophoresis, affinity chromatography, and enzyme immunoassay. Clin. Chem., 39 (1993): 138-142.

[89] Frantzen, F., Grimsrud, K., Heggli, D.E., Sundrehagen, E. Protein-boronic acid conjugates and their binding to low-molecular-mass *cis*-diols and glycated hemoglobin. J. Chromatogr. B, 670 (1995): 37-45.

[90] Liu, G., Iyengar, S.G., Gooding, J.J. An electrochemical impedance immunosensor based on gold nanoparticle-modified electrodes for the detection of HbA1c in human blood. Electroanalysis, 24 (2012): 1509-1516.

[91] Wangoo, N., Kaushal, J., Bhasin, K., Mehta, S., Suri, C. Zeta potential based colorimetric immunoassay for the direct detection of diabetic marker HbA1c using gold nanoprobes. Chem. Commun., 46 (2010): 5755-5757.

[92] Tanaka, T., Tsukube, S., Izawa, K., Okochi, M., Lim, T.K., Watanabe, S., Harada, M., Matsunaga, T. Electrochemical detection of HbA_{1c}, a maker

for diabetes, using a flow immunoassay system. Biosens. Bioelectron., 22 (2007): 2051-2056.

[93] Song, S.Y., Han, Y.D., Park, Y.M., Jeong, C.Y., Yang, Y.J., Kim, M.S., Ku, Y., Yoon, H.C. Bioelectrocatalytic detection of glycated hemoglobin (HbA_{1c}) based on the competitive binding of target and signaling glycoproteins to a boronate-modified surface. Biosens. Bioelectron., 35 (2012): 355-362.

[94] Song, S.Y., Yoon, H.C. Boronic acid-modified thin film interface for specific binding of glycated hemoglobin (HbA_{1c}) and electrochemical biosensing. Sens. Actuator-B Chem., 140 (2009): 233-239.

[95] Kiran, M., Itoh, T., Yoshida, K., Kawashima, N., Biju, V., Ishikawa, M. Selective detection of HbA1c using surface enhanced resonance Raman spectroscopy. Anal. Chem., 82 (2010): 1342-1348.

[96] Fang, L., Li, W., Zhou, Y., Liu, C.C. A single-use, disposable iridium-modified electrochemical biosensor for fructosyl valine for the glycoslated hemoglobin detection. Sens. Actuator-B Chem., 137 (2009): 235-238.

[97] Raistrick, I.D., Franceschetti, D.R., Macdonald, J.R.. In: Barsoukov, E., Macdonald, J.R. (Ed.) Impedance Spectroscopy: Theory, Experiment, and Applications. John Wiley & Sons, Inc., Hoboken, New Jersey, (2005): 37.

[98] Tanvir, S., Pantigny, J., Boulnois, P., Pulvin, S. Covalent immobilization of recombinant human cytochrome CYP2E1 and glucose-6-phosphate dehydrogenase in alumina membrane for drug screening applications. J. Membr. Sci., 329 (2009): 85-90.

[99] Deng, J., Toh, C.S. Impedimetric DNA biosensor based on a nanoporous alumina membrane for the detection of the specific oligonucleotide sequence of dengue virus. Sensors, 13 (2013): 7774-7785.

[100] Durmuş, E., Celik, I., Ozturk, A., Ozkan, Y., Aydin, M. Evaluation of the potential beneficial effects of ostrich eggshell combined with eggshell membranes in healing of cranial defects in rabbits. J. Int. Med. Res., 31 (2003): 223-230.

[101] Yang, J.Y., Chuang, S.S., Yang, W.G., Tsay, P.K. Egg membrane as a new biological dressing in split-thickness skin graft donor sites: a preliminary clinical evaluation. Chang Gung Med. J., 26 (2003): 153-159.

[102] Xiao, D., Choi, M.M. Aspartame optical biosensor with bienzyme-immobilized eggshell membrane and oxygen-sensitive optode membrane. Anal. Chem., 74 (2002): 863-870.

[103] Tang, J., Liu, Z., Kang, J., Zhang, Y. Determination of salbutamol using R-phycoerythrin immobilized on eggshell membrane surface as a fluorescence probe. Anal. Bioanal. Chem., 397 (2010): 3015-3022.

[104] Yeni, F., Odaci, D., Timur, S. Use of eggshell membrane as an immobilization platform in microbial sensing. Anal. Lett., 41 (2008): 2743-2758.

[105] Liu, S., Wollenberger, U., Halámek, J., Leupold, E., Stöcklein, W., Warsinke, A., Scheller, F.W. Affinity Interactions between Phenylboronic Acid- Carrying Self- Assembled Monolayers and Flavin Adenine Dinucleotide or Horseradish Peroxidase. Chem.-Eur. J., 11 (2005): 4239-4246.

[106] Tan, C., Chen, T., Chan, H., Ng, L. A scanning and transmission electron microscopic study of the membranes of chicken egg. Histol. Histopath. 7 (1992): 339-345.

[107] Takiguchi, M., Igarashi, K., Azuma, M., Ooshima, H. Flowerlike agglomerates of calcium carbonate crystals formed on an eggshell membrane. Cryst. Growth Des., 6 (2006): 2754-2757.

[108] Li, N., Niu, L.N., Qi, Y.P., Yiu, C.K., Ryou, H., Arola, D.D., Chen, J.H., Pashley, D.H.,Tay, F.R. Subtleties of biomineralisation revealed by manipulation of the eggshell membrane. Biomaterials, 32 (2011): 8743-8752.

[109] Yan, J., Springsteen, G., Deeter, S., Wang, B. The relationship among pK_a, pH, and binding constants in the interactions between boronic acids and diols—it is not as simple as it appears. Tetrahedron, 60 (2004): 11205-11209.

[110] Li, B., Lan, D., Zhang, Z. Chemiluminescence flow-through biosensor for glucose with eggshell membrane as enzyme immobilization platform. Anal. Biochem., 374 (2008): 64-70.

[111] Zhang, G., Liu, D., Shuang, S., Choi, M.M. A homocysteine biosensor with eggshell membrane as an enzyme immobilization platform. Sens. Actuator-B Chem., 114 (2006): 936-942.

[112] Wu, B., Zhang, G., Shuang, S., Choi, M.M. Biosensors for determination of glucose with glucose oxidase immobilized on an eggshell membrane. Talanta, 64 (2004): 546-553.

[113] Choi, M.M., Yiu, T.P. Immobilization of beef liver catalase on eggshell membrane for fabrication of hydrogen peroxide biosensor. Enzyme Microb. Technol., 34 (2004): 41-47.

[114] Tembe, S., Kubal, B., Karve, M., D'Souza, S. Glutaraldehyde activated eggshell membrane for immobilization of tyrosinase from *Amorphophallus companulatus*: Application in construction of electrochemical biosensor for dopamine. Anal. Chim. Acta, 612 (2008): 212-217.

[115] Choi, M.M., Pang, W.S., Xiao, D., Wu, X. An optical glucose biosensor with eggshell membrane as an enzyme immobilisation platform. Analyst, 126 (2001): 1558-1563.

[116] Nys, Y., Gautron, J., Garcia-Ruiz, J.M., Hincke, M.T. Avian eggshell mineralization: biochemical and functional characterization of matrix proteins. C. R. Palevol, 3 (2004): 549-562.

[117] Bard, A.J., Faulkner, L.R.. Electrochemical Methods: Fundmentals and Applications. John Wiley & Sons, Inc., Hoboken, New Jersey, (2001).

[118] Sacks, D.B., Arnold, M., Bakris, G.L., Bruns, D.E., Horvath, A.R., Kirkman, M.S., Lernmark, A., Metzger, B.E., Nathan, D.M. Guidelines and recommendations for laboratory analysis in the diagnosis and management of diabetes mellitus. Diabetes Care, 34 (2011): e61-e99.

[119] Bry, L., Chen, P.C., Sacks, D.B. Effects of hemoglobin variants and chemically modified derivatives on assays for glycohemoglobin. Clin. Chem., 47 (2001): 153-163.

[120] Jaisson, S., Leroy, N., Desroches, C., Tonye-Libyh, M., Guillard, E., Gillery, P. Interference of the most frequent haemoglobin variants on quantification of HbA_{1c}: Comparison between the LC–MS (IFCC reference method) and three routinely used methods. Diabetes Metab., 39 (2013): 363-369.

[121] Dungchai, W., Chailapakul, O., Henry, C.S. Electrochemical detection for paper-based microfluidics. Anal. Chem., 81 (2009): 5821-5826.

[122] Zhao, C., Thuo, M.M., Liu, X. A microfluidic paper-based electrochemical biosensor array for multiplexed detection of metabolic biomarkers. Sci. Technol. Adv. Mater., 14 (2013): 1-7.

[123] Wang, J., Profitt, J.A., Pugia, M.J., Suni, I.I. Au nanoparticle conjugation for impedance and capacitance signal amplification in biosensors. Anal. Chem., 78 (2006): 1769-1773.

[124] Shervedani, R.K., Mozaffari, S.A. Impedimetric sensing of uranyl ion based on phosphate functionalized cysteamine self-assembled monolayers. Anal. Chim. Acta, 562 (2006): 223-228.

[125] Shervedani, R.K., Hatefi-Mehrjardi, A. Electrochemical characterization of directly immobilized glucose oxidase on gold mercaptosuccinic anhydride self-assembled monolayer. Sens. Actuator-B Chem., 126 (2007): 415-423.

[126] Shervedani, R.K., Bagherzadeh, M., Sabzyan, H., Safari, R. One-impedance for one-concentration impedimetry as an electrochemical method for determination of the trace zirconium ion. J. Electroanal. Chem., 633 (2009): 259-263.

[127] Katz, E., Alfonta, L., Willner, I. Chronopotentiometry and Faradaic impedance spectroscopy as methods for signal transduction in immunosensors. Sens. Actuator-B Chem., 76 (2001): 134-141.

[128] La Belle, J.T., Demirok, U.K., Patel, D.R., Cook, C.B. Development of a novel single sensor multiplexed marker assay. Analyst, 136 (2011): 1496-1501.

[129] Fairchild, A.B., McAferty, K., Demirok, U.K., La Belle, J.T. A label-free, rapid multimarker protein impedance-based immunosensor. In: Complex Medical Engineering, 2009. CME. ICME International Conference on, IEEE (2009): 1-5

[130] Demirok, U., Verma, A., La Belle, J. The Development of a Label-Free Electrochemical Impedance Based Point-of-care Technology for Multimarker Detection. J. Biosens. Bioelectron., 12 (2013): 1-7.

[131] Adamson, T.L., Eusebio, F.A., Cook, C.B., LaBelle, J.T. The promise of electrochemical impedance spectroscopy as novel technology for the management of patients with diabetes mellitus. Analyst, 137 (2012): 4179-4187.

[132] Adamson, T.L., Cook, C.B., LaBelle, J.T. Detection of 1, 5-Anhydroglucitol by Electrochemical Impedance Spectroscopy. J. Diabetes Sci. Technol., 8 (2014): 350-355.

[133] Consensus Committee. Consensus statement on the worldwide standardisation of the HbA1c measurement. Diabetologia, 50 (2007): 2042-2043.

[134] Ogawa, K., Stöllner, D., Scheller, F., Warsinke, A., Ishimura, F., Tsugawa, W., Ferri, S., Sode, K. Development of a flow-injection analysis (FIA) enzyme sensor for fructosyl amine monitoring. Anal. Bioanal. Chem., 373 (2002): 211-214.

[135] Sakaguchi, A., Tsugawa, W., Ferri, S., Sode, K. Development of highly-sensitive fructosyl-valine enzyme sensor employing recombinant fructosyl amine oxidase. Electrochemistry, 71 (2003): 442-445.

[136] Tsugawa, W., Ishimura, F., Ogawa, K., Sode, K. Development of an enzyme sensor utilizing a novel fructosyl amine oxidase from a marine yeast. Electrochemistry, 68 (2000): 869-871.

[137] Boonyasit, Y., Heiskanen, A., Chailapakul, O., Laiwattanapaisal, W. Selective label-free electrochemical impedance measurement of glycated haemoglobin on 3-aminophenylboronic acid-modified eggshell membranes. Anal. Bioanal. Chem., 407 (2015): 5287-5297.

[138] Carrilho, E., Martinez, A.W., Whitesides, G.M. Understanding wax printing: a simple micropatterning process for paper-based microfluidics. Anal. Chem., 81 (2009): 7091-7095.

[139] Yakovleva, J., Davidsson, R., Lobanova, A., Bengtsson, M., Eremin, S., Laurell, T., Emnéus, J. Microfluidic enzyme immunoassay using silicon microchip with immobilized antibodies and chemiluminescence detection. Anal. Chem., 74 (2002): 2994-3004.

[140] Kitzmiller, J.L., Block, J.M., Brown, F.M., Catalano, P.M., Conway, D.L., Coustan, D.R., Gunderson, E.P., Herman, W.H., Hoffman, L.D., Inturrisi, M. Managing Preexisting Diabetes for Pregnancy Summary of

evidence and consensus recommendations for care. Diabetes Care, 31 (2008): 1060-1079.

[141] Eckerbom, S., Bergqvist, Y., Jeppsson, J. Improved method for analysis of glycated haemoglobin by ion exchange chromatography. Ann. Clin. Biochem., 31 (1994): 355-360.

[142] Takahashi, S., Anzai, J.I. Phenylboronic acid monolayer-modified electrodes sensitive to sugars. Langmuir, 21 (2005): 5102-5107.

[143] Wannapob, R., Kanatharana, P., Limbut, W., Numnuam, A., Asawatreratanakul, P., Thammakhet, C., Thavarungkul, P. Affinity sensor using 3-aminophenylboronic acid for bacteria detection. Biosens. Bioelectron., 26 (2010): 357-364.

[144] Elmas, B., Onur, M., Şenel, S., Tuncel, A. Temperature controlled RNA isolation by N-isopropylacrylamide–vinylphenyl boronic acid copolymer latex. Colloid Polym. Sci., 280 (2002): 1137-1146.

[145] Nie, H., Chen, Y., Lü, C., Liu, Z. Efficient selection of glycoprotein-binding DNA aptamers via boronate affinity monolithic capillary. Anal. Chem., 85 (2013): 8277-8283.

[146] Liu, H., Li, Y., Sun, K., Fan, J., Zhang, P., Meng, J., Wang, S., Jiang, L. Dual-responsive surfaces modified with phenylboronic acid-containing polymer brush to reversibly capture and release cancer cells. J. Am. Chem. Soc., 135 (2013): 7603-7609.

[147] Liu, S., Zhang, X., Wu, Y., Tu, Y., He, L. Prostate-specific antigen detection by using a reusable amperometric immunosensor based on reversible

binding and leasing of HRP-anti-PSA from phenylboronic acid modified electrode. Clin. Chim. Acta, 395 (2008): 51-56.

[148] Zhang, X., Wu, Y., Tu, Y., Liu, S. A reusable electrochemical immunosensor for carcinoembryonic antigen via molecular recognition of glycoprotein antibody by phenylboronic acid self-assembly layer on gold. Analyst, 133 (2008): 485-492.

[149] Katz, E., Willner, I. Probing biomolecular interactions at conductive and semiconductive surfaces by impedance spectroscopy: routes to impedimetric immunosensors, DNA-sensors, and enzyme biosensors. Electroanalysis, 15 (2003): 913-947.

[150] Lasseter, T.L., Cai, W., Hamers, R.J. Frequency-dependent electrical detection of protein binding events. Analyst, 129 (2004): 3-8.

[151] Boonyasit, Y., Chailapakul, O., Laiwattanapaisal, W. A Multiplexed Three-Dimensional Paper-Based Electrochemical Impedance Device for Simultaneous Label-Free Affinity Sensing of Total and Glycated Haemoglobin: the Potential of using a Specific Single-Frequency Value for Analysis. Anal. Chim. Acta, (2016).

[152] American Diabetes Association. Consensus statement on the worldwide standardization of the hemoglobin A1C measurement. Diabetes Care, 30 (2007): 2399-2400.

[153] Dimaki, M., Vergani, M., Heiskanen, A., Kwasny, D., Sasso, L., Carminati, M., Gerrard, J.A., Emneus, J., Svendsen, W.E. A compact microelectrode array chip with multiple measuring sites for electrochemical applications. Sensors, 14 (2014): 9505-9521.

[154] Zor, K., Heiskanen, A., Caviglia, C., Vergani, M., Landini, E., Shah, F., Carminati, M., Martínez-Serrano, A., Moreno, T.R., Kokaia, M. A compact multifunctional microfluidic platform for exploring cellular dynamics in real-time using electrochemical detection. RSC Adv., 4 (2014): 63761-63771.

[155] Heiskanen, A.R., Spegel, C.F., Kostesha, N., Ruzgas, T., Emnéus, J. Monitoring of Saccharomyces cerevisiae cell proliferation on thiol-modified planar gold microelectrodes using impedance spectroscopy. Langmuir, 24 (2008): 9066-9073.

[156] Pardo-Yissar, V., Katz, E., Lioubashevski, O., Willner, I. Layered polyelectrolyte films on Au electrodes: characterization of electron-transfer features at the charged polymer interface and application for selective redox reactions. Langmuir, 17 (2001): 1110-1118.

[157] Lvovich, V.F., Impedance spectroscopy: applications to electrochemical and dielectric phenomena. John Wiley & Sons, Inc., Hoboken, (2012)

[158] Hsu, C., Mansfeld, F. Technical note: concerning the conversion of the constant phase element parameter Y0 into a capacitance. Corrosion, 57 (2001): 747-748.

[159] Hisamitsu, I., Kataoka, K., Okano, T., Sakurai, Y. Glucose-responsive gel from phenylborate polymer and poly (vinyl alcohol): prompt response at physiological pH through the interaction of borate with amino group in the gel. Pharm. Res., 14 (1997): 289-293.

[160] Mohapatra, S., Panda, N., Pramanik, P. Boronic acid functionalized superparamagnetic iron oxide nanoparticle as a novel tool for adsorption of sugar. Mater. Sci. Eng. C-Mater. Biol. Appl., 29 (2009): 2254-2260.

[161] Heiskanen, A., Coman, V., Kostesha, N., Sabourin, D., Haslett, N., Baronian, K., Gorton, L., Dufva, M., Emnéus, J. Bioelectrochemical probing of intracellular redox processes in living yeast cells—application of redox polymer wiring in a microfluidic environment. Anal. Bioanal. Chem., 405 (2013): 3847-3858.

[162] Sabourin, D., Snakenborg, D., Dufva, M. Interconnection blocks with minimal dead volumes permitting planar interconnection to thin microfluidic devices. Microfluid. Nanofluid., 9 (2010): 87-93.

[163] Skafte-Pedersen, P., Sabourin, D., Dufva, M., Snakenborg, D. Multi-channel peristaltic pump for microfluidic applications featuring monolithic PDMS inlay. Lab Chip, 9 (2009): 3003-3006.

APPENDIX

Reagent preparation

1. Bromcresol green working solution (1X, pH 4.2)

Bromcresol green sodium salt	50 mg
Succinic acid	4.425 g
Sodium azide	50 mg
Brij® 35 (30% w/v)	2 mL
Milli-Q water	400 mL

The pH was adjusted to a desired pH at 4.2 with NaOH (40 g dL^{-1}) or succinic acid (50 g L^{-1}) before adjusting the final volume with Milli-Q water to 500 mL. The working solution was stored in brown bottle at 4 °C.

2. Carbonate buffer (0.1 M, pH 10.3)

Sodium carbonate	1.25 g
Sodium bicarbonate	1.11 g
Milli-Q water	250 mL

3. Hemolysing buffer

(26 mM NaH_2PO_4, 7.4 mM Na_2HPO_4, and 13.5 mM KCN)

Sodium phosphate monobasic monohydrate	0.897 g
Sodium phosphate dibasic	0.263 g
Potassium cyanide	0.220 g
Milli-Q water	250 mL

4. 4-ethylmorpholine solution (10 mM, pH 8.5)

4-ethylmorpholine	326.37 µL
Milli-Q water	200 mL

The pH was adjusted to 8.5 with HCl (1M) before adjusting the final volume with Milli-Q water to 250 mL.

5. Sodium acetate buffer (10 mM, pH 5)

Sodium acetate trihydrate	215.94 mg
Glacial acetic acid	52.22 µL
Milli-Q water	250 mL

6. Phosphate buffer solution (100 mM, pH 7)

Potassium phosphate monobasic	834.48 mg
Potassium phosphate dibasic	673.92 mg
Milli-Q water	100 mL

7. Urea solution containing 0.15 M sodium chloride (5 M, pH 11)

Urea	15 g
Sodium chloride	438.3 mg
Milli-Q water	40 mL

The pH was adjusted to 11 before adjusting to the final volume with Milli-Q water to 50 mL.

VITA

Yuwadee Boonyasit obtained her B.Sc. in Medical Technology, and M.Sc. in Clinical Biochemistry and Molecular Medicine Program from Chulalongkorn University in 2008 and 2011, respectively. When she was undergraduate student, she received the Thailand Advanced Institute of Science and Technology's Pilot Project scholarship from the National Science and Technology Development Agency (NSTDA). She also received the Thailand Graduate Institute of Science and Technology scholarship (under the contract no. TG-44-09-51-094M), the CU Graduate School Thesis Grant, and the financial support for Master's students to present academic papers in a foreign country from the Graduate School.

From 2014 to 2015, she spent a one-year period at the Department of Micro- and Nanotechnology, Technical University of Denmark, Kongens Lyngby, Denmark, under the supervision of Prof. Jenny Emnéus. During her stay at DTU, she was trained in various academic and industrial microfabrication techniques.

Currently, she is pursuing a PhD degree in Clinical Biochemistry and Molecular Medicine Program at the Faculty of Allied Health Sciences, Chulalongkorn University, Thailand, under the supervision of Asst. Prof. Wanida Laiwattanapaisal. Her main interests focus on the development of analytical devices for detection of diabetic markers, microfluidic paper-based analytical device, electrochemical biosensors, sequential injection analysis system, and Lab-on-Chip devices for clinical diagnostics. She also has a keen interest in the interdisciplinary aspects of these areas. She wishes to acknowledge the financial support from the Thailand Research Fund through the Royal Golden Jubilee Ph.D. Program (under grant No. PHD/0164/2553), and the Graduate School, Chulalongkorn University for the Tuition Free Scholarship.